Supporting Information

Membrane-Tethered Activation Design of Photosensitizer Boosts Systemic Antitumor Immunity via Pyroptosis

Pei Lu, Xianjun Liu, Xia Chu, Fenglin Wang*, Jian-Hui Jiang

State Key Laboratory of Chemo/Bio-Sensing and Chemometric, College of Chemistry and Chemical Engineering, Hunan University Changsha, 410082 (P. R. China)

E-mail: fengliw@hnu.edu.cn

Table of contents

1. Experimental Procedures

1.1 Reagents and instruments

Dihydrorhodamine 123 (DHR123), 1,3-diphenlisobenzofuran (DPBF) and 2′,7′-dichlorofluorescin diacetate (DCFH-DA) were obtained from Sigma-Aldrich (MO, USA). Singlet oxygen sensor green (SOSG), hydroxyphenyl fluorescein (HPF) and CellMask Green plasma membrane stain (Dil) were purchased from Invitrogen (CA, USA). Paraformaldehyde (PFA, 4%), Hoechst 33342, immunol staining blocking buffer, immunol staining primary antibody dilution buffer, phenylmethanesulfonyl fluoride (PMSF), RIPA-lysis buffer (middle), sodium dodecyl sulphate-polyacrylamide gel electrophoresis (SDS-PAGE) loading buffer, high mobility group box 1 (HMGB1) Rabbit monoclonal antibody, calreticulin (CRT) Rabbit monoclonal antibody, Annexin V-FITC apoptosis detection kit and Calcein/ propidium iodide (PI) cell cytotoxicity assay kit, hematoxylin and eosin (H&E) were purchased from Beyotime (Shanghai, China). Cell counting Kit-8 (CCK-8) was obtained from Topscience (Shanghai, China). Recombinant human aminopeptidase N (APN) was obtained from R&D Systems (MN, USA). Caspase-1 rabbit antibody was purchased from Cell Signaling Technology (MA, USA). Anti-CD4-mouse-PE, anti-CD3-mouse-FITC, anti-CD8a-mouse-APC, anti-CD11c-mouse-FITC, anti-CD80-mouse-APC and anti-CD86-mouse-PE were purchased from Biolegend (CA, USA). β-Actin rabbit monoclonal antibody, horse radish peroxidase (HRP)-conjugated goat anti-rabbit IgG and Alexa Fluor 488-conjugated goat anti-rabbit IgG were obtained by Sangon Biotech (Shanghai, China). ELISA kits for mouse interleukin-18 (IL-18), IL-1β, TNFα and IL-10 were obtained from Solarbio (Beijing China). HepG2 cells (human hepatoma cell line) and 4T1 cells (mouse breast cancer cell line) were obtained from Cell Bank of Type Culture Collection of Chinese Academy of Sciences (Beijing, China). HeLa cells (human cervical carcinoma cell line), MCF-7 cells (human breast adenocarcinoma cell line), HEK293T cells (human embryonic kidney cell line) and A549 cells (non-small cell lung cancer cell line) were purchased from the cell bank of central laboratory at Xiangya Hospital (Changsha, China). Dulbecco's modified Eagle's medium (DMEM), penicillin, streptomycin and 100% heat-inactivated fetal bovine serum were obtained from Thermo Scientific HyClone (MA, USA). All other reagents were commercially purchased and used without purification unless otherwise indicated. Ultrapure water was obtained through a Millipore Milli-Q water purification system (Billerica, MA, USA) and had an electric resistance >18.25 MΩ. The stock solutions of **aPYCI** (2.5 mM) and **aPYCI4** (2.5 mM) were prepared in DMSO.

Thin-layer chromatography (TLC) was performed on silica gel aluminum sheets with an F-254 indicator. Column chromatography was conducted using 200-300 mesh SiO_2 (Qingdao Ocean Chemical Products). Mass spectroscopy (MS) analysis was performed on an LCQ advantage ion trap mass spectrometry (Thermo Fisher Scientific, Bremen, Germany). ^{1}H NMR and ^{13}C NMR spectra were recorded on a Bruker Avance-III 400 instrument (Bruker) using tetramethylsilane (TMS) as an internal standard. UV-vis absorbance spectra were recorded on a Shimadzu UV-2450 spectrophotometer with an interval of 2 nm. Fluorescence spectra were recorded on an FS5 spectrofluorometer (Edinburgh, UK). Confocal fluorescence imaging was performed on a Nikon A1+ confocal microscope (Japan) with 20× or 60× objective lens. In vivo fluorescence imaging was performed on an IVIS Lumina XR small animal imaging system (Caliper, Switzerland).

1.2 In vitro Assays

Absorption and fluorescence measurements. Both UV-Vis absorption and fluorescence measurements were carried out in PBS (10 mM, pH = 7.4) buffer solution containing 10% DMSO as a co-solvent. Absorbance spectrum for **aPYCI4** was recorded in the range from 500 nm to 800 nm.

Fluorescence spectrum of **aPYCI4** was recorded in the range from 660 nm to 850 nm with an excitation wavelength of 640 nm.

To study the absorbance response of **aPYCI4** towards APN, **aPYCI4** (2.5 μM) was incubated with APN (100 ng/mL) in PBS at 37 °C for 1 h and absorbance spectrum was recorded in the range from 500 nm to 800 nm. To study the fluorescence responses of **aPYCI4** towards APN, **aPYCI4** (2.5 μM) was incubated with different concentrations of APN (0-200 ng/mL) in PBS at 37 °C for 1 h. The limit of detection was calculated using the following equation:

$$\text{Detection limit} = 3\sigma/k$$

Where σ is the standard deviation of the blank measurements, k is the slope between the fluorescence intensity at 680 nm versus various APN concentrations in the linear region.

For selectivity studies, solutions of various testing substances including $MgCl_2$ (100 μM), BSA (100 ng/mL), serum (20%), H_2O_2 (100 μM), GSH (5 mM), Cys (100 μM), nitroreductase (NTR, 100 ng/mL), carboxylesterases, (CE, 100 ng/mL), NAD(P)H quinone dehydrogenase 1 (NQO1, 100 ng/mL), gamma-glutamyl transferase (γ-GGT, 100 ng/mL) and APN (100 ng/mL) were incubated with **aPYCI4** (2.5 μM) at 37 °C for 1 h. For APN inhibition, **aPYCI4** (2.5 μM) was treated with bestatin (100 μM) and APN (100 ng/mL) in PBS at 37 °C for 1 h. Fluorescence spectra were recorded in the range from 660 nm to 850 nm with an excitation wavelength of 640 nm.

Photostability studies. For photostability studies, **PYCI4** and cyanine 5 (Cy5) in PBS (10 mM, pH = 7.4) containing 10% DMSO was irradiated with a xenon lamp (100 W) and maximum fluorescence intensities were recorded at different time points for 2 h.

HR-MS-ESI analysis. Probe **aPYCI4** (10 μM) was incubated with APN (400 ng/mL) in PBS (10 mM, pH 7.4) for 1 h at 37°C. The reaction was quenched by 250 μL of acetonitrile, vortexed and centrifuged at 10000 rpm for 15 min. HR-MS-ESI analysis was performed.

Reactive oxygen species (ROS) detection. Probe **aPYCI4** (2.5 μM) was incubated with or without APN (100 ng/mL) at 37 °C for 1 h. Afterwards, DCFH-DA (10 μM) was added, and the resulting mixture was irradiated with a 640 nm laser (10 mW/cm^2) for different times (0, 1, 2, 3, 4, 5, 6, 7, 8, 9, 10 min). Fluorescence spectra for DCFH-DA were obtained upon excitation at 488 nm. Probe **aPYCI4** without incubation with APN was used as a control.

Singlet oxygen ($^1O_2$) detection. Probe **aPYCI4** (2.5 μM) was incubated with or without APN (100 ng/mL) at 37 °C for 1 h. Afterwards, SOSG (2.5 μM) was added, and the resulting mixture was irradiated with a 640 nm laser (10 mW/cm^2) for different times (0, 2, 5, 8, 10 min). Fluorescence spectra for SOSG were obtained upon excitation at 488 nm.

Superoxide radical ($O_2^{-\bullet}$) detection. Probe **aPYCI4** (2.5 μM) was incubated with or without APN (100 ng/mL) at 37 °C for 1 h. Afterwards, DHR123 (2.5 μM) was added, and the resulting mixture was irradiated with a 640 nm laser (10 mW/cm^2) for different times (0, 2, 5, 8, 10 min). Fluorescence spectra for DHR123 were obtained upon excitation at 488 nm.

Hydroxyl radical (OH•) detection. Probe **aPYCI4** (2.5 μM) was incubated with or without APN (100 ng/mL) at 37 °C for 1 h. Afterwards, HPF (2.5 μM) was added, and the resulting mixture was irradiated with a 640 nm laser (10 mW/cm^2) for different times (0, 2, 5, 8, 10 min). Fluorescence spectra for HPF were obtained upon excitation at 488 nm.

$^1O_2$ quantum yield calculation. The quantum yield for $^1O_2$ production was determined by decomposing 1,3-diphenlisobenzofuran (DPBF) using methylene blue (MB) as the reference. **PYCI4** (10 μM) or MB (10 μM) was mixed with DPBF (10 μM) in PBS/EtOH (v/v = 50/50) and the resulting

mixture was irradiated with a 640 nm laser (10 mW/cm^2) for different times (0, 30, 60, 90, 120, 150, 180 s). Absorption spectra for DPBF were recorded after irradiation. The $^1O_2$ quantum yield was calculated using the following equation:

$$\Phi_{Probe} = \Phi_{MB} \frac{K_{Probe} A_{MB}}{K_{MB} A_{Probe}}$$

where K_{Probe} and K_{MB} were the decomposition rates of DPBF in the presence of the probe and MB, respectively. Φ_{MB} was the $^1O_2$ quantum yield of MB (Φ_{MB} = 0.52). The natural logarithm of the absorbance ratio (A_0/A) of DPBF at 410 nm was plotted against irradiation time and the slopes were determined as the decomposition rates.

1.3 Cellular Studies

Cell culture. Cells of HepG2, HEK293T, 4T1, HeLa, MCF-7 and A549 were cultured in DMEM supplemented with 10% fetal bovine serum, 100 U/mL penicillin and 100 g/mL streptomycin at 37°C in a humidified atmosphere containing 5% CO_2. The cells were plated on 35-mm sterilized dishes with 14 mm wells and grown to a confluency of 50–70%.

Confocal laser scanning microscopy (CLSM) imaging. To test the ability of photosensitizers (PSs) to localize on plasma membrane, cells including HepG2, HEK293T and 4T1 were incubated with **PYCI1-4** (2.5 μM) for 30 min, stained with a membrane tracker Dil (2 μg/mL) for 15 min and then stained with Hoechst 33342 (2 μg/mL). The cells were washed with PBS for three times and replenished with fresh medium.

To determine the activities of endogenous APN, cells including HepG2, HEK293T and 4T1 were treated with probe **aPYCI4** (2.5 μM) at 37 °C for 1 h, washed thrice with PBS (pH = 7.4) and co-stained with Dil (2 μg/mL) for 15 min. To investigate the specific activation of the probe by APN, the cells were pretreated with bestatin (100 μM) before incubation with **aPYCI4**.

CLSM images were acquired on a Nikon TI-E+A1 SI confocal laser scanning microscope using an oil immersion objective lens of 60× or a dry objective lens of 20× with the following parameters. Red channel for **aPYCI4**: Ex = 640 nm, Em = 650 - 700 nm; Green channel for Dil: Ex = 488 nm, Em = 500 - 550 nm; blue channel for Hoechst 33342: Ex = 405 nm, Em = 430–470 nm.

Flow cytometry assays. All the cells were cultured in 6-well plates at a density of 2 × 10^5 cells/well for 24 h and then incubated with probe **aPYCI4** (2.5 μM) at 37 °C for 1 h. The cells were washed twice with PBS (pH = 7.4), treated with 0.25% trypsin and centrifuged at 1500 rpm for 3 min at room temperature. The cell pellet was washed and suspended in PBS for flow cytometry analysis on a FACSVerseTM flow cytometer (BD Biosciences, USA). Data was analyzed with Flow Jo software.

Intracellular detection of ROS. HepG2 cells were treated with probe **aPYCI4** (2.5 μM) for 1 h and irradiated with/without a 640 nm laser (10 mW/cm^2,10 min). The cells were washed twice with PBS and incubated with DCFH-DA (10 μM) in FBS-free DMEM for 1 h in the dark. The cells were washed twice with PBS and CLSM images were obtained using the following parameters: Ex = 488 nm, Em = 500 - 550 nm. To test the specific production of ROS by APN-mediated activation of **aPYCI4**, the cells were pretreated with the APN inhibitor bestatin (100 μM) for 2 h. For flow cytometry assays, the cells were treated with 0.25% trypsin and centrifuged at 1500 rpm for 3 min at room temperature. The cell pellets were washed and suspended in PBS for flow cytometry analysis.

For determination of the type of ROS, the cells were pretreated with **aPYCI4** (2.5 μM) for 1 h, and treated with specific ROS scavengers for 1 h at 37 °C. Particularly, the cells were treated with sodium azide[1] (5 mM), D-mannitol[2] (50 mM) or Tiron[3] (10 mM) to scavenge $^1O_2$, ·OH and $O_2^{-\bullet}$, respectively. Afterwards, the cells were irradiated with a 640 nm laser (10 mW/cm^2,10 min), treated with DCFH-DA (10 μM) for 1 h and CLSM images were obtained. For flow cytometry assays, the cells were treated

with 0.25% trypsin and centrifuged at 1500 rpm for 3 min at room temperature. The cell pellet was washed and suspended in PBS for flow cytometry analysis.

Cytotoxicity assay. Cells were seeded in 96-well plates at a density of 1×10^4 cells per well and cultured for 24 h. The cells were incubated with different concentrations of **aPYCI4** (0 μM - 4 μM) for 1 h and irradiated with/without a 640 nm laser (10 mW/cm^2,10 min). The cells were cultured for 24 h before addition of CCK-8 solution (10 μL). The cells were incubated at 37°C for 2 h and optical density (OD) values at 450 nm were measured with a microplate reader. Cell viability was determined using the following equation:

$$\text{Cells viability (\%)} = (OD_{probe} - OD_{blank})/(OD_{control} - OD_{blank}) \times 100$$

where OD_{probe} are the OD values for cells treated with **aPYCI4** (0 μM - 4 μM).

Live/Dead cell co-staining assay. For live/dead cell assays, 2×10^5 cells were seeded and cultured in 35-mm sterilized dishes with 14 mm wells for 24 h. HepG2 and HEK293T cells were treated with **aPYCI4** (2.5 μM) at 37°C for 1 h and irradiated with a 640 nm laser (10 mW/cm^2,10min). Cells without treatment of **aPYCI4** or without laser irradiation were used as controls. The cells were co-stained with Calcein AM and PI according to the instruction manual. CLSM images were obtained using the following parameters: Calcein AM: Ex = 488 nm, Em = 505 - 545 nm; PI: Ex = 561 nm, Em = 600 -700 nm.

Quantification of apoptosis/necrosis by flow cytometry. HepG2 cells were seeded in the 6-well plate at a density of 2×10^5 cells/well and cultured for 24 h. The cells were treated with probe **aPYCI4** (2.5 μM) or control probe **aPYCI** (2.5 μM) at 37 °C for 1 h, irradiated with a 640 nm laser (10 mW/cm^2,10min) and cultured for another 4 h. Afterwards, the cells were detached using trypsin, co-stained with Annexin V-FITC and PI according to the manufacturer's instructions. The cells were washed and suspended in PBS for flow cytometry analysis.

Lactate dehydrogenase (LDH) and cytokine release assays. HepG2 cells were cultured in 6-well plates at a density of 2×10^5 cells/well for 24 h and incubated with probe **aPYCI4** (2.5 μM) or **aPYCI** (2.5 μM) at 37 °C for 1 h. The cells were irradiated with or without a 640 nm laser (10 mW/cm^2,10min) and cultured for another 4 h. The amounts of LDH in the supernatants were detected with the LDH kit according to the manufacturer's instructions. Meanwhile, the levels of IL-18 and IL-1β in the supernatants were quantified by ELISA method. Cells without incubation of the probe were used as controls.

Western blotting analysis. Western blotting assay for cleaved caspase-1 and N-terminal GSDMD was performed according to the manufacturer's protocols with slight modifications. HepG2 cells treated with **aPYCI4** (2.5 μM) or **aPYCI** (2.5 μM) were irradiated with or without a 640 nm laser (10 mW/cm^2,10min). Cells irradiated with the laser only were used as controls. The cells were lysed in lysis buffer and total proteins were extracted. The extracted proteins were separated by SDS-PAGE and transferred to polyvinylidene difluoride (PVDF) membranes. The membranes were blocked with I-Block reagent (0.2%) containing bovine saline albumin (5%) and incubated with primary antibodies (1: 1000 dilution, cleaved N-terminal GSDMD, or cleaved caspase-1) at room temperature overnight. The membranes were washed with 1x TBST buffer and incubated with HRP-conjugated secondary antibodies (1: 3000 dilution) for 2 h. A chemiluminescence (ECL) system (Thermo Fisher) was used to visualize the immunoreactive bands. For control, β-actin was analyzed using the same protocol using the corresponding primary antibody.

Immunofluorescence assay. Immunofluorescence staining was performed to study the levels of HMGB1/CRT for HepG2 cells under different treatments. The cells with various treatments (control, **aPYCI4** and **aPYCI**) were irradiated with the laser for 10 min or kept in dark. The cells were cultured for another 4 h, washed with PBS, fixed with paraformaldehyde (4%) at 4°C for 20 min, permeabilized and treated with blocking reagent (10 % bovine serum in PBS). The cells were then stained with rabbit monoclonal antibodies for HMGB1/CRT at 4°C overnight. Afterwards, the cells were washed thrice with PBS, stained with Alexa Fluor 488-labeled goat anti-rabbit IgG for 1 h in the dark. The cells were incubated with Hoechst 33342 and CLSM images were acquired using the following parameters: Channel for Hoechst 33342: Ex = 405 nm, Em = 430 - 470 nm; Channel for Alexa Fluor 488: Ex = 488 nm, Em = 500 - 550 nm.

1.4 Vivo Studies

In Vivo Imaging. All mice experiments were approved by the Hunan Provincial Science & Technology Department and performed in compliance with the guidelines of the Institutional Animal Care and Use Committee of Human University (approval number: SYXK2018-0006). Female Balb/c mice (4-5 weeks of age) were obtained from Hunan Shrek Jingda Experimental Animal Cooperation (Changsha, China). 4T1 tumor cells (2×10^6 cells in 100 μL 1 × PBS) were subcutaneously inoculated on the left flanks of mice. Tumors were grown to ~100 mm^3 before imaging. For fluorescence imaging, **aPYCI4** or **aPYCI** (100 μM, 100 μL) was injected to the tumor-bearing mice via tail vein. Fluorescence images were acquired at different time post-injection (0, 4, 8,12, 24, 48, 72, 120, 168 h) using the IVIS Lumina XR small animal imaging system.

Blood circulation analysis. Healthy female Balb/c mice (n = 3) were intravenously injected with **PYCI4** (100 μM,100 μl), blood samples were collected at different time points via the orbital venous plexus and incubated at 4 °C. Fluorescence spectra for **PYCI4** were recorded. The blood concentrations of **PYCI4** at different times were determined based on their standard curves. Pharmacokinetic parameters were calculated as following[4]:

$C = A'e^{-\alpha t} + B'e^{-\beta t} - C'e^{-k_a t}$

C is the concentration of the PS at a specific time, t is the specific time, α is distribution rate constant, β is elimination rate constant.

When t is long enough,

$k_a \gg \alpha, \alpha \gg \beta$

So $e^{-\beta t} \to 0$, $e^{-k_a} \to 0$, the above equation is simplified as follows:

$C = B'e^{-\beta t}$, so $\lg C = \lg B' - 0.4343\,\beta t$

A semi-logarithmic graph was plotted for $\lg C$ *vs* t, and the elimination rate constant (β) was calculated based on the slope. For **PYCI4**, β= 0.3357, so $t_{1/2} = 0.693/\beta = 2.06$ h.

Blood partition analysis. To determine the partition of **PYCI4**, healthy female Balb/c mice (n = 3) were intravenously injected with **PYCI4** (100 μM,100 μl). Blood samples were immediately collected and stored at room temperature for 2 h. The blood samples were centrifuged at 3000 rpm for 15 min and the upper layer was collected as serum. The serum was separated by ultrafiltration (13000 rpm, 30 min), and serum protein and supernatant were collected. Fluorescence spectra for the blood sample, serum, serum protein and supernatant were recorded in the range from 660 nm to 850 nm with an excitation wavelength of 640 nm.

In vivo treatment of primary tumors via PDT. To determine the ability of **aPYCI4**-mediated PDT for treating primary tumors, mice bearing tumors (n = 5) were randomly divided into four groups and intravenously injected with one dosage of PBS (group I and group II),) and **aPYCI4** (group III

and IV) via tail-vein injection. The tumor regions of mice in group II and IV were irradiated with a 640 nm laser (10 mW/cm^2,10 min) every other day for four times. The mice weight and tumor sizes were monitored every other day for 14 days. Tumor volume (V) was calculated using $V = W^2 \times L/2$, where W is the maximal transverse diameter (width) and L is the largested longitudinal diameter (length) of the tumor. The mice were euthanized on day 14. The tumors and major organs (including heart, liver, spleen, lung and kidney) were excised for further studies. Ex vivo fluorescence images of the tumors and major organs were acquired using the IVIS Lumina XR small animal imaging system.

The excised tumors and organs were fixed with 4% formaldehyde, embedded in paraffin and sliced into 5 μm in thickness. For H&E analysis, the sliced tissues were stained with haematoxylin, eosin and DAPI. For immunofluorescence staining analysis, the sliced tissues were stained with anti-CD8-PE and DAPI or anti-CD4-FITC and DAPI. Fluorescence images were collected by a fluorescence microscope with a magnification of 100 times.

In vivo treatment of primary and distant tumors via PDT. To explore the abscopal effect of **aPYCI** for treatment of distant tumors, primary tumors were established by subcutaneously inoculating 4T1 tumor cells to the left flanks of BALB/c. Mice bearing tumors (n = 5) with sizes of ~100 mm^3 were randomly divided into five groups and intravenously injected with one dosage of PBS (group I), **aPYCI** (group II and III) or **aPYCI4** (group IV and V) via tail-vein injection. Distant tumors were inoculated onto the right leg of mice after the primary tumors were irradiated once with 640 nm laser (10 mW/cm^2,10 min). Afterwards, the primary tumors were irradiated for three more times whereas the distant tumors were not irradiated. The mice weights and tumor sizes of primary and distant tumors were monitored every other day. The mice were euthanized on day 14, and the tumors and major organs (including heart, liver, spleen, lung and kidney) were excised for further studies.

In vivo anti-tumor immunity and abscopal effect. To determine the maturation of dendritic cells, tumor bearing mice were randomly divided into 5 groups (n = 3) and treated under the same conditions as described in the section of in vivo treatment of primary and distant tumors via PDT. The tumors were harvested after the first irradiation. The tumors were cut into small pieces and immersed in collagenase IV (1 mg/mL) and DNase I (0.1 mg/mL) for 1 h at 37 °C to obtain single cell suspensions. The cells were filtered with a 70 μm nylon cell strainer and blood cells were removed by a red blood cell lysis buffer. The cells were stained with anti-CD80-mouse-APC, anti-CD86-mouse-PE and anti-CD11c-mouse-FITC, and analyzed with flow cytometry. To determine intratumor-infiltrating T lymphocytes, the tumors were harvested after irradiation for three times. The tumors were suspended, filtered and removed with blood cells using the same procedures as described above. The cells were stained with anti-CD3-mouse-FITC, anti-CD8a-mouse-APC or anti-CD4-mouse-PE, and analyzed with flow cytometry. To determine the levels of the cytokines in serum, the tumor bearing mice were treated under the same conditions in the section of in vivo treatment of primary tumors via PDT. Serum samples were collected after irradiation for three times. The levels of TNF-α, IL-10, IL-18 and IL-1β were measured by ELISA Kit according to the manufacturer's protocols.

Statistical analysis. All the experiments were replicated and the specific number of replicates was either annotated in the figure captions or specific sections. Unless otherwise specified, statistical significance was determined by the unpaired, two-tailed Student's t-test at ****$p < 0.0001$, ***$p < 0.001$, **$p < 0.01$ and *$p < 0.05$. Data were presented as mean ± standard deviation (SD).

1.5 Synthesis of compounds

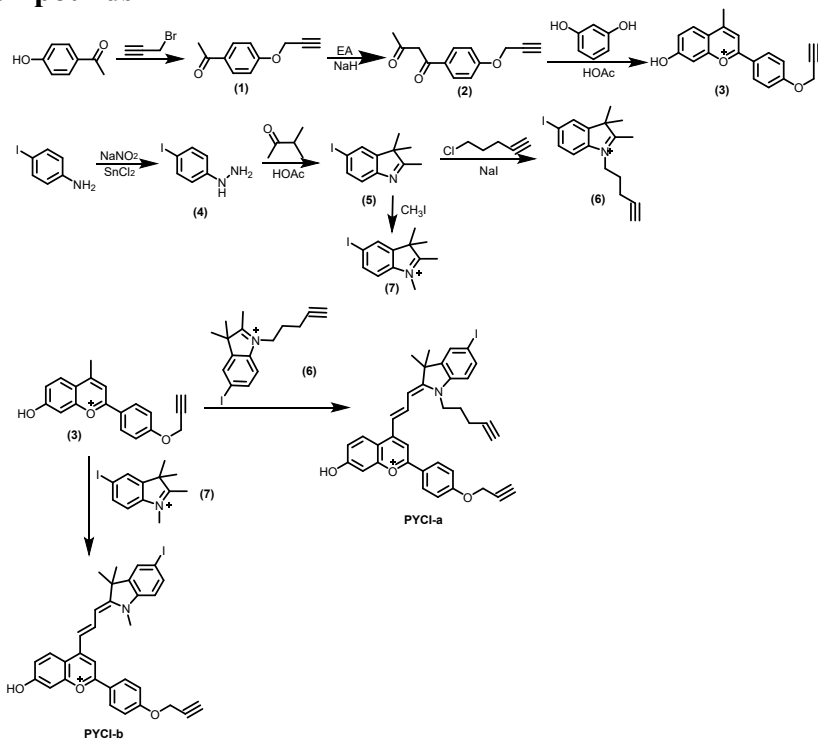

Scheme S1. Synthetic routes for **PYCI-a** and **PYCI-b**.

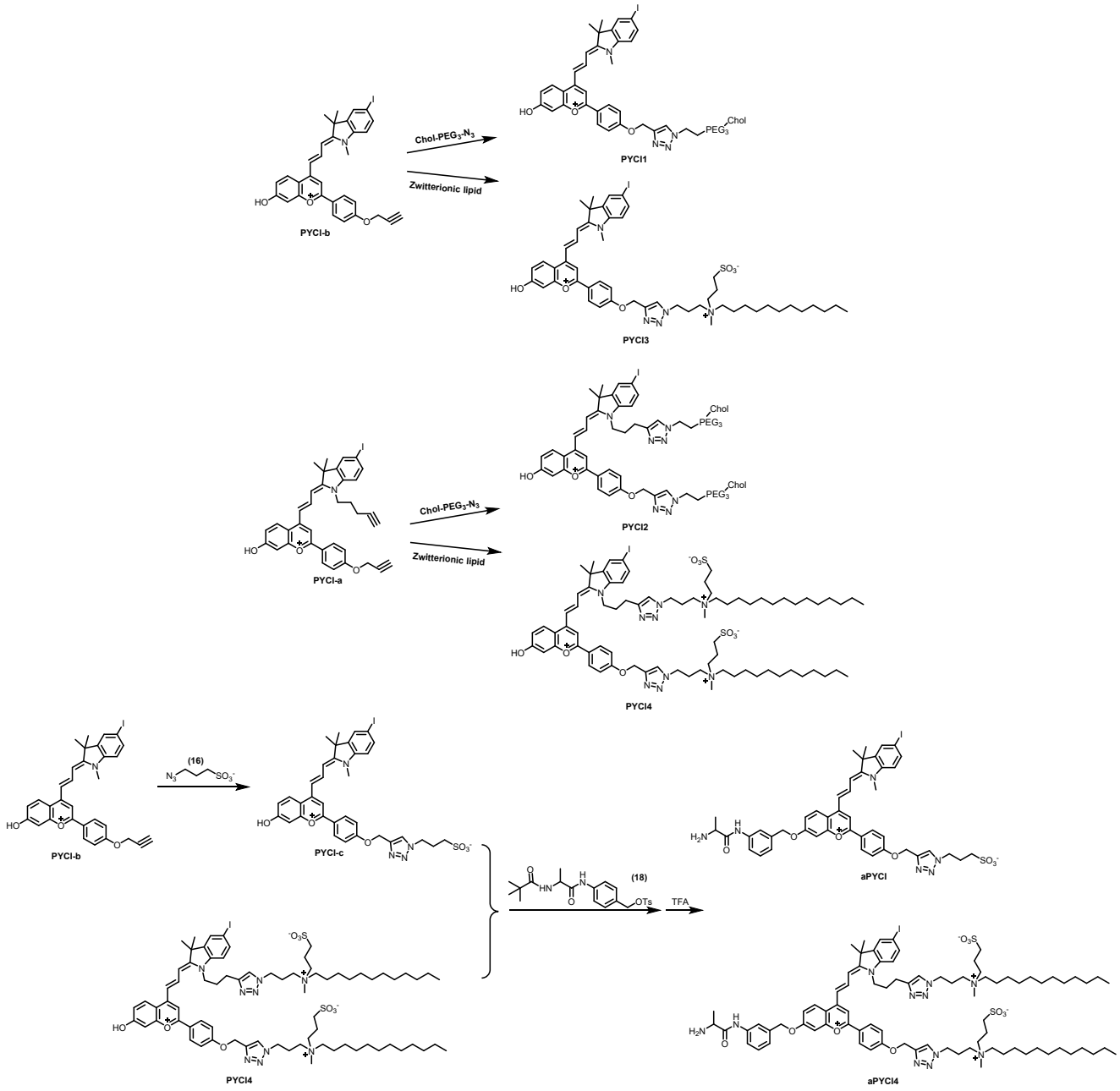

Scheme S2. Synthetic routes for **PYCI1**, **PYCI2**, **PYCI3**, **PYCI4**, **aPYCI** and **aPYCI4**.

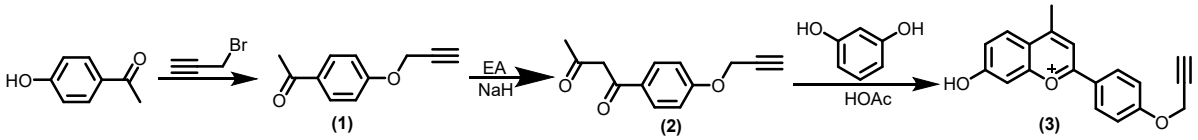

Compound 1: 4'-Hydroxyacetophenone (2.72 g, 20 mmol) was dissolved in N, N-dimethylformamide (DMF, 20 mL), followed by addition of propargyl bromide (3.57 g, 30 mmol) and KOH (1.23 g, 22 mmol). The resulting mixture was stirred at room temperature for 3 h, and the solvent was removed under reduced pressure. The residue was dissolved in ethyl acetate (EA) and extracted with water. The organic solvent was evaporated and subjected to silica gel chromatography and eluted with PE: EA (10:1 to 5:1, v/v) to yield compound **1** as a white solid (2.2 g, yield: 93%). ^{1}H NMR (400 MHz, 298 K, $CDCl_3$): δ 7.96 (d, *J* = 8.8 Hz, 2 H), 7.05 (d, *J* = 8.8 Hz, 2 H), 4.78 (d, *J* = 2.0 Hz, 2 H), 2.58 (s, 3 H), 2.57 (t, *J* = 2.4 Hz, 1 H). ^{13}C NMR (100 MHz, 298 K, $CDCl_3$): δ 196.68, 161.28, 131.08, 130.51, 114.58, 77.76, 76.14, 55.85, 26.37. HR-ESI-MS: m/z calcd for compound **1** ($C_{11}H_{10}O_2$, $[M+H]^+$), 175.07; found, 175.02.

Compound 2: To a suspension of NaH (1.60 g of dispersion in oil, 40 mmol) in EA (20 mL) was slowly added with a solution of compound **1** (1.74 g, 10 mmol) in EA (20 mL) at 0 °C. The mixture was stirred at room temperature for 12 h and treated with 10% aqueous NH_4Cl (30 mL). pH was adjusted to 5 using HCl and the aqueous phase was separated and extracted with EA. The combined organic extracts were dried over anhydrous Na_2SO_4 and concentrated under reduced pressure. The residues were purified by flash column chromatography on silica (PE: EA=7:1, v/v) to yield compound **2** as a yellow oil (1.9 g, yield: 88%). ^{1}H NMR (400 MHz, 298 K, $CDCl_3$): δ 7.88 (d, *J* = 8.8 Hz, 2 H), 7.03 (d, *J* = 8.8 Hz, 2 H), 6.14 (s, 1 H), 4.78 (d, *J* = 2.4 Hz, 2 H), 2.58 (t, *J* = 2 Hz, 1H), 2.20 (s, 3 H). ^{13}C NMR (100 MHz, 298 K, $CDCl_3$): δ 191.94, 183.79, 160.86, 129.04,114.81, 77.83, 76.71, 55.86, 54.79, 25.39 . HR-ESI-MS: m/z calcd for compound **2** ($C_{13}H_{12}O_3$, $[M+H]^+$), 217.08; found, 216.87.

Compound 3: Compound **2** (1.73 g, 8 mmol) and resorcinol (0.88 g, 8 mmol) were dissolved in acetic anhydride (20 mL), and passed with HCl gas. The mixture was stirred at room temperature for 2 h. The resulting precipitate was filtered, washed with water 3 times and dried in a vacuum oven to afford compound **3** (1.28 g, yield: 55%) as an orange solid. ^{1}H NMR (400 MHz, 298 K, CD_3OD): δ 8.50 (d, *J* = 8.8 Hz, 2 H), 8.39 (d, *J* = 4.8 Hz, 2 H), 7.52 (d, *J* = 2.0 Hz, 1 H), 7.47 (s, 1 H), 7.38 (d, *J* = 8.8 Hz, 2 H), 5.00 (d, *J* = 2.0 Hz, 2 H), 3.33 (d, *J* = 1.2 Hz, 3 H), 3.14-3.13 (m, 1 H). ^{13}C NMR (100 MHz, 298 K, CD_3OD): δ170.17, 168.58, 164.43, 158.29, 131.49, 129.04, 121.77, 120.81, 118.57, 116.27, 113.82. HR-ESI-MS: m/z calcd for compound **3** ($C_{19}H_{15}O_3$+, $[M]^+$), 291.10; found, 291.65.

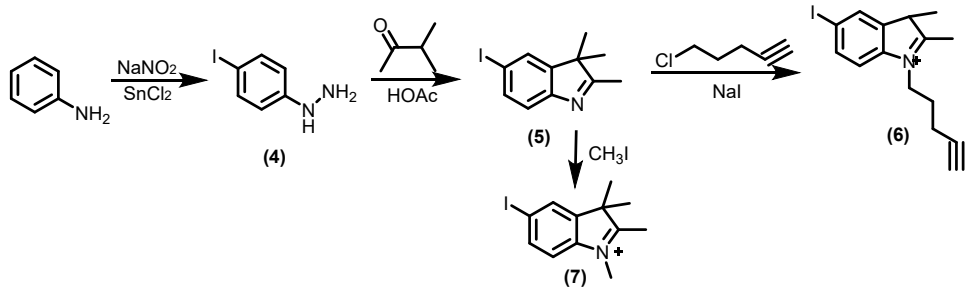

Compound 4: To a solution of 4-iodoaniline (8.76 g, 40 mmol) in HCl (20%, 45 mL) was added dropwise with $NaNO_2$(2.84 g, 41.2 mmol) in water (65 mL) at 0°C. After stirring for 30 min, a solution of $SnCl_2$ (21.9 g, 97.2 mmol) in concentrated HCl (30 mL) was slowly added at 0°C.The resulting suspension was stirred for 30 min, filtered and washed with water. The free base from the obtained solid was liberated using NaOH solution (1 M) and extracted 3 times with CH_2Cl_2. The combined

organic phase was dried over anhydrous Na_2SO_4, filtered and evaporated to give compound **4** (6.78 g, yield: 72%) as a brown solid which was directly used without further purification.

Compound 5: A solution of 4-iodophenylhydrazine **4** (6.69 g, 28.6 mmol) and 3-mthyl-2-butanone (3.52 mL, 32.9 mmol) in acetic acid (220 mL) was refluxed for 3 h. After reaction, the residue was neutralized with Na_2CO_3 and extracted twice with EA. The combined organic phase was washed with saturated brine, dried over anhydrous Na_2SO_4, filtered and evaporated. The crude product was purified on silica gel chromatography and eluted with PE: EA (10:1 to 3:1, v/v) to yield compound **5** (4.59 g, yield: 56%) as a yellow oil. ^{1}H NMR (400 MHz, 298 K, $CDCl_3$): δ 7.63 (d, J = 8.0 Hz, 1 H), 7.61 (s, 1 H), 7.29 (d, J = 3.2 Hz, 1 H), 2.27 (s, 3 H), 1.31 (s, 6 H). ^{13}C NMR (100 MHz, 298 K, $CDCl_3$): δ 188.46, 153.27, 148.00, 136.42, 130.66, 121.82, 89.77, 53.87, 22.76, 15.38. HR-ESI-MS: m/z calcd for compound **5** ($C_{13}H_{12}O_3$, $[M+H]^+$), 286.00; found, 286.96.

Compound 6: NaI (3.3 g, 22 mmol) was added to a solution of **5** (2.85 g,10 mmol) and 5-chloro-1-pentyne (1.02 g, 10 mmol) in acetonitrile (8 mL). The resulting mixture was refluxed for 24 h. A light brown precipitate was obtained and filtered under reduced pressure. The residue was recrystallized with acetone to afford compound **6** as a light brown powder (2.35 g, yield: 67%). ^{1}H NMR (400 MHz, 298 K, DMSO-d_6): δ 8.31 (s, 1 H), 8.02 (d, J = 8.0 Hz, 1 H), 7.80 (d, J = 8.4 Hz, 1 H), 4.47 (t, J = 7.2 Hz, 2 H), 2.93 (s, 1 H), 2.83 (s, 3 H), 2.40 (t, J = 5.2 Hz, 2 H), 2.04 (m, 2 H) 1.54 (s, 6 H). ^{13}C NMR (100 MHz, 298 K, DMSO-d_6): δ 171.5, 156.2, 137.5, 136.7, 128.9, 127.6, 119.8, 115.3, 80.5, 65.2, 64.9, 50.8, 38.6, 28.4, 18.1. HR-ESI-MS: m/z calcd for compound **6** ($C_{16}H_{19}IN$, $[M+H]^+$), 353.24; found, 353.03.

Compound 7: Compound **5** (1.42 g, 5 mmol) was dissolved in toluene (20 mL) and heated to reflux. Then iodomethane (2.13 g, 15 mmol) in toluene (5 mL) was added through a syringe under continuous stirring. After stirring for 6 h, a pink precipitate was obtained, filtered under reduced pressure, washed with EA for 3 times and dried over a vacuum oven to afford compound **7** (1.05 g, yield: 70%). ^{1}H NMR (400 MHz, 298 K, DMSO-d_6): δ 8.29 (s, 1 H), 8.01 (d, J = 8.4 Hz, 1 H), 7.73 (d, J = 8.4 Hz, 1 H), 3.94 (s, 3 H), 2.74 (s, 3 H), 1.52 (s, 6 H). ^{13}C NMR (100 MHz, 298 K, DMSO-d_6): δ 196.57, 144.25, 142.41, 137.93, 132.66, 117.58, 96.46, 54.51, 35.25, 22.95, 14.63. HR-ESI-MS: m/z calcd for compound **7** ($C_{12}H_{15}IN$, $[M+H]^+$), 301.02; found, 300.79.

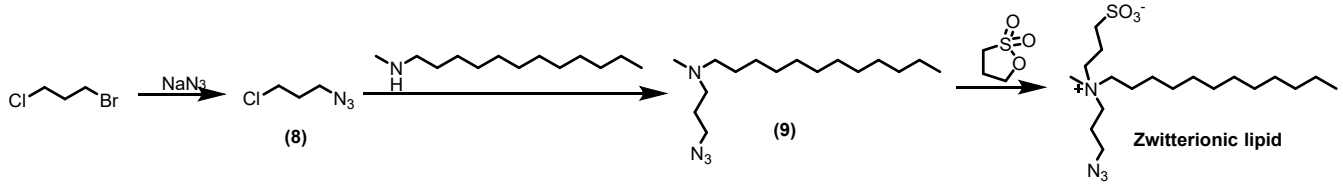

Compound 8: NaN_3 (1.0 g, 6.35 mmol) was added to a solution of 1-bromo-3-chloropropane (0.41 g, 6.35 mmol) in DMF (20 mL). The reaction mixture was stirred for 20 h at room temperature, and partitioned between ether and water. The organic layer was washed with water for 3 times, dried over anhydrous Na_2SO_4 and concentrated to give compound **8** (0.71 g, yield: 94%) as a colorless oil which was directly used without further purification.

Compound 9: Compound **8** (0.602 g, 5 mmol) and dodecyl(methy)amine (1 g, 5 mmol) were dissolved in CH_3CN (15 mL). The mixture was heated at 80°C in a sealed flask for 6 h. The solvent was removed under reduced pressure and the crude product was purified by column chromatography using CH_2Cl_2/MeOH (5 to 10% of MeOH) as an eluent to give compound **9** (0.77 g**,** yield: 38%) as a yellowish oil. ^{1}H NMR (400 MHz, 298 K, DMSO-d_6): δ 3.33 (t, J = 6.4 Hz, 2 H), 2.40 (t, J = 7.2 Hz,

2 H), 2.31 (t, J = 7.6 Hz, 2 H), 2.20 (s, 3 H), 1.78-1.71 (m, 2 H), 1.48-1.43 (m, 2 H), 1.31-1.26 (m, 18 H), 0.88 (t, J = 6.4 Hz, 3 H). ^{13}C NMR (100 MHz, 298 K, DMSO-d_6): δ 57.91, 54.57, 49.56, 42.18, 31.87, 29.67, 29.35, 27.51, 27.26, 26.77, 22.73, 14.11. HR-ESI-MS: m/z calcd for compound **9** ($C_{16}H_{34}N_4$, $[M+H]^+$), 283.28; found, 283.13.

Compound Zwitterionic lipid: N-(3-azidopropyl)-N-methyldodecan-1-amine **9** (500 mg,1.77 mmol) dissolved in CH_3CN (15 mL), was added with 1,3-propanesultone (1.1 g, 8.85 mmol). The mixture was refluxed for 12 h. The white solid was filtered, washed with CH_3CN and dried to obtain zwitterionic lipid as a white powder (430 mg, yield: 60%). ^{1}H NMR (400 MHz, 298 K, CD_3OD): δ 3.55-3.51 (m, 4 H), 3.34-3.32 (m, 2 H), 3.08 (s, 3 H), 2.90 (t, J = 6.8 Hz, 2 H), 2.23-2.15 (m, 2 H), 2.07-2.00 (m, 2 H), 1.83-1.77 (m, 2 H), 1.48-1.31 (m, 18 H), 0.92 (t, J = 6.4 Hz, 3 H). ^{13}C NMR (100 MHz, 298 K, CD_3OD): δ 61.84, 60.08, 58.95, 48.45, 31.66, 29.33, 29.22, 29.15, 29.05, 28.81, 26.00, 22.32, 21.72, 21.68, 18.14, 13.02. HR-ESI-MS: m/z calcd for **Zwitterionic lipid** ($C_{19}H_{40}N_4O_3S$, $[M+23]^+$), 427.28; found, 427.26.

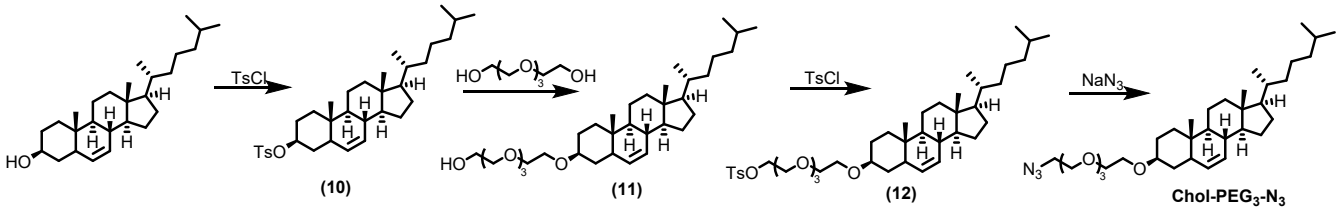

Compound 10: To a solution of cholesterol (0.52 g, 1.34 mmol) in $CHCl_3$ (6 mL) at 0°C, p-tosyl chloride (0.41 g, 2.15 mmol) and pyridine (1 mL) were added. The reaction mixture was allowed to stir for 6 h at 0°C and another 12 h at room temperature. Then, NH_4Cl (15 mL) was added and the solvents were removed in vacuo. The resulting residue was dissolved in $CHCl_3$(100 mL) and washed with water (3 × 50 mL). The organic layer was dried over Na_2SO_4, filtered and concentrated in vacuo to afford compound **10**. The mixture was recrystallized with acetone (50 mL) to get a white crystal (690 mg, yield: 85%). ^{1}H NMR (400 MHz, 298 K, $CDCl_3$): δ 7.81 (d, J = 8.0 Hz, 2 H), 7.34 (d, J = 8.0 Hz, 2 H), 5.32 (d, J = 2.0 Hz, 1 H), 4.38-4.30 (m, 1 H), 2.47 (s, 3 H), 2.31-1.06 (m, 28 H), 0.98 (s, 3 H), 0.93 (d, J = 4.0 Hz, 3 H), 0.92 (d, J = 1.6 Hz, 6 H), 0.68 (s, 3 H). ^{13}C NMR (100 MHz, 298 K, $CDCl_3$): δ 144.39, 138.87, 134.70, 129.74, 127.64, 123.53, 82.42, 56.65, 56.11, 49.92, 42.30, 39.66, 39.51, 36.36, 35.77, 31.76, 28.64, 28.02, 23.81, 22.83, 22.57, 21.65, 19.16, 18.71, 11.84.

Compound 11: Tetraethyleneglycol (971 mg, 5 mmol) and **10** (540 mg, 1 mmol) were dissolved in dioxane (50 mL) and refluxed for 48 h. The solvent was removed removed in vacuo, and the mixture were extracted with water and dichloromethane (DCM). The organic layer was collected and dried with anhydrous Na_2SO_4. The solution was filtered and concentrated in vacuo. The residue was purified by silica gel chromatography and eluated with EA/hexane (1:20) to yield compound **11** as a white oil (400 mg, yield: 76% yield). HR-ESI-MS: m/z calcd for compound **11** ($C_{35}H_{62}O_5$, $[M+23]^+$), 585.46; found, 585.57.

Compound 12: To a solution of compound **11** (281 mg, 0.5 mmol) in $CHCl_3$ (6 mL) at 0°C, p-tosyl chloride (0.15 mg, 0.8 mmol) and pyridine (0.5 mL) were added. The reaction mixture was stirred at 0 °C for 6 h and another 12 h at room temperature. The mixture was added with aqueous NH_4Cl (10 mL) and the solvents were removed in vacuo. The residue was dissolved in $CHCl_3$ (50 mL) and washed with water (3 × 25 mL). The organic layer was dried over Na_2SO_4, filtered and concentrated in vacuo to afford compound **12**. The mixture was recrystallized with acetone (50 mL) to get a white crystal (294 mg, yield: 82%).

Compound Chol-PEG$_3$-N$_3$: Compound **12** (215 mg, 0.3 mmol) was dissolved in N,N'-dimethyl-N,N'-trimethyleneurea (DMPU, 10 mL) under an argon atmosphere. Sodium azide (39 mg, 0.6 mmol) was added and the mixture was stirred at 50°C for 24 h. Et_2O (40 mL) was added and the organic phase was washed with HCl (10%, 2 × 30 mL) and brine (50 mL) and dried with Na_2SO_4.The solvents were removed under reduced pressure and crystalized from ethanol to obtain **Chol-PEG$_3$-N$_3$** as white crystalline needles (158 mg, yield: 90%). ^{1}H NMR (400 MHz, 298 K, $CDCl_3$): δ 5.35 (d, *J* = 1.6 Hz, 1 H), 3.70-3.65 (m, 14 H), 3.41 (t, *J* = 4.4 Hz, 2 H), 3.27-3.17 (m, 1 H), 2.43-1.07 (m, 28 H), 1.01 (s, 3 H), 0.92 (d, *J* = 6.4 Hz, 3 H), 0.87 (d, *J* = 6.4 Hz, 6 H), 0.69 (s, 3 H). ^{13}C NMR (100 MHz, 298 K, $CDCl_3$): δ 144.39, 138.87, 134.70, 129.74, 127.64, 123.53, 82.42, 56.65, 56.11, 49.92, 42.30, 39.66, 39.51, 36.36, 35.77, 31.76, 28.64, 28.02, 23.81, 22.83, 22.57, 21.65, 19.16, 18.71, 11.84. HR-ESI-MS: m/z calcd for compound **Chol-PEG$_3$-N$_3$** ($C_{35}H_{62}O_5$, [M+23] $^+$), 610.79; found, 611.15.

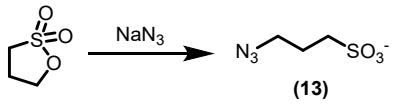

Compound 13: A solution of NaN_3 (0.65 g, 10 mmol) in H_2O (4 mL) was slowly added to a stirring solution of 1,3-propane sultone (1.22 g,10 mmol) in acetone (20 mL) at room temperature. The resulting mixture was stirred for 4 h at room temperature. The solvent was removed under vacuum and the final sodium salt was suspended in Et_2O and filtered to obtain compound **13** as a white powder. ^{1}H NMR (400 MHz, 298 K, CD_3OD): δ 3.49 (t, *J* = 6.8 Hz, 2 H), 2.89 (t, *J* = 7.2 Hz, 2 H), 2.09-2.01 (m, 2 H). ^{13}C NMR (100 MHz, 298 K, CD_3OD): δ 49.94, 48.21, 24.52.

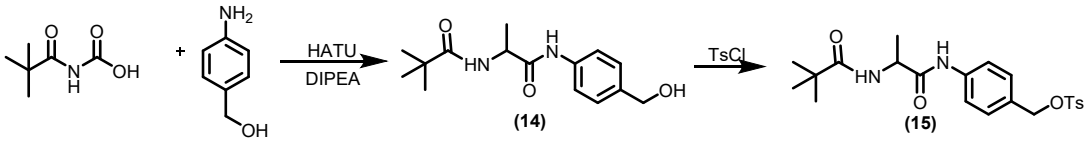

Compound 14: 4-Aminobenzyl alcohol (1.23 g, 10 mmol), (tert-butoxycarbonyl)-L-alanine (1.45 g, 10 mmol), O-(7-azabenzotriazol-1-yl)-N,N,N',N'-tetramethyluronium hexafluorophosphate (HATU, 3.8 g, 10 mmol) and N,N-diisopropylethylamine (DIPEA, 2.59 g, 10 mmol) were dissolved in anhydrous THF (15 mL). The mixture was stirred at 0°C under nitrogen for 10 min and at room temperature overnight. The solvent was removed under vacuum and the dark crude product was purified by silica gel column chromatography using PE/EA (2:1, v/v) as the eluent to obtain compound **14** as a white yellow solid (2.28 g, yield: 82%). ^{1}H NMR (400 MHz, 298 K, $CDCl_3$): δ 8.90 (s, 1 H), 7.42 (d, *J* = 8.4 Hz, 2 H), 7.18 (d, *J* = 8.0 Hz, 2 H), 5.40 (s, 1 H), 4.59 (s, 2 H), 4.40 (s, 1 H), 1.47 (s, 9 H), 1.44 (d, *J* = 7.2 Hz, 3 H). ^{13}C NMR (100 MHz, 298 K, $CDCl_3$): δ 171.11, 137.11, 136.41, 127.56, 119.76, 115.19, 64.83, 50.57, 38.71, 28.44, 17.77. HR-ESI-MS: m/z calcd for compound **14** ($C_{15}H_{22}N_2O_3$, [M+39] $^+$), 317.16; found, 317.04.

Compound 15: Triethylamine (0.5 mL) was slowly added to compound **14** (2 g, 7.2 mmol) and 4-toluene sulfonyl chloride (1.64 g,8.64 mmol) in anhydrous DCM (15 mL). The mixture was stirred at 0°C for 3 h under nitrogen. The solvent was removed at vacuum and the crude product was purified by silica gel column chromatography using DCM as an eluent to obtain compound **15** (0.68 g, yield:22%) as a white solid, which was directly used in next step.

Compound PYCI-a: Compound **3** (291 mg, 1 mmol) and compound **6** (300 mg,1 mmol) were dissolved in a mixture of acetic anhydride (25 mL) and acetic acid (25 mL), trimethoxymethane (106 mg, 1 mmol) and pyridine (85 mg, 1 mmol) were added. Then the mixture was stirred at 140°C for 30

min. The solvent was removed under reduced pressure. The crude product was dissolved in a mixture of acetone (10 mL) and HCl (10 mL, 2 M) and refluxed for 2 h. The mixture was neutralized by $NaHCO_3$, and the crude product was purified by silica gel column chromatography using CH_2Cl_2/MeOH (5 to 10% of MeOH) as an eluent to obtain compound **PYAI-a** as a dark bule solid (120 mg, yield: 20%). ^{1}H NMR (400 MHz, 298 K, CD_3OD): δ 7.44 (t, *J* = 13.2 Hz, 1 H), 7.19 (d, *J* = 8.0 Hz, 3 H), 6.89 (d, *J* = 8.4 Hz, 1 H), 6.85 (s, 1 H), 6.61 (s, 1 H), 6.48 (s, 1 H), 6.38 (d, *J* = 8.8 Hz, 2 H), 6.24 (d, *J* = 13.6 Hz, 1 H), 6.19 (d, *J* = 2.0 Hz, 1 H), 6.13 (d, *J* = 8.0 Hz, 1 H), 6.03 (d, *J* = 2.0 Hz, 1 H), 4.04 (d, *J* = 2.0 Hz, 2 H), 1.92 (t, *J* = 2.0 Hz, 1 H), 1.63 (d, *J* = 6.4 Hz, 2 H), 1.47 (d, *J* = 2.0 Hz, 1 H), 1.28-1.21 (m, 2 H), 0.96 (s, 6 H), 0.45 (d, *J* = 13.2 Hz, 2 H). ^{13}C NMR (100 MHz, 298 K, CD_3OD): δ 174.01, 169.95, 160.80, 159.50, 157.94, 150.63, 143.88, 142.40, 142.34, 137.53, 131.18, 128.25, 126.41, 124.20, 122.30, 115.67, 114.21, 112.50, 111.54, 103.91, 101.89, 99.84, 86.94, 82.59, 76.48, 70.38, 56.00, 49.43, 48.32, 48.15, 42.51, 28.69, 25.64, 15.97. HR-ESI-MS: m/z calcd for compound **PYCI-a** ($C_{36}H_{31}INO_3$, $[M]^+$), 652.13; found, 652.33.

Compound PYCI-b: **Compound PYCI-b**, prepared similarly as **Compound PYCI-a** using compound **3** (291 mg, 1 mmol) and compound **7** (352 mg,1 mmol), was obtained as a dark bule solid (138 mg, yield: 23%). ^{1}H NMR (400 MHz, $CDCl_3$): δ 7.40 (t, *J* = 13.2 Hz, 1 H), 7.26 (d, *J* = 8.8 Hz, 2 H), 7.17 (d, *J* = 9.6 Hz, 1 H), 6.92 (d, *J* = 8.0 Hz, 1 H), 6.86 (s, 1 H), 6.67 (s, 1 H), 6.48 (t, *J* = 4.4 Hz, 3 H), 6.22-6.15 (m, 2 H), 6.05 (d, *J* = 8.4 Hz, 1 H), 5.98 (d, *J* = 2.0 Hz, 1 H), 5.29 (d, *J* = 12.8 Hz, 1 H), 4.12 (d, *J* = 2.0 Hz, 2 H), 2.72 (s, 3 H), 1.98 (d, *J* = 2.0 Hz, 1 H), 1.01 (s, 6 H), 0.45 (d, *J* = 13.2 Hz, 2 H). ^{13}C NMR (100 MHz, $CDCl_3$): δ 164.44, 163.25, 154.18, 149.68, 147.28, 145.68, 141.11, 141.02, 134.73, 131.85, 129.75, 128.78, 128.33, 119.49, 118.07, 117.93, 115.96, 114.50, 107.89, 103.82, 103.11, 81.56, 81.34, 80.37, 59.85, 51.62, 32.51. HR-ESI-MS: m/z calcd for compound **PYCI-b** ($C_{32}H_{27}INO_3$, $[M+H]^+$), 601.10; found, 601.53.

Compound PYCI1: **PYCI-b** (60 mg, 0.1 mmol), compound **Chol-PEG$_3$-N$_3$** (45 mg, 0.1 mmol), coppersulfatepentahydrate (30 mg, 0.1 mmol) and sodiumascorbate (19.8 mg, 0.1 mmol) were dissolved in dry DMF (10 mL). The mixture was stirred at room temperature for 8 h under nitrogen. The solvent was removed under vacuum and the crude product was purified by silica gel column chromatography using CH_2Cl_2/MeOH (5 to 30% of MeOH) as an eluent to obtain compound **PYCI1** as a dark bule solid (32 mg, yield: 27%). ^{1}H NMR (400 MHz, CD_3OD/ $CDCl_3$): δ 8.16 (t, *J* = 13.2 Hz, 1 H), 7.89 (d, *J* = 9.2 Hz, 2 H), 7.83 (d, *J* = 9.2 Hz, 1 H), 7.55 (d, *J* = 8.4 Hz, 1 H), 7.49 (s, 1 H), 7.27 (d, *J* = 8.8 Hz, 1 H), 7.05 (t, *J* = 8.8 Hz, 2 H), 6.95-6.90 (m, 2 H), 6.79 (s, 1 H), 6.75 (d, *J* = 8.4 Hz, 1 H), 6.27 (d, *J* = 13.2 Hz, 1 H), 5.71 (d, *J* = 12.8 Hz, 1 H), 4.40 (t, *J* = 4.4 Hz, 1 H), 3.71 (t, *J* = 4.4 Hz, 1 H), 3.44-3.42 (m, 10 H), 3.22 (s, 2 H), 3.18 (s, 3 H), 2.98-2.92 (m, 3 H), 2.84-2.78 (m, 1 H), 2.16-1.22 (m, 28 H), 1.17 (s, 6 H), 0.77(s, 3 H), 0.71-0.66 (m, 9 H), 0.46 (s, 3 H) . ^{13}C NMR (100 MHz, CD_3OD/ $CDCl_3$): δ 174.45, 170.26, 163.31, 148.72, 140.50, 138.30, 137.64, 137.05, 131.23, 128.53, 128.49, 124.22, 123.95, 121.59, 120.01, 114.69, 100.46, 99.99, 79.58, 70.63, 70.39, 70.36, 69.88, 67.09, 56.73, 56.12, 50.50, 50.20, 42.20, 39.73, 39.39, 38.84, 37.09, 36.68, 36.06, 35.72, 31.84, 31.78, 28.14, 28.07, 27.84, 24.09, 23.66, 23.02, 22.29, 22.04, 20.93, 20.37, 18.93, 18.30, 11.44. HR-ESI-MS: m/z calcd for compound **PYCI1** ($C_{67}H_{88}IN_4O_7$, $[M]^+$), 1187.57; found, 1187.52.

Compound PYCI2: **PYCI2**, prepared similarly as **PYCI1** using **PYCI-a** (65 mg, 0.1 mmol) and compound **Chol-PEG$_3$-N$_3$** (90 mg, 0.2 mmol), was obtained as a dark bule solid (34 mg, yield: 19%). ^{1}H NMR (400 MHz, CD_3OD/ $CDCl_3$): δ 7.85 (t, *J* = 12.8 Hz, 1 H), 7.72 (s, 1 H), 7.67 (d, *J* = 8.4 Hz, 2 H), 7.39 (s, 1 H), 7.28 (d, *J* = 4.8 Hz, 1 H), 7.09 (d, *J* = 4.4 Hz, 1 H), 6.93 (t, *J* = 4.0 Hz, 1 H), 6.9 (d, *J* = 8.4 Hz, 2 H), 6.67-6.60 (m, 2 H), 6.49 (d, *J* = 4.0 Hz, 1 H), 6.44 (s, 1 H), 5.84 (d, *J* = 12.4 Hz, 1 H), 4.98 (s, 2 H), 4.29-4.23 (m, 4 H), 3.91-3.86 (m, 10 H), 3.68 (t, *J* = 6.8 Hz, 2 H), 3.60-3.55 (m, 4 H), 2.31-3.28 (m, 20 H), 2.86-2.80 (m, 2 H), 2.56 (t, *J* = 6.8 Hz, 2 H), 2.01-0.65 (m, 62 H), 0.63 (s, 3 H), 0.56 (d, *J* = 6.0 Hz, 6 H), 0.52 (d, *J* = 6.4 Hz, 12 H), 0.32 (s, 3 H) . ^{13}C NMR (100 MHz, CD_3OD/

$CDCl_3$): δ 167.74, 161.53, 159.45, 158.48, 154.91, 142.85, 140.56, 137.44, 128.28, 124.90, 124.04, 122.97, 121.73, 121.69, 115.55, 114.08, 112.16, 111.26, 104.03, 99.32, 79.58, 70.71, 70.44, 70.32, 69.31, 69.18, 67.11, 61.75, 56.68, 56.10, 50.43, 50.24, 50.11, 42.23, 39.69, 39.44, 38.91, 37.09, 36.75, 36.11, 35.72, 31.81, 29.59, 28.68, 28.20, 28.14, 27.92, 26.03, 24.19, 23.76, 22.64, 22.47, 22.38, 20.98, 19.21, 18.57, 11.71. HR-ESI-MS: m/z calcd for compound **PYCI2** ($C_{106}H_{153}IN_7O_{11}$, $[M]^+$), 1828.07; found, 1827.94.

Compound PYCI3: **PYCI3**, prepared similarly as **PYCI1** using **PYCI-b** (60 mg, 0.1 mmol) and compound **zwitterionic lipid** (40 mg, 0.1 mmol), was obtained as a dark bule solid (17 mg, yield: 16%). ^{1}H NMR (400 MHz, CD_3OD/ $CDCl_3$): δ 7.74 (t, *J* = 13.2 Hz, 1 H), 7.50 (d, *J* = 8.0 Hz, 2 H), 7.42 (d, *J* = 9.2 Hz, 1 H), 7.15 (d, *J* = 12.4 Hz, 1 H), 7.04 (s, 1 H), 6.82 (s, 1 H), 6.68 (t, *J* = 8.0 Hz, 2 H), 6.48 (d, *J* = 13.6 Hz, 1 H), 6.41-6.36 (m, 2 H), 6.23 (s, 1 H), 5.59 (d, *J* = 2.0 Hz, 1 H), 5.29 (d, *J* = 12.4 Hz, 1 H), 4.35 (s, 2 H), 3.05-3.03 (m, 4 H), 3 .00 (s, 3 H), 2.85-2.80 (m, 4 H), 2.77-2.71 (m, 2 H), 2.55 (s, 3 H), 2.42-2.32 (m, 2 H), 1.73-1.60 (m, 2 H), 1.57-1.41 (m, 2 H), 1.35 (s, 6 H), 0.88-0.77 (m, 18 H), 0.38 (t, *J* = 5.2 Hz, 3 H). ^{13}C NMR (100 MHz, CD_3OD/ $CDCl_3$): δ168.95, 160.77, 159.37, 158.50, 150.74, 143.36, 143.17, 142.24, 137.35, 130.99, 128.16, 126.10, 124.31, 123.46, 115.53, 113.84, 111.86, 111.18, 104.01, 101.06, 99.60, 86.21, 76.44, 62.21, 60.43, 58.98, 55.90, 49.31, 49.09, 47.90, 47.81, 46.97, 31.78, 29.47, 29.35, 29.31, 29.19, 29.00, 28.33, 26.31, 22.52, 21.97, 21.87, 18.28, 13.48. HR-ESI-MS: m/z calcd for compound PYCI3 ($C_{51}H_{67}IN_5O_6S$, $[M+H]^+$), 1006.39; found, 1006.55.

Compound PYCI4: **PYCI4**, prepared similarly as **PYCI1** using **PYCI-a** (60 mg, 0.1 mmol) and compound **zwitterionic lipid** (80 mg, 0.2 mmol), was obtained as a dark bule solid (16 mg, yield: 11%). ^{1}H NMR (400 MHz, CD_3OD/ $CDCl_3$): δ 7.89 (t, *J* = 13.2 Hz, 1 H), 7.78 (s, 1 H), 7.60 (d, *J* = 8.8 Hz, 1 H), 7.48 (s, 1 H), 7.18 (d, *J* = 8.4 Hz, 1 H), 7.03 (s, 1 H), 6.93 (t, *J* = 6.0 Hz, 1 H), 6.87 (s, 1 H), 6.73 (t, *J* = 9.6 Hz, 2 H), 6.62 (d, *J* = 8.4 Hz, 1 H), 6.53 (d, *J* = 8.0 Hz, 1 H), 6.46-6.42 (m, 1 H), 6.26 (s, 1 H), 5.89 (d, *J* = 12.4 Hz, 1 H), 4.82 (s, 2 H), 4.07 (d, *J* = 8.4 Hz, 4 H), 3.01 (t, *J* = 13.2 Hz, 2 H), 2.88-2.85 (m, 2H), 2.84-2.78 (m, 10 H), 2.52 (d, *J* = 13.2 Hz, 4 H), 2.44-2.26 (m, 4 H), 2.00-1.88 (m, 2 H), 1.69 (t, *J* = 7.6 Hz, 2 H), 1.59-1.50 2.44-2.26 (m, 4 H), 1.43-1.40 (m, 4 H), 1.30-1.25 (m, 2 H), 1.17-1.01 (m, 4 H), 0.93-0.85 (m, 4 H), 0.82 (s, 6 H), 0.80-0.72 (m, 36 H), 0.40-0.34 (m, 6 H). ^{13}C NMR (100 MHz, CD_3OD/ $CDCl_3$): δ 170.27, 163.42, 148.74, 138.26, 137.82, 137.06, 131.34, 128.60, 126.32, 126.32, 126.42, 120.07, 117.48, 114.81, 112.80, 103.28, 100.77, 99.96, 98.96, 89.13, 62.18, 60.42, 58.98, 55.39, 49.02, 46.99, 31.77, 29.45, 29.34, 29.30, 29.18, 28.98, 27.88, 26.20, 24.03, 23.21, 22.50, 21.99, 21.86, 20.50, 18.27, 13.66. HR-ESI-MS: m/z calcd for compound **PYCI4** ($C_{74}H_{111}IN_9O_9S_2$, $[M]^+$), 1460.70; found, 1460.64.

Compound aPYCI: Compound **PYCI-b** (60 mg, 0.1 mmol) and compound **13** (16.5 mg, 0.1 mmol), coppersulfatepentahydrate (30 mg, 0.1 mmol) and sodiumascorbate (19.8 mg, 0.1 mmol) were dissolved in dry DMF (10 mL). The mixture was stirred at room temperature for 8 h under nitrogen. The solvent was removed under vacuum and the crude product was purified by silica gel column chromatography using CH_2Cl_2/MeOH (5 to 10% of MeOH) as an eluent to obtain compound **PYCI-c** as a dark blue solid. Compound **PYCI-c** (76.4 mg, 0.1 mmol), compound **15** (43.2 mg, 0.1 mmol), potassium carbonate (63 mg, 0.5 mmol) and sodium iodide (15 mg, 0.1 mmol) were dissolved in DMF (20 mL). The mixture was stirred at 80 °C for 5 h. The solvent was removed by vacuum and the crude product was purified by silica gel column chromatography using DCM/MeOH=8/1 as an eluent to obtain Boc-aPYCI as a dark blue solid (Yield: 77%).

Boc-aPYCI (50.2 mg, 0.05 mmol) dissolved in anhydrous DCM (10 mL) was slowly added with trifluoroacetic acid (1 mL) in dry DCM (1 mL) at 0°C. The resulting mixture was stirred at room temperature for another 1 h. The solvent was removed under reduced pressure and the crude product was purified by silica gel column chromatography using DCM/MeOH=5/1 as an eluent to obtain

aPYCI as a dark blue solid with metallic sheen (27.2 mg, Yield: 68%). ^{1}H NMR (400 MHz, CD_3OD/ $CDCl_3$): δ 7.85 (t, *J* = 13.2 Hz, 1 H), 7.62 (d, *J* = 8.4 Hz, 2 H), 7.51 (d, *J* = 9.2 Hz, 1 H), 7.25 (s, 2 H), 7.17 (d, *J* = 8.4 Hz, 2 H), 6.92 (t, *J* = 8.4 Hz, 3 H), 6.76 (d, *J* = 8.4 Hz, 2 H), 6.56 (d, *J* = 13.6 Hz, 1 H), 6.50-6.46 (m, 2 H), 6.30 (s, 1 H), 5.73 (d, *J* = 12.8 Hz, 1 H), 4.44 (s, 2 H), 4.18 (s, 2 H), 3.10 (s, 3 H), 3.06 (t, *J* = 13.2 Hz, 2 H), 2.97-2.93 (m, 2 H), 2.75-2.70 (m, 2 H), 2.52-2.47 (m, 3H), 1.70-1.62 (m, 2 H), 1.34 (s, 6 H), 0.46 (d, *J* = 8.0 Hz, 3 H). ^{13}C NMR (100 MHz, CD_3OD/ $CDCl_3$): δ 169.23, 160.79, 159.28, 158.39, 150.80, 143.73, 143.18, 142.37, 137.31, 136.97, 130.95, 128.12, 127.45, 126.10, 124.28, 119.91, 115.51, 113.77, 111.71, 111.29, 103.92, 101.26, 99.62, 86.22, 77.66, 76.41, 63.71, 55.82, 50.12, 48.35, 46.42, 31.08, 30.99, 29.95, 29.79, 29.51, 29.19, 28.10, 24.60, 22.49, 19.57, 13.61, 8.46. HR-ESI-MS: m/z calcd for compound a**PYCI** ($C_{45}H_{45}IN_6O_7S$, $[M+23]^+$), 964.21; found, 964.77.

Compound aPYCI4: **aPYCI4**, prepared similarly as **aPYCI** using **PYCI4** (74.4 mg, 0.05 mmol), compound **15** (21.6 mg, 0.05 mmol) potassium carbonate (31.5 mg, 0.25 mmol) and sodium iodide (7.5 mg, 0.05 mmol), was obtained as a dark bule solid (21.6 mg, Yield: 52%). ^{1}H NMR (400 MHz, CD_3OD/ $CDCl_3$): δ 7.83 (t, *J* = 13.2 Hz, 1 H), 7.59 (d, *J* = 8.4 Hz, 2 H), 7.49 (d, *J* = 9.2 Hz, 1 H), 7.25 (s, 2 H), 7.19 (s, 1 H), 7.16 (d, *J* = 8.0 Hz, 1 H), 7.03 (t, *J* = 8.0 Hz, 3 H), 6.99-6.90 (m, 1 H), 6.81 (d, *J* = 8.4 Hz, 3 H), 6.67 (d, *J* = 8.4 Hz, 1 H), 6.54-6.46 (m, 1 H), 6.37 (d, *J* = 9.6 Hz, 1 H), 6.18 (s, 1 H), 5.79 (d, *J* = 12.8 Hz, 1 H), 5.63-5.60 (m, 1 H), 4.05 (s, 2 H), 3.91-3.86 (m, 1 H), 3.24 (t, *J* = 7.2 Hz, 2 H), 3.05-2.94 (m, 8 H), 2.86-2.74 (m, 12 H), 2.65-2.59 (m, 4 H), 2.53 (s, 3 H), 2.37 (t, *J* = 6.4 Hz, 4 H), 1.70-1.61 (m, 4 H), 1.50-1.47 (m, 4 H), 1.24 (s, 6 H), 0.92 (d, *J* = 4.4 Hz, 3 H), 0.86-0.84 (m, 4 H), 0.82-0.76 (m, 36 H), 0.37 (t, *J* = 4.8 Hz, 6 H. ^{13}C NMR (100 MHz, CD_3OD/ $CDCl_3$): δ 170.26, 148.70, 140.49, 138.32, 137.05, 128.50, 124.22, 123.92, 121.54, 119.98, 114.66, 79.57, 70.61, 70.37, 70.33, 69.86, 67.08, 56.74, 56.12, 50.48, 42.18, 39.74, 39.38, 38.83, 37.08, 36.66, 36.05, 35.72, 31.84, 31.76, 29.41, 28.12, 28.05, 27.82, 24.06, 23.64, 22.92, 22.45, 22.22, 21.97, 18.86, 18.24, 11.37. HR-ESI-MS: m/z calcd for compound a**PYCI4** ($C_{84}H_{123}IN_{11}O_{10}S_2$, $[M]^+$), 1636.79; found, 1636.81.

2. Additional Figures

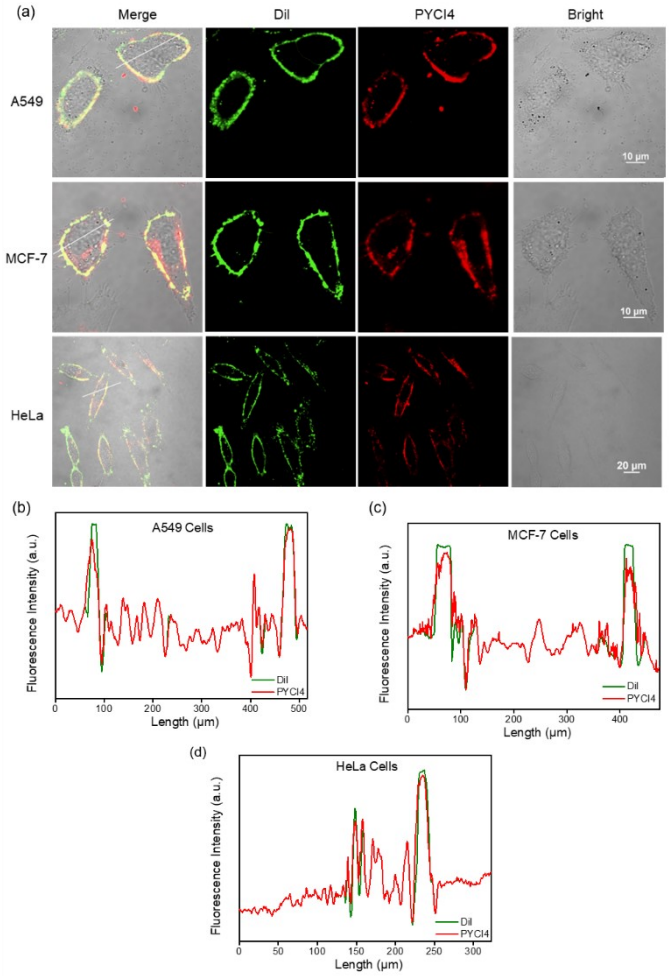

Fig. S1 (a) CLSM images of different cells incubated with **PYCI4** (2.5 μM) for 30 min and membrane tracker Dil (2 μg/mL) for 15 min. Red fluorescence (PYCI4: Ex: 640 nm, Em: 650-700 nm); green fluorescence (Dil: Ex=488 nm, Em=500-550 nm). (b), (c), (d) Fluorescence intensities profiles for Dil (green) and **PYCI4** (red) along the white dotted lines in the merged images.

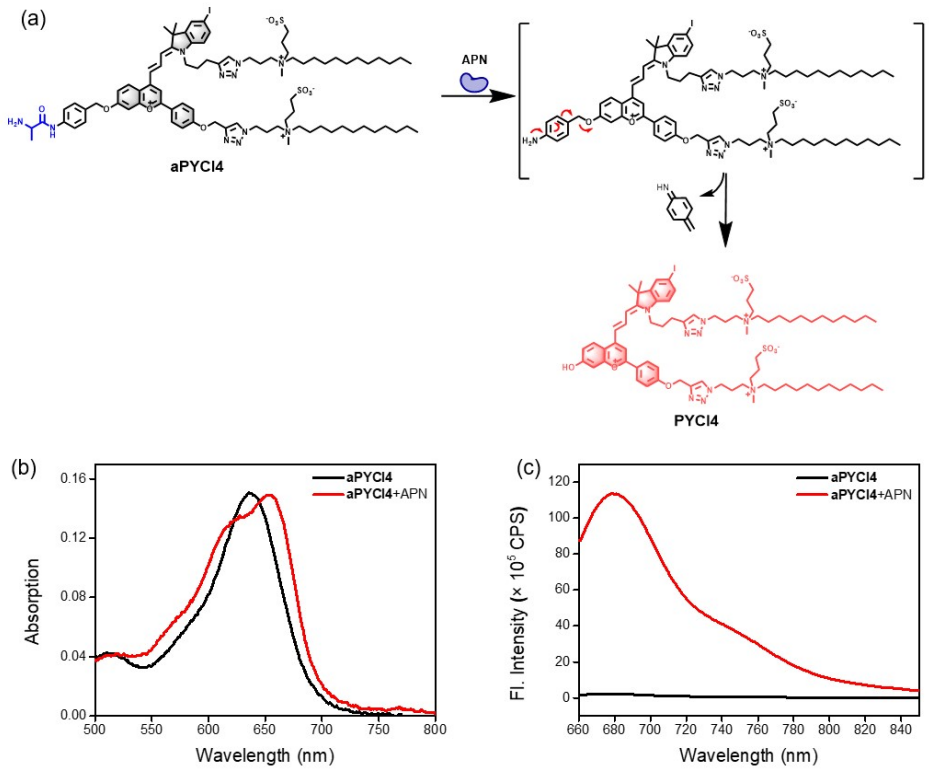

Fig. S2 (a) Schematic illustration of the reaction mechanism for APN-catalyzed activation of **aPYCI4**. (b) Absorption spectra of **aPYCI4** (2.5 μM) in the absence or presence of APN (100 ng/mL) in PBS at 37 °C for 1 h. (c) Fluorescence spectra of **aPYCI4** (2.5 μM) in the absence or presence of APN (100 ng/mL) in PBS at 37 °C for 1 h.

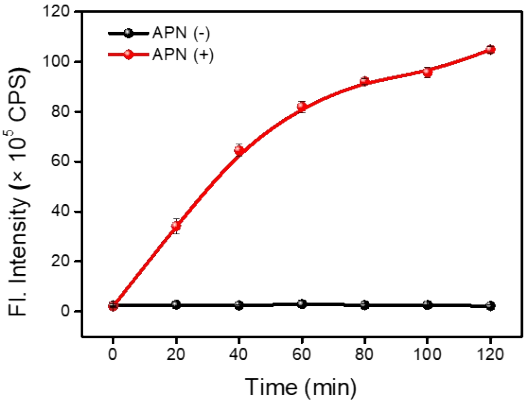

Fig. S3 Time-dependent fluorescence intensities at 680 nm for **aPYCI4** (2.5 μM) treated with or without APN (100 ng/mL). Data are presented as mean ± SD from three independent experiments.

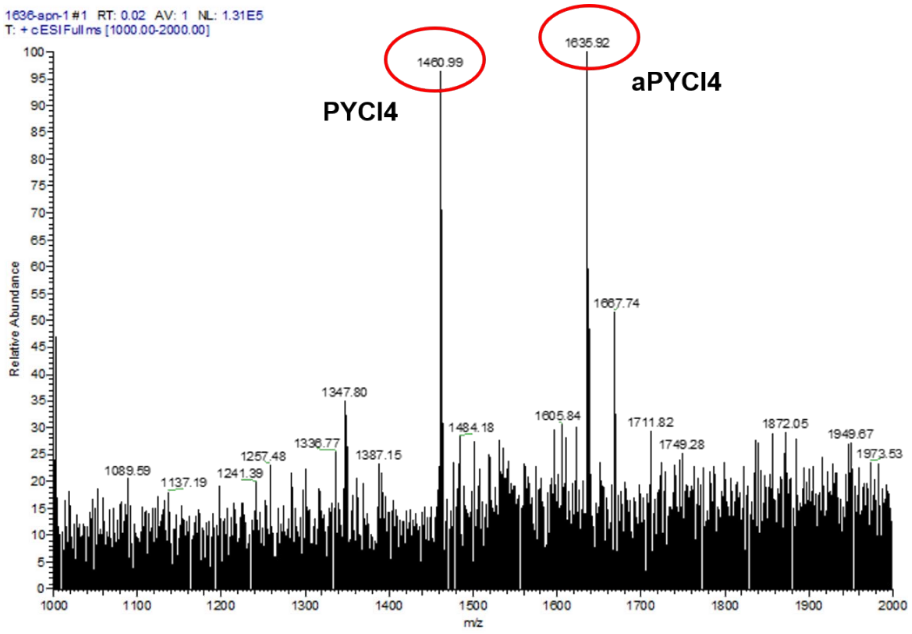

Fig. S4 HR-ESI MS analysis of the reaction products of APN-catalyzed **aPYCI4**.

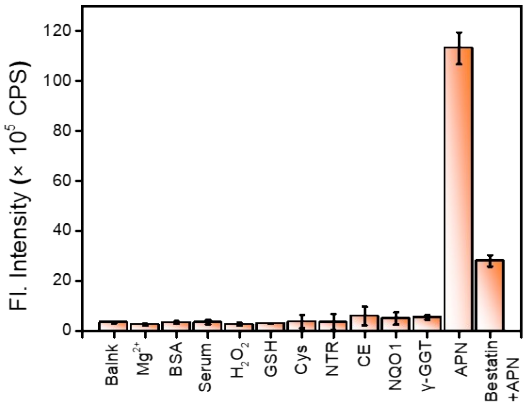

Fig. S5 Fluorescence intensities at 680 nm for **aPYCI4** (2.5 μM) in the prescence of Mg^{2+} (100 μM), BSA (100 ng/mL), serum (20%), H_2O_2 (100 μM), GSH (5 mM), Cys (100 μM), nitroreductase (NTR, 100 ng/mL), carboxylesterases, (CE, 100 ng/mL), NAD(P)H quinone dehydrogenase 1 (NQO1, 100 ng/mL), gamma-glutamyl transferase (γ-GGT, 100 ng/mL) and APN (100 ng/mL) pretreated with bestatin (100 μM) in aqueous solution (PBS/DMSO =1 : 9, v/v, 10 mM, pH = 7.4). Data are presented as mean ± SD from three independent experiments.

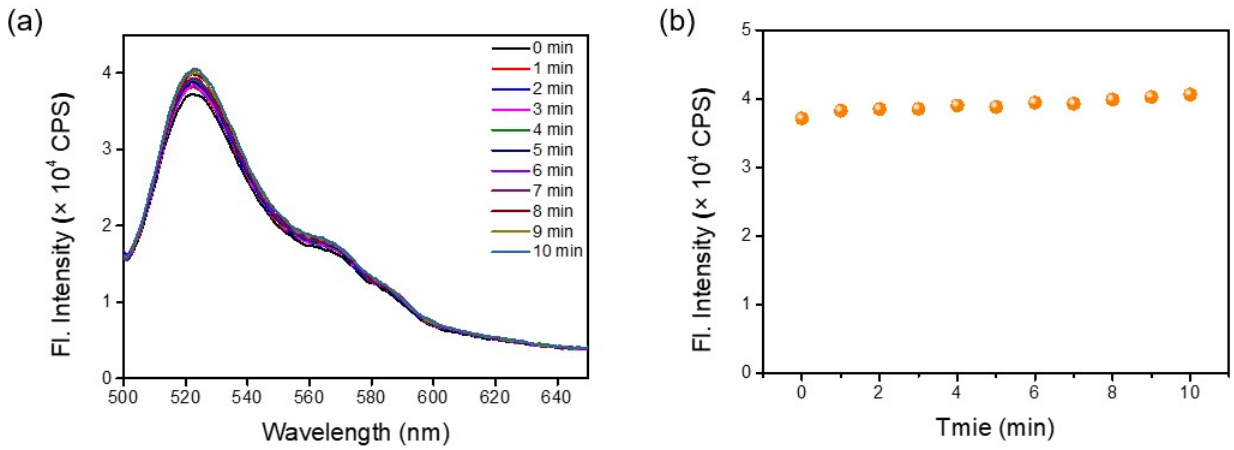

Fig. S6 Fluorescence spectra (a) and fluorescence intensities at 525 nm (b) for DCFH-DA in the prescencce of **aPYCI4** (2.5 μM) irradiated with a 640 nm laser for different time periods.

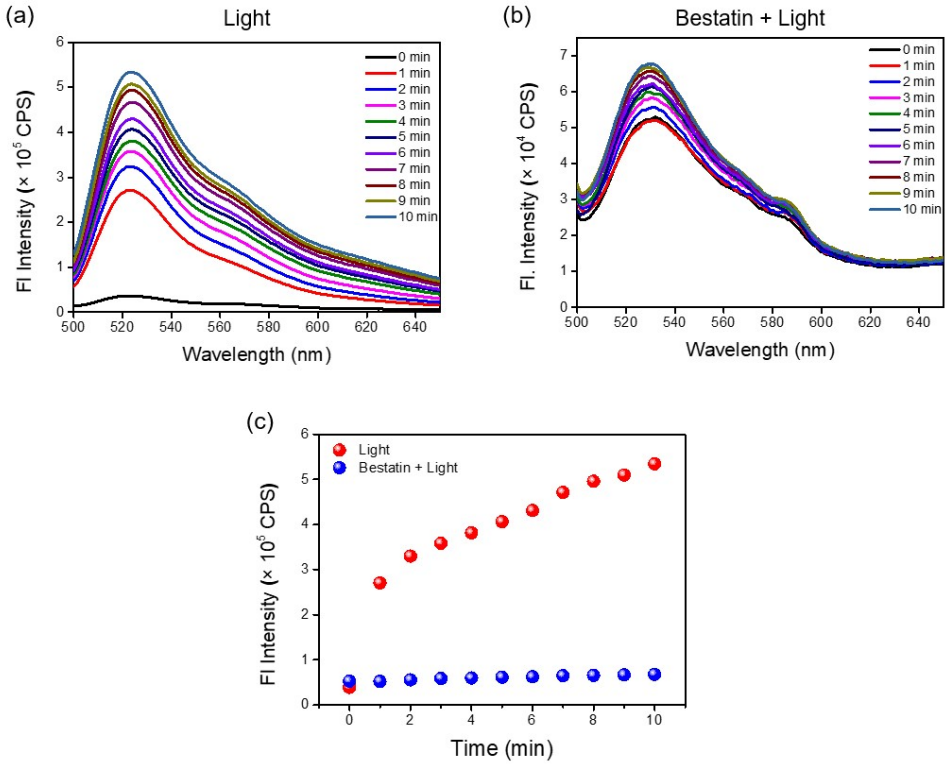

Fig. S7 Fluorescence spectra of DCFH-DA in the prescence of **aPYCI4** (2.5 μM) treated with APN (100 ng/mL) (a) or APN (100 ng/mL) and bestatin (100 μM) (b) at 37 °C for 1 h and irradiated with a 640 nm laser for 0 - 10 min. (c) Fluorescence intensities for DCFH-DA at 525 nm after different treatments in (a) and (b).

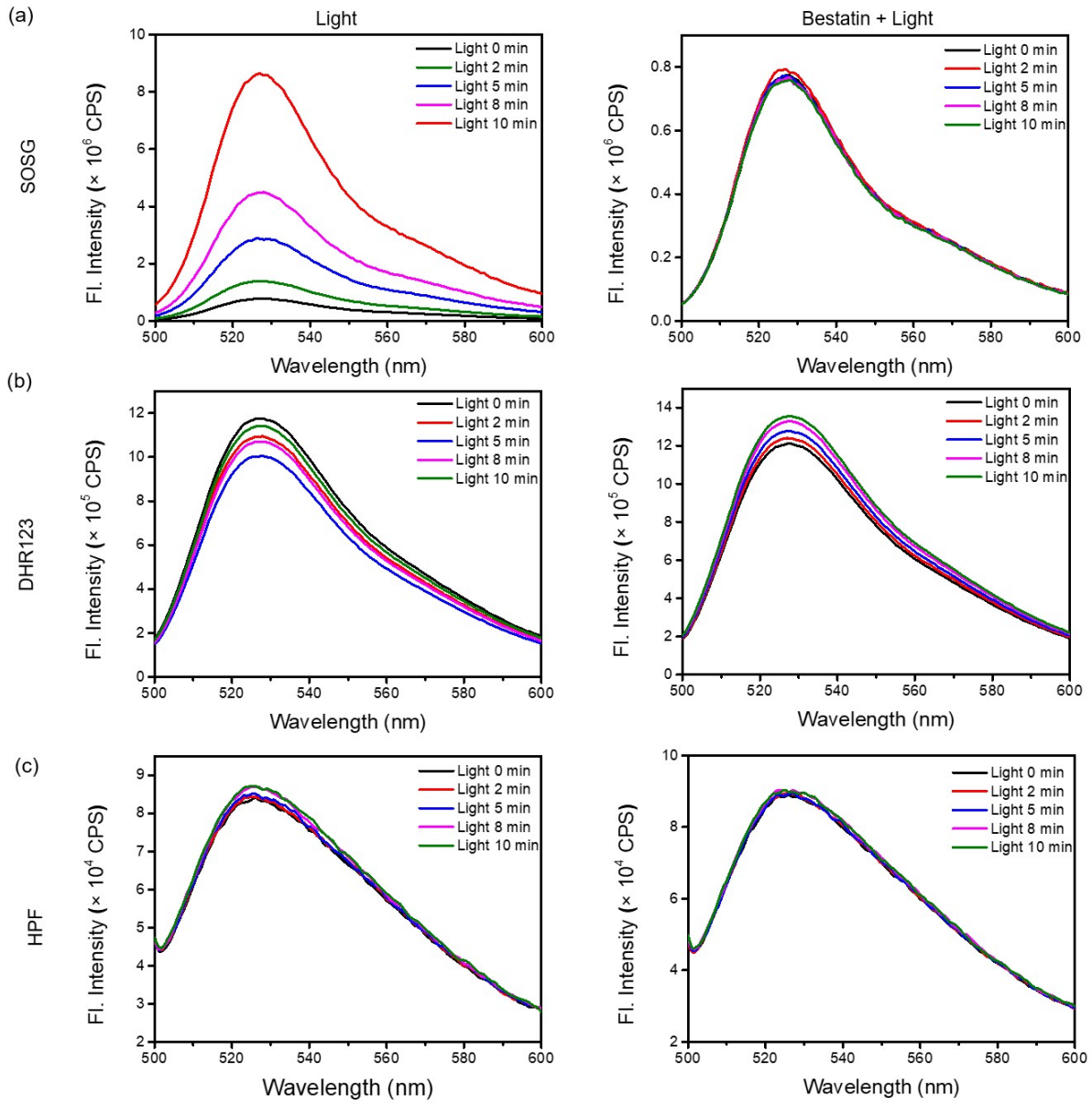

Fig. S8 Fluorescence spectra for SOSG (a), DHR123 (b) and HPF (c) in the prescence of **aPYCI4** (2.5 μM) treated with APN (100 ng/mL) or APN (100 ng/mL) and bestatin (100 μM) at 37 °C for 1 h and irradiated with a 640 nm laser for 0 - 10 min.

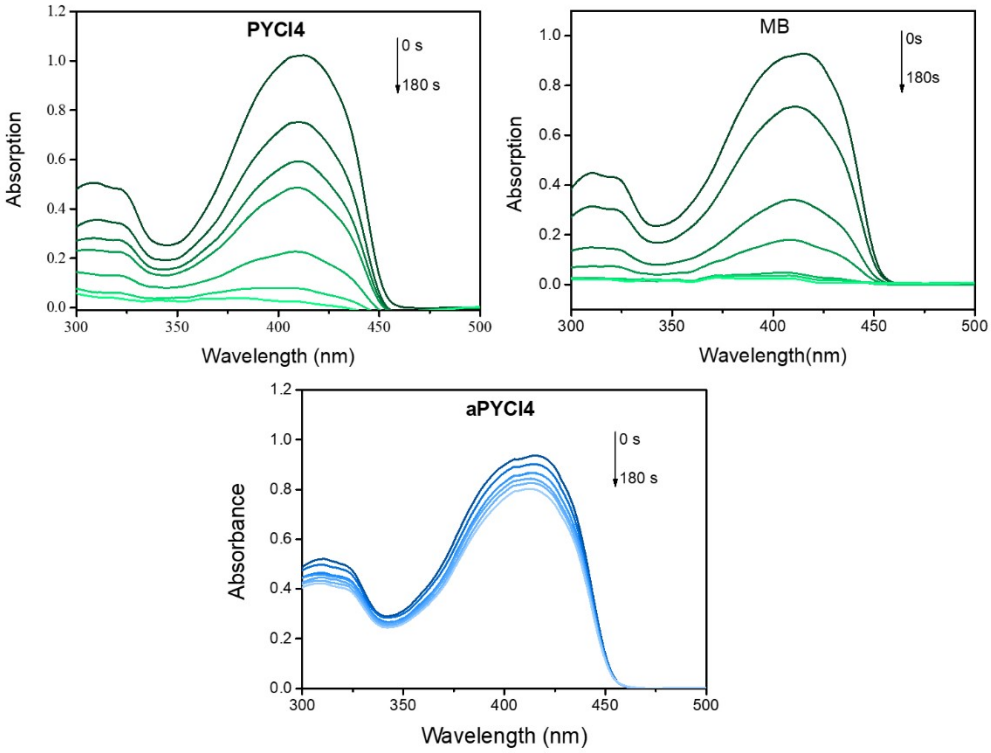

Fig. S9 Absorptions spectra of DPBF in the presence of **PYCI4**, MB and **aPYCI4** irradiated with a 640 nm laser for different times (0, 30, 60, 90, 120, 150, 180 s).

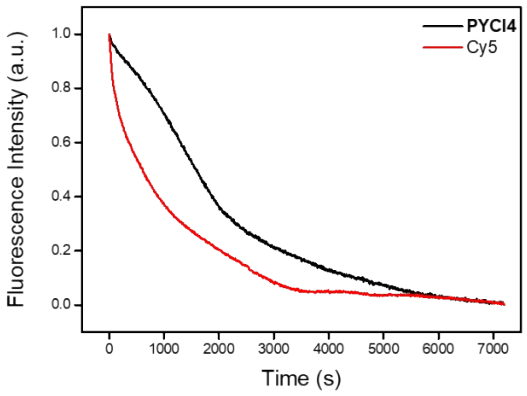

Fig. S10 Time-dependent fluorescence intensities for **PYCI4** and Cy5 after irradiation for different times. Fluorescence intensities at 680 nm and 670 nm were recorded and normalized for **PYCI4** and Cy5, respectively.

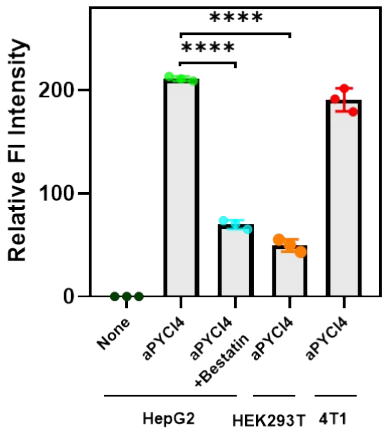

Fig. S11 Quantitative analysis of **aPYCI4** fluorescence intensities for cells under different treatments in Fig. 1h in the maintext. Data are presented as mean ± SD from three independent experiments. Statistical comparison was performed by two-tailed t-test, ****p < 0.0001.

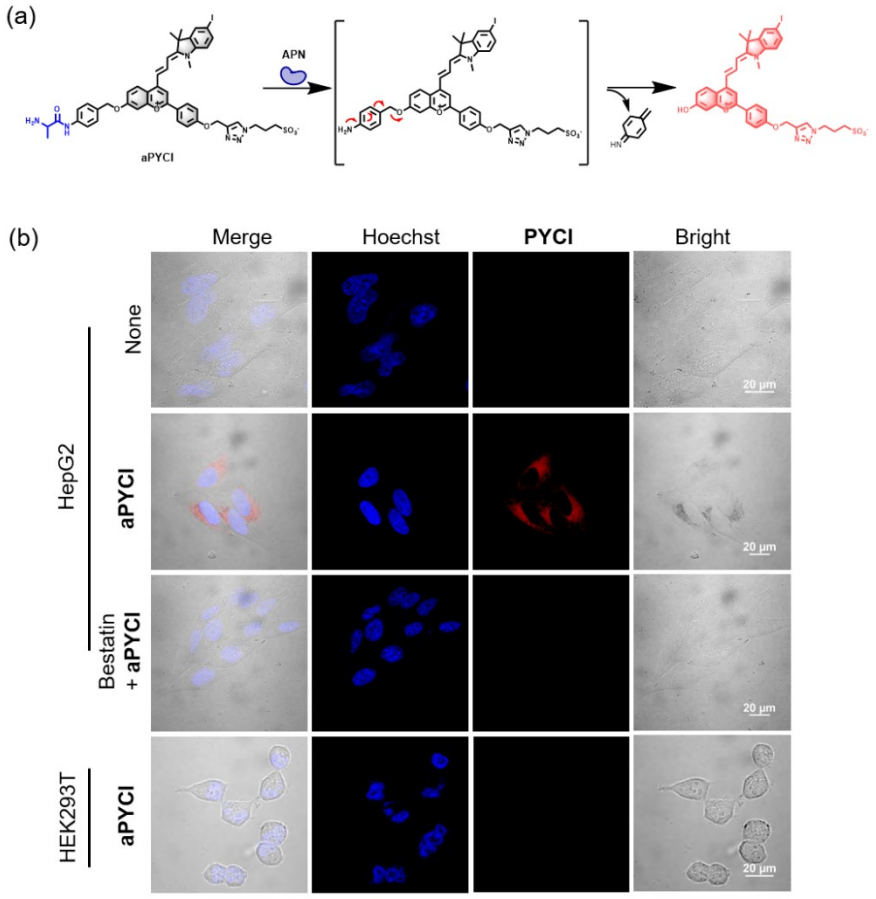

Fig. S12 (a) Schematic illustration of the reaction mechanism for APN-catalyzed activation of **aPYCI**. (b)CLSM images of HepG2 and HEK293T cells under different treatments. Red fluorescence (**aPYCI**,

Ex: 640 nm, Em: 650–700 nm); blue fluorescence (Hoechst 33342: Ex: 405 nm, Em: 430–470 nm). Scale bar: 20 μm.

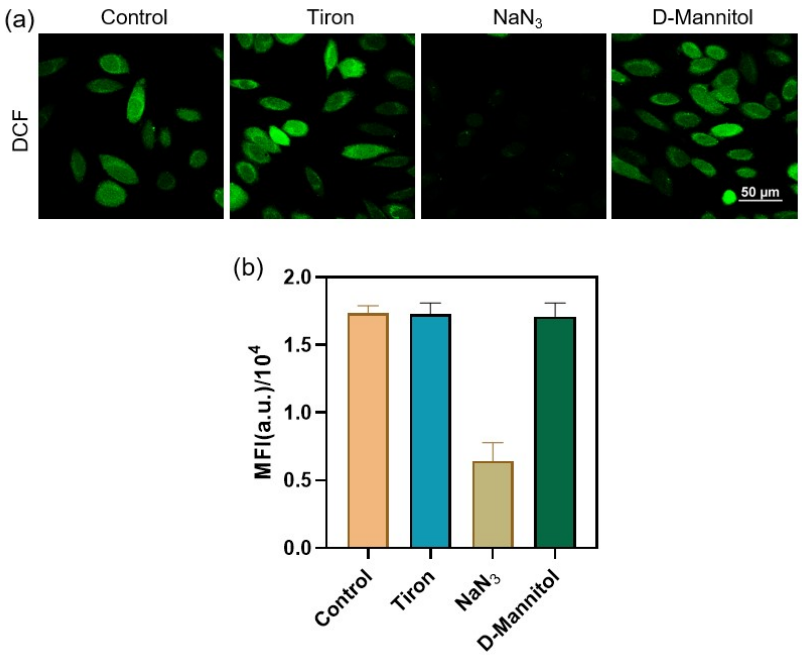

Fig. S13 CLSM images (a) and flow cytometry anlysis (b) for HepG2 cells preincubated with DCFH-DA and different ROS scavengers, treated with **aPYCI4** (2.5 μM) and irradiated with a 640 nm laser (DCF: Ex: 488 nm, Em: 500–550 nm). Data are presented as mean ± SD from three independent experiments. Scale bar: 50 μm.

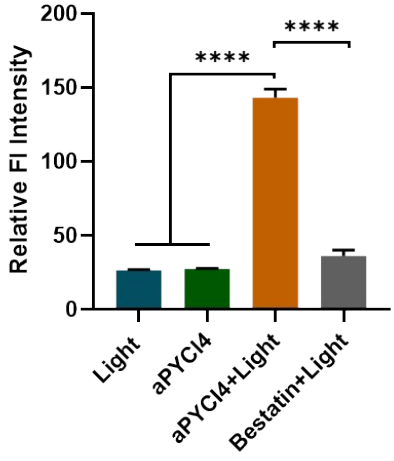

Fig. S14. Quantitative analysis of SOSG fluorescence intensities for cells under different treatments in Fig. 2e in the maintext. Statistical comparison was performed by two-tailed t-test (****$p < 0.0001$, $n = 3$).

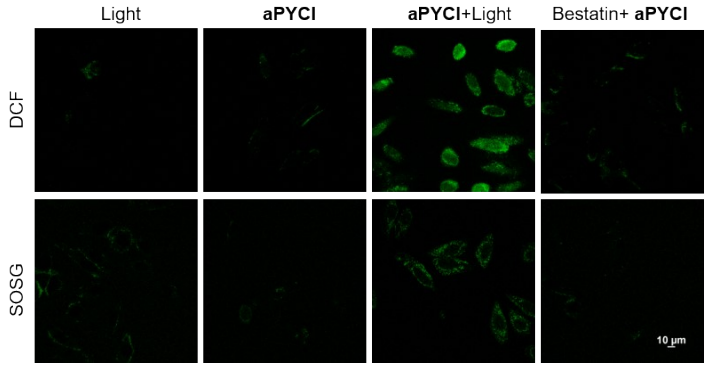

Fig. S15 CLSM images for HepG2 cells pretreated with DCFH-AD or SOSG, incubated with **aPYCI** (2.5 μM) and irradiated with a 640 nm laser (DCF and SOSG: Ex=488 nm, Em=500–550 nm). Scale bar: 10 μm.

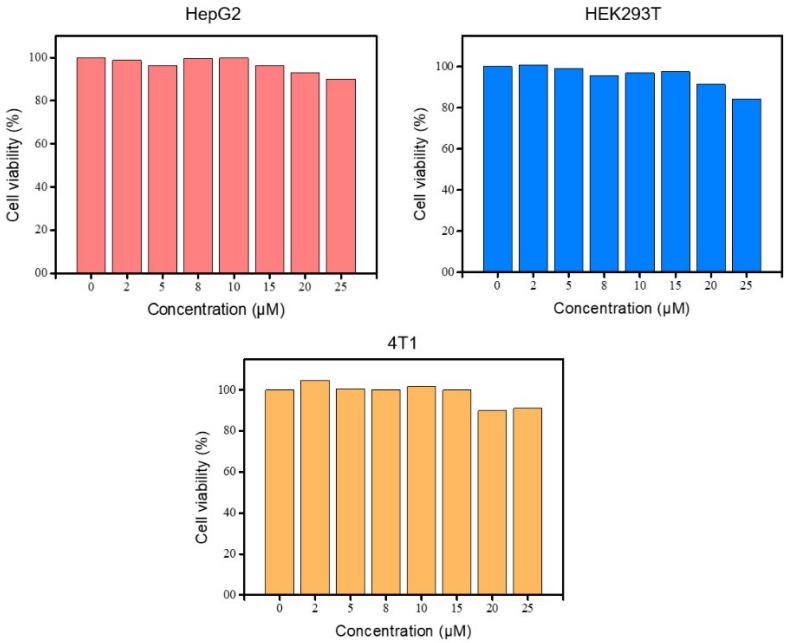

Fig. S16 Dark cytotoxicity effect of **aPYCI4** (0 - 25 μM) on HepG2, HEK293T and 4T1 cells.

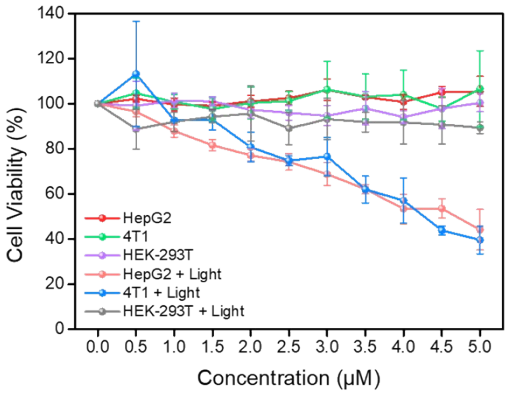

Fig. S17 Cytotoxicitis of **aPYCI** toward various cells under dark or irradiated with a 640 nm laser (n = 3). Data are presented as mean ± SD from three independent experiments.

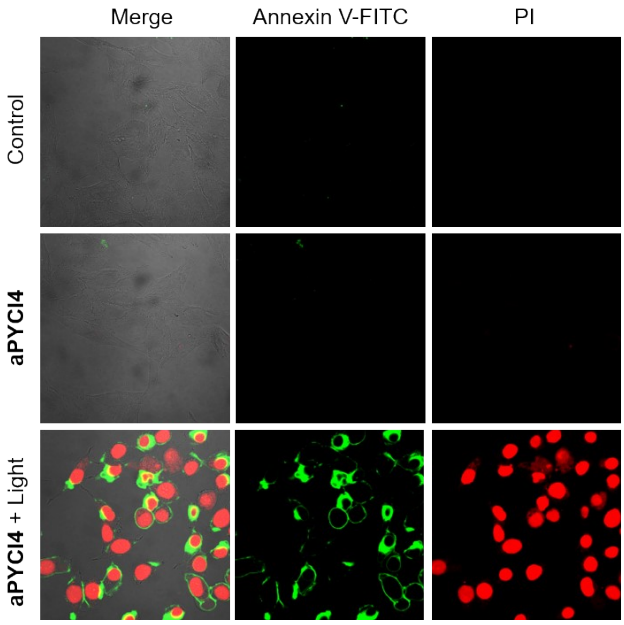

Fig. S18 CLSM images for HepG2 cells co-stained with Annexin V-FITC and PI under different treatments (Annexin V-FITC: Ex = 488 nm, Em = 500–550 nm; PI: Ex = 561 nm, Em = 590–640 nm).

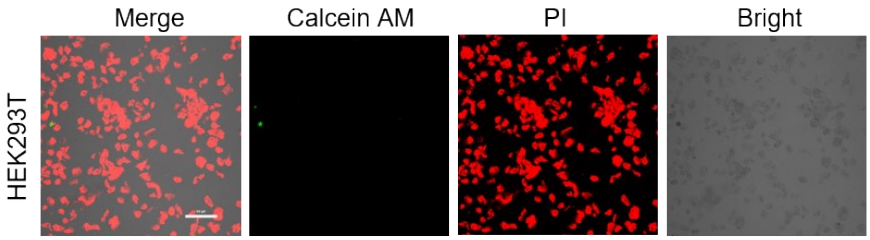

Fig. S19 Fluorescence imaging of calcein AM and PI for **PYC4**-treated HEK293T cells under irradiated with a 640 nm laser (10 mW/cm^2). Scale bar: 100 μm.

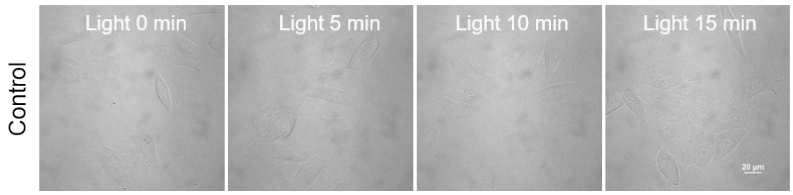

Fig. S20 Merged images for HepG2 cells irradiated with a 640 nm laser (10 mW/cm^2) for different time periods. Scale bar: 20 μm.

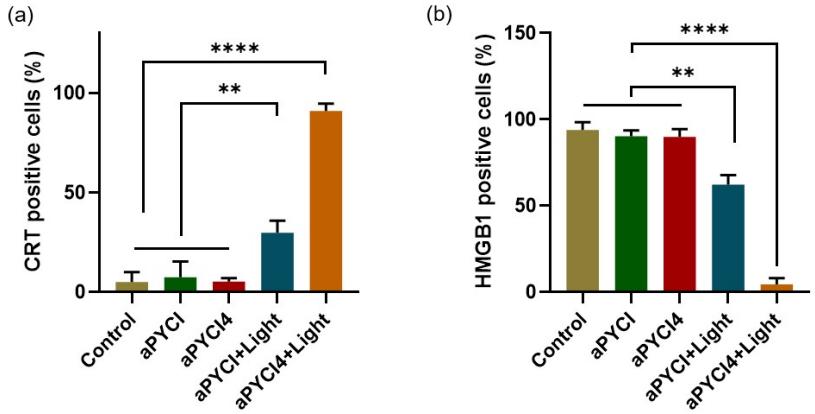

Fig. S21 Qutantitative analysis of fluorescence intensities for CRT (a) and HMGB1 (b) in HepG2 cells after different treatments in Fig. 3h and 3i in the maintext. Statistical comparison was performed by two-tailed t-test (****p < 0.0001, ***p < 0.001, **p < 0.01, n = 3).

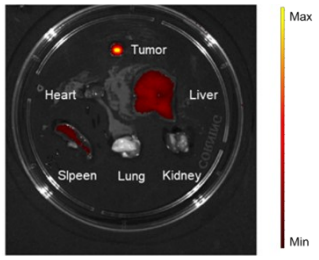

Fig. S22 Representative ex vivo fluorescence imaging of various organs and tumor in Balb/c mice upon intravenous injection with **aPYCI4** (100 μL, 100 μM) on the 7th day.

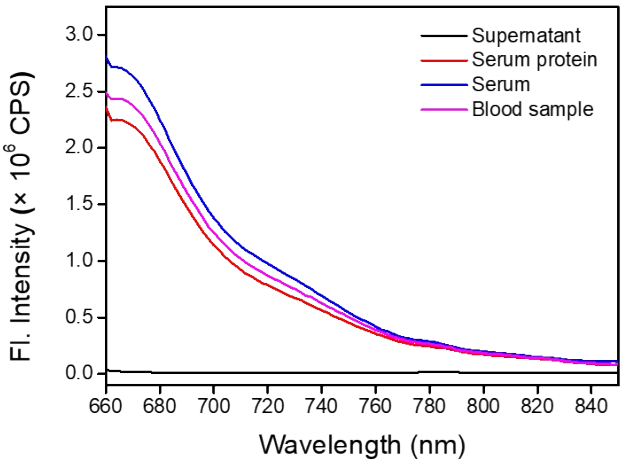

Fig. S23 Fluorescence spectra for determing the partition of **PYCI4** in different components of blood. Blood sample was collected from healthy mice upon intravenous injection with **PYCI4** (100 μL, 100 μM) and separated with different procedures. The slight higher fluorescence for serum sample was propably due to the slight decreased volume after centrifugation.

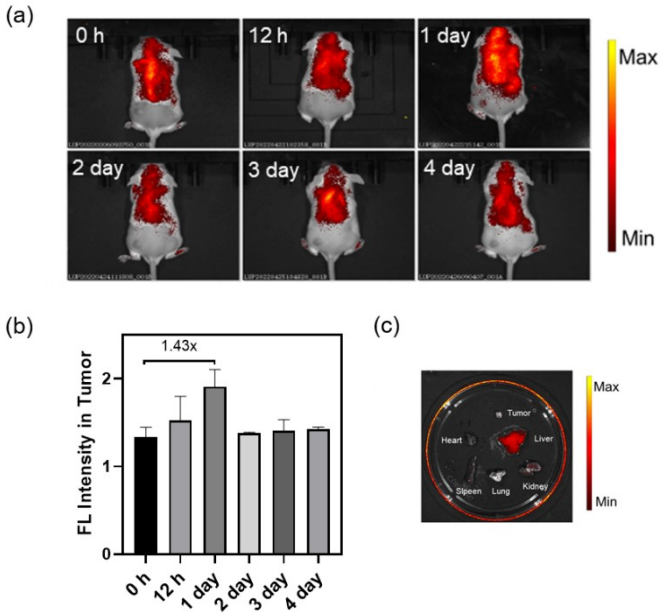

Fig. S24 (a) In vivo fluorescence imaging for 4T1 tumor-bearing mice at different time intervals upon injection with **aPYCI** (100 μM, 100 μL) via tail-vein. (b) Average fluorescence intensities from the tumor regions as a function of time (n=3). (c) Ex vivo fluorescence imaging of various organs and tumor in 4T1 tumor-bearing mice upon intravenous injection with **aPYCI** (100 μL, 100 μM) on the 4th day.

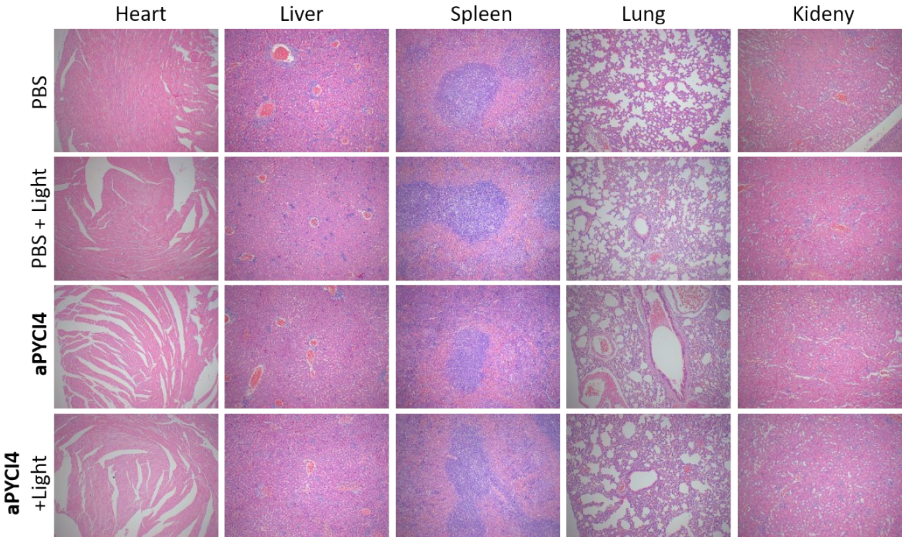

Fig. S25 H&E staining of major organs including heart, liver, spleen, lung, and kidneys for 4T1 tumor-bearing mice under different treatments on the 14th day.

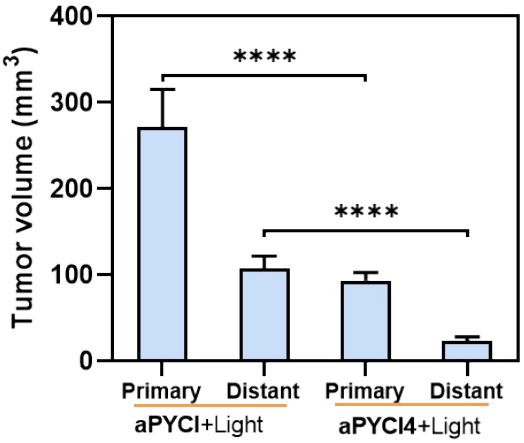

Fig. S26 Tumor volumes of primary (left) and distant (right) tumors in 4T1-tumor-bearing mice under different treatments after NIR irradiation. Statistical comparison was performed by two-tailed t-test (****$p < 0.0001$, $n = 5$).

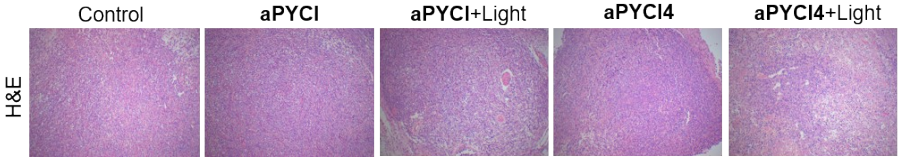

Fig. S27 H&E staining of distant tumors for 4T1-tumor-bearing mice under different treatments on the 14th day.

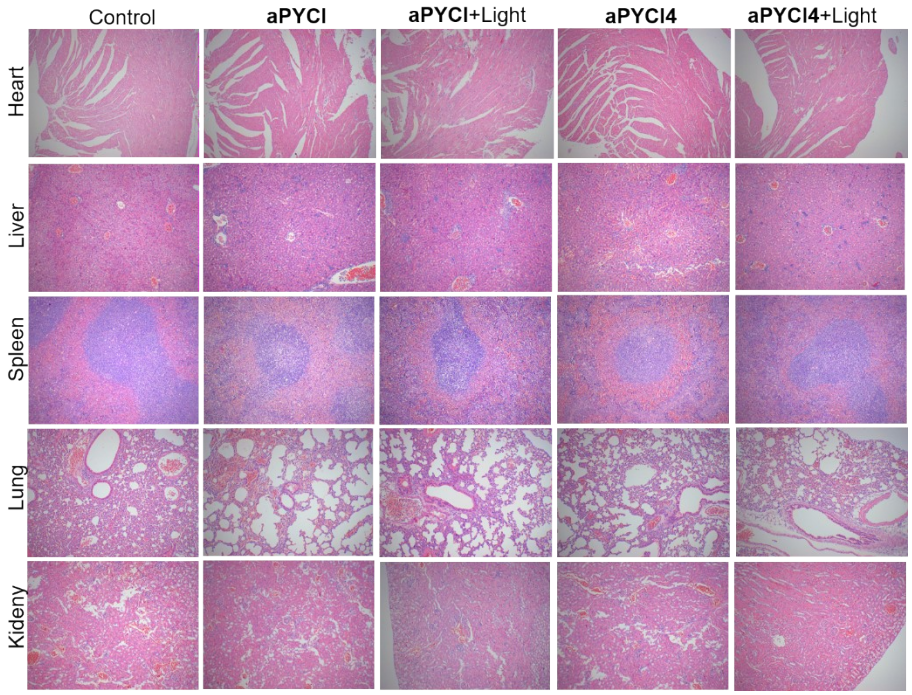

Fig. S28 H&E staining of major organs including heart, liver, spleen, lung, and kidneys for mice bearing primary and distant tumors under different treatments on the 14th day.

3. NMR and MS spectra

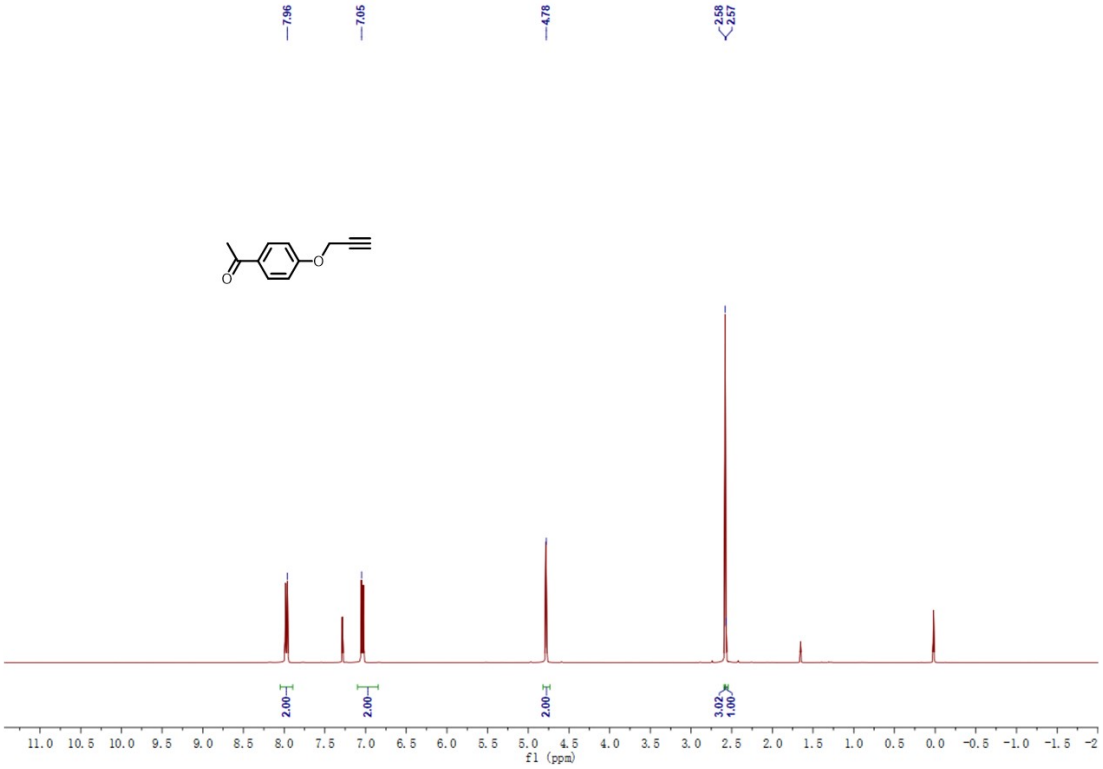

Fig S29 ^{1}H NMR (400 MHz, 298 K, $CDCl_3$) spectrum for compound **1**.

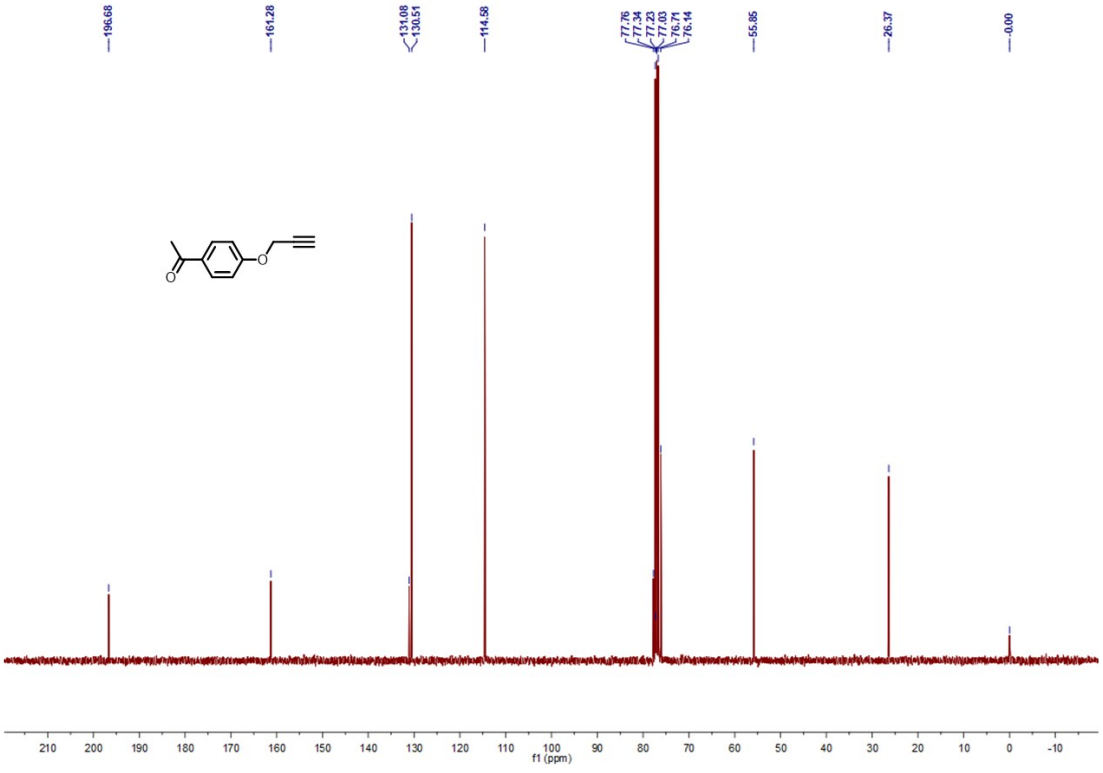

Fig. S30 ^{13}C NMR (100 MHz, 298 K, $CDCl_3$) spectrum for compound **1**.

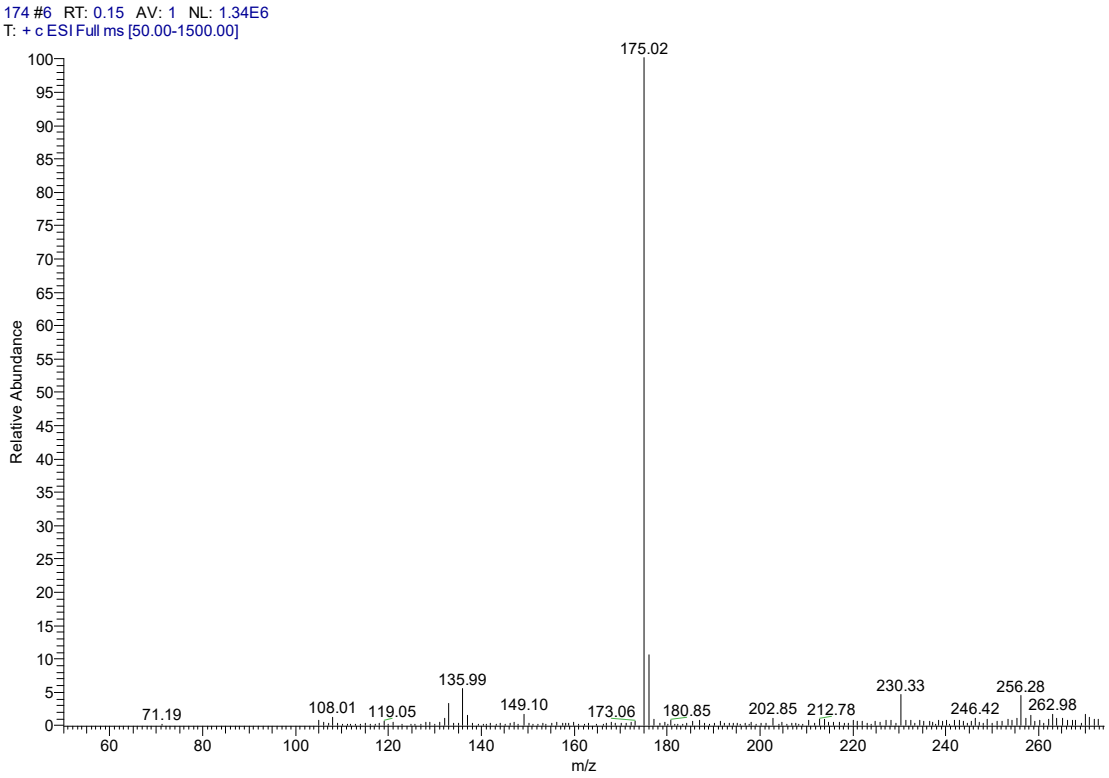

Fig. S31 HR-MS-ESI spectrum for compound **1**.

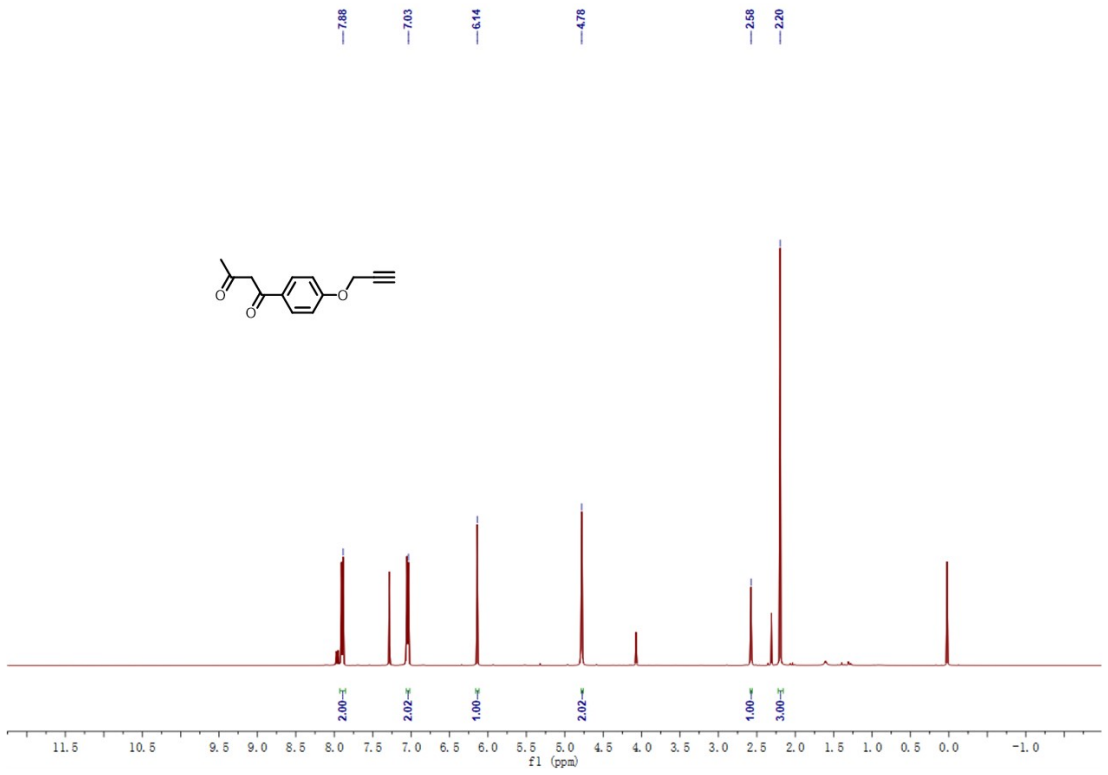

Fig. S32 ^{1}H NMR (400 MHz, 298 K, $CDCl_3$) spectrum for compound **2**.

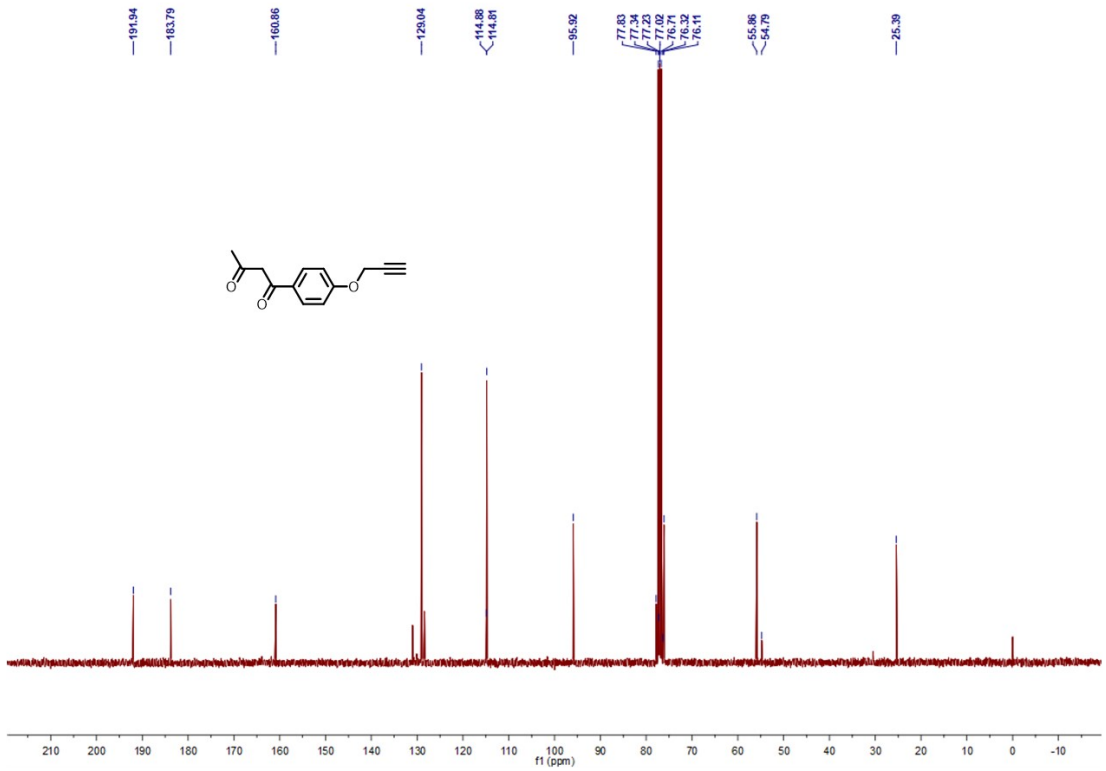

Fig. S33 ^{13}C NMR (100 MHz, 298 K, $CDCl_3$) spectrum for compound **2**.

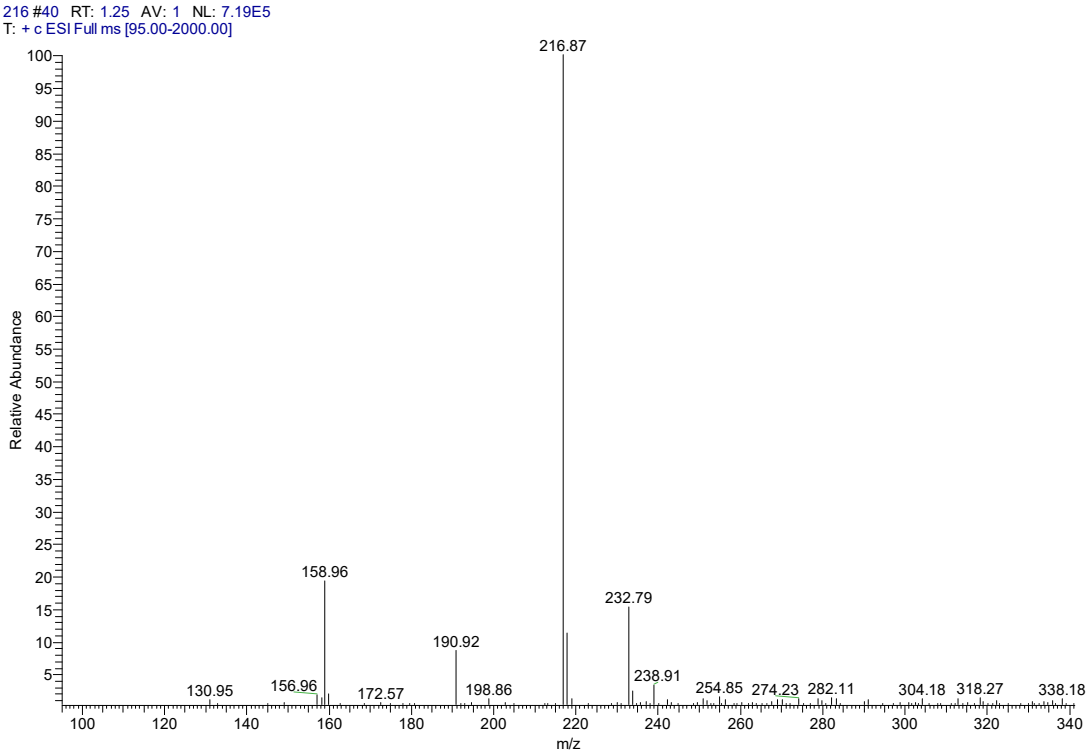

Fig. S34 HR-MS-ESI spectrum for compound **2**.

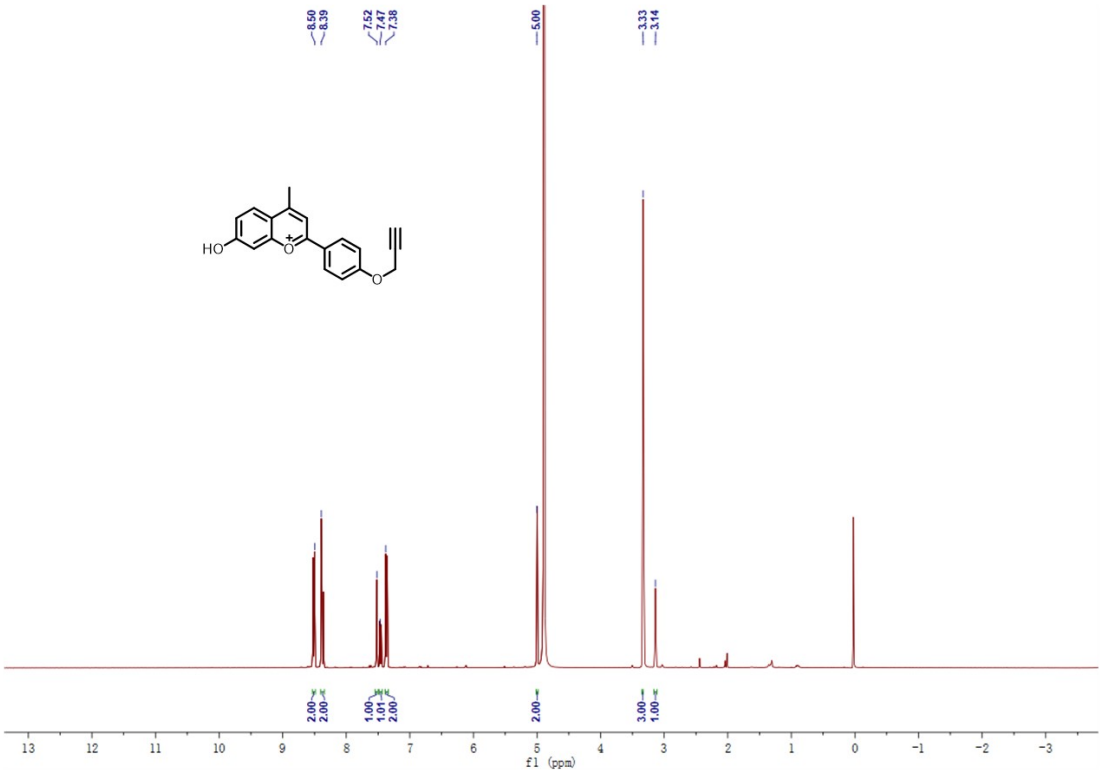

Fig. S35 ^{1}H NMR (400 MHz, 298 K, CD_3OD) spectrum for compound **3**.

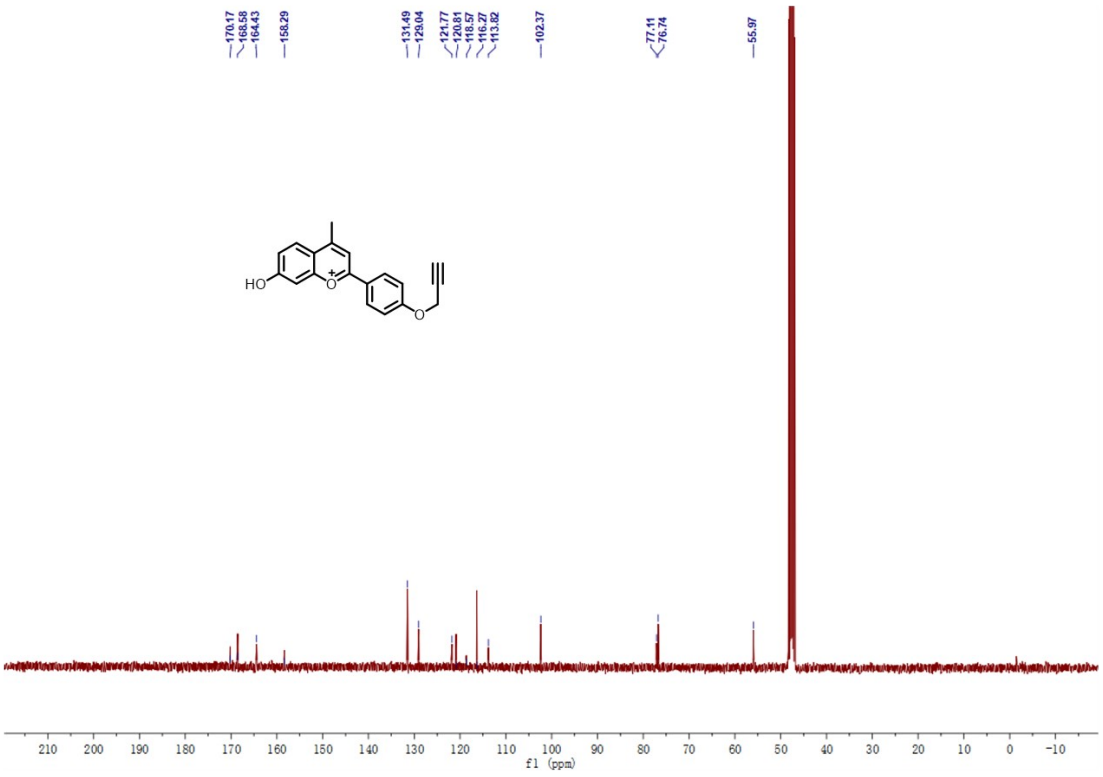

Fig. S36 ^{13}C NMR (100 MHz, 298 K, CD_3OD) spectrum for compound **3**.

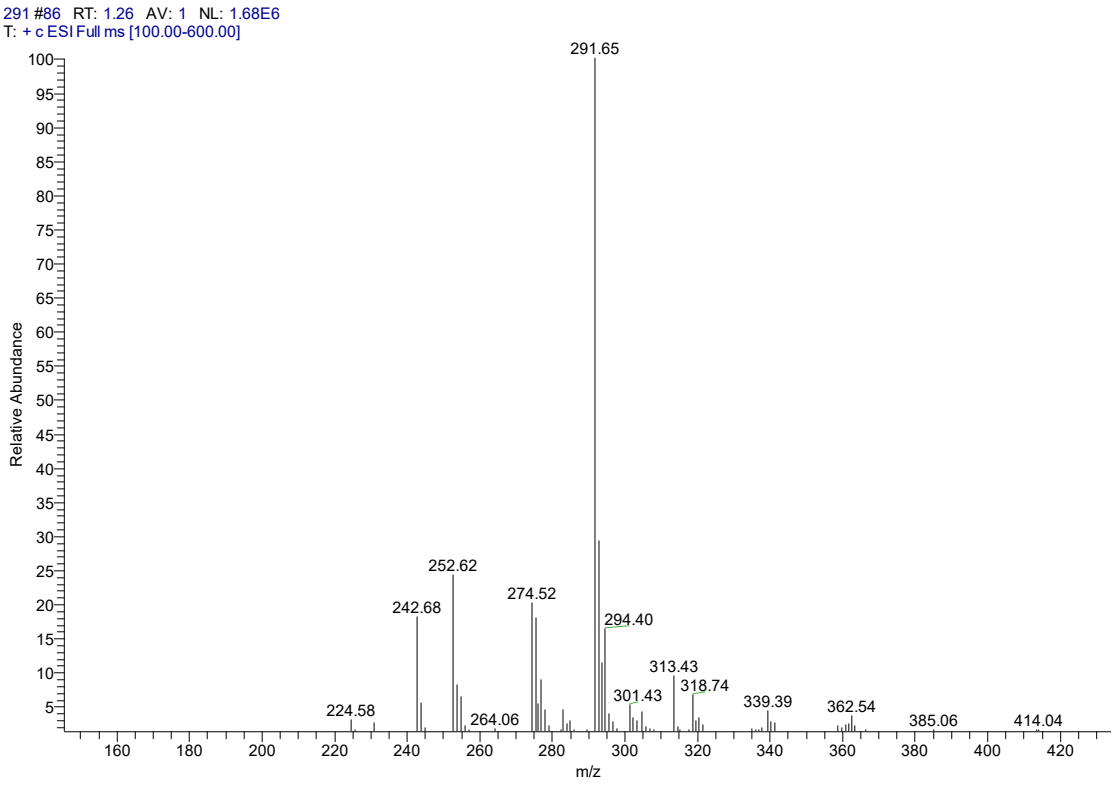

Fig. S37 HR-MS-ESI spectrum for compound **3**.

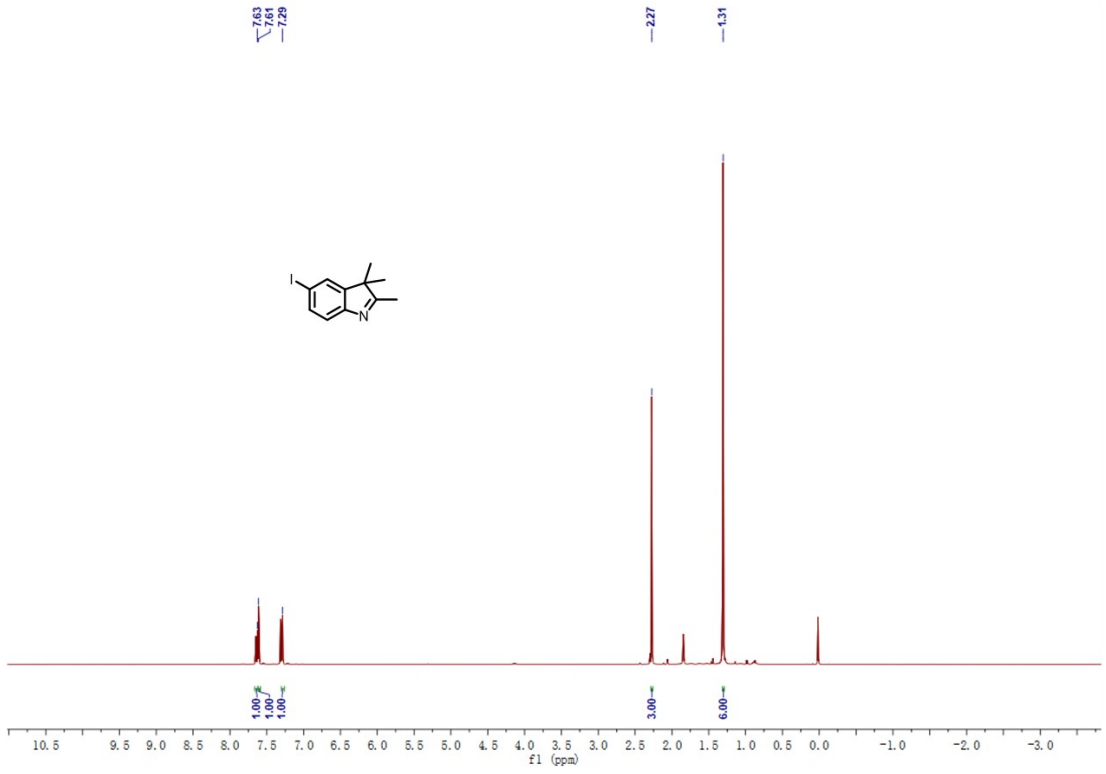

Fig. S38 ^{1}H NMR (400 MHz, 298 K, $CDCl_3$) spectrum for compound **5**.

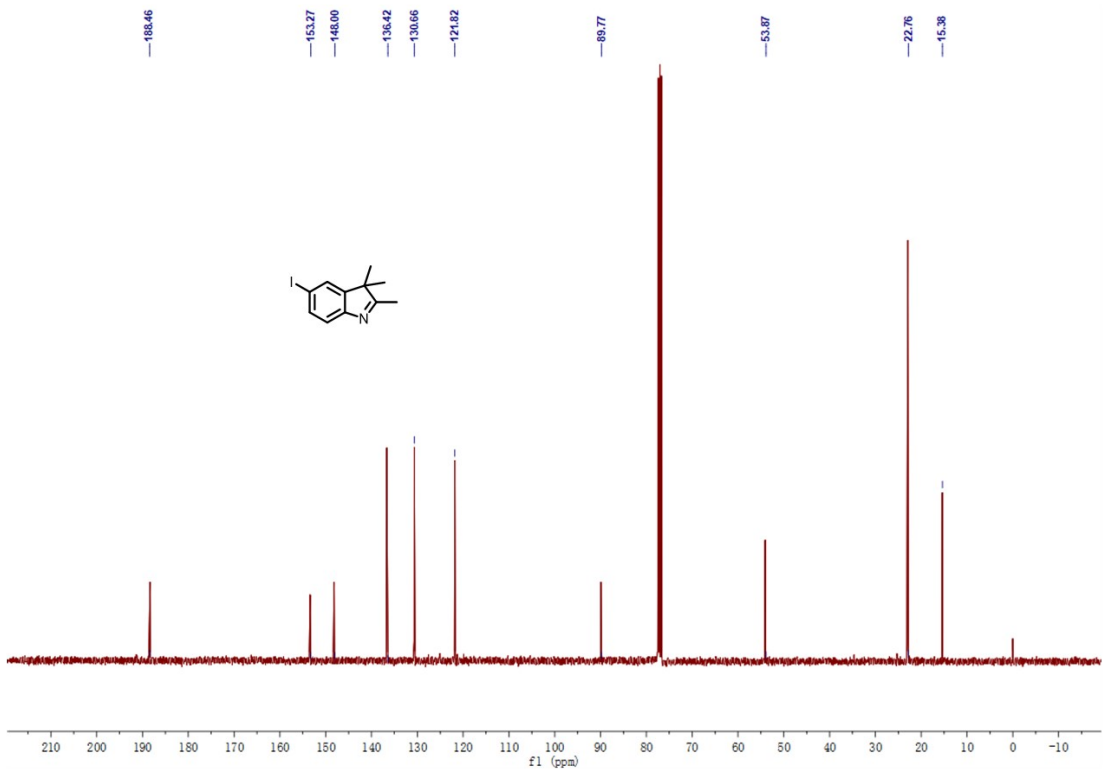

Fig. S39 ^{13}C NMR (100 MHz, 298 K, $CDCl_3$) spectrum for compound **5**.

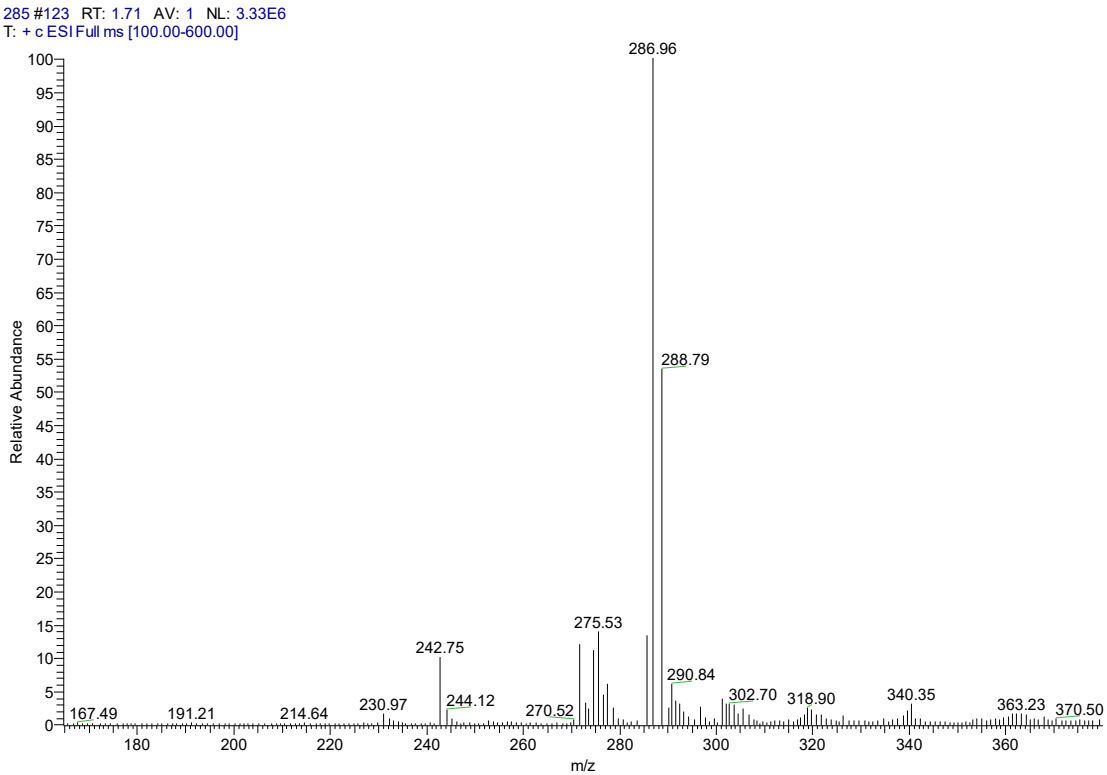

Fig. S40 HR-MS-ESI spectrum for compound **5**.

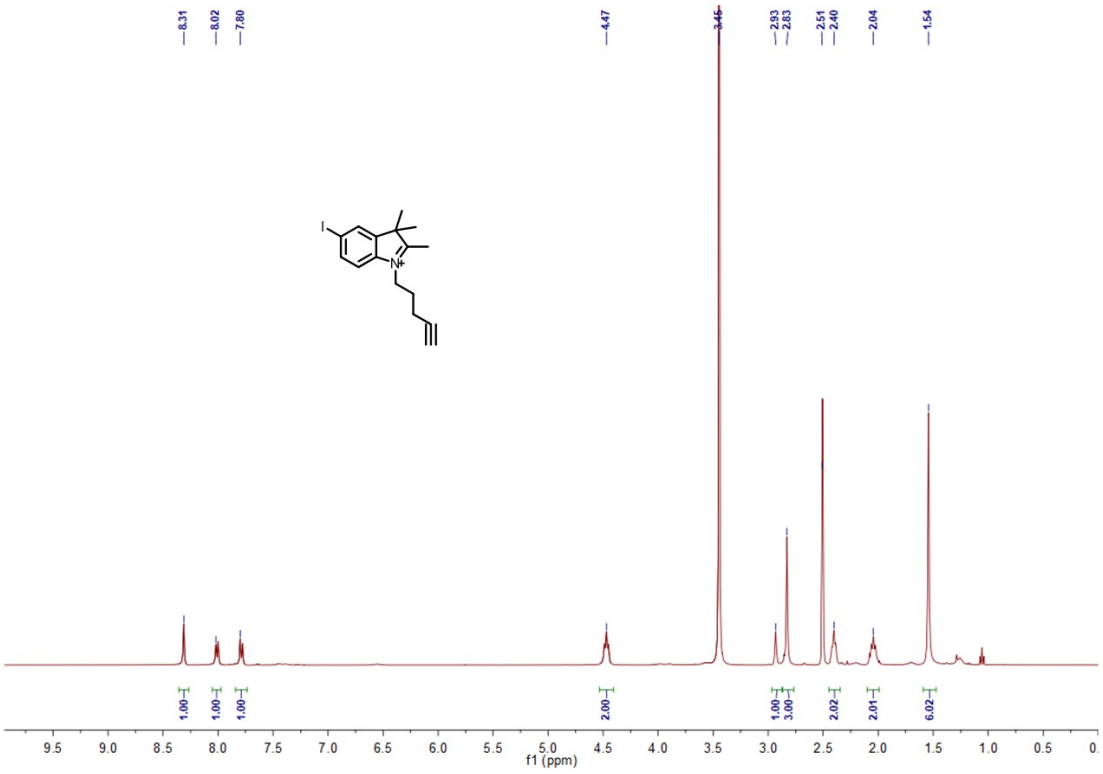

Fig. S41 ^{1}H NMR (400 MHz, 298 K, DMSO-d_6) spectrum for compound **6**.

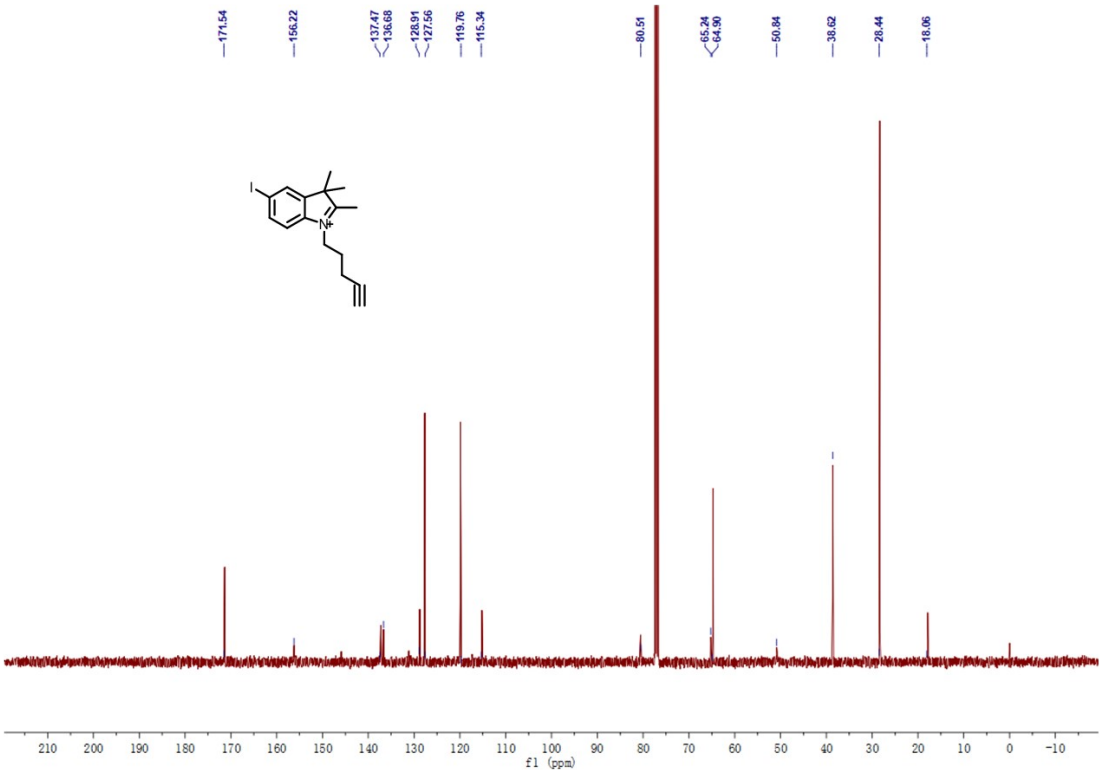

Fig. S42 ^{13}C NMR (100 MHz, 298 K, DMSO-d_6) spectrum for compound **6**.

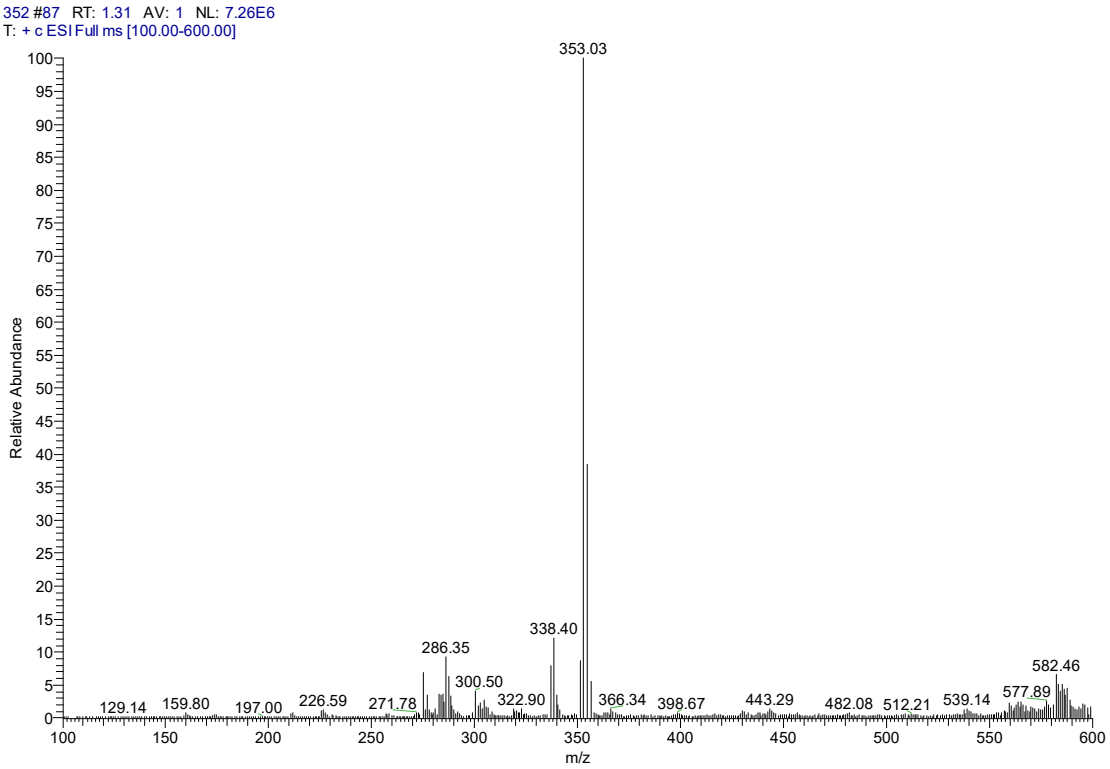

Fig. S43 HR-MS-ESI spectrum for compound **6**.

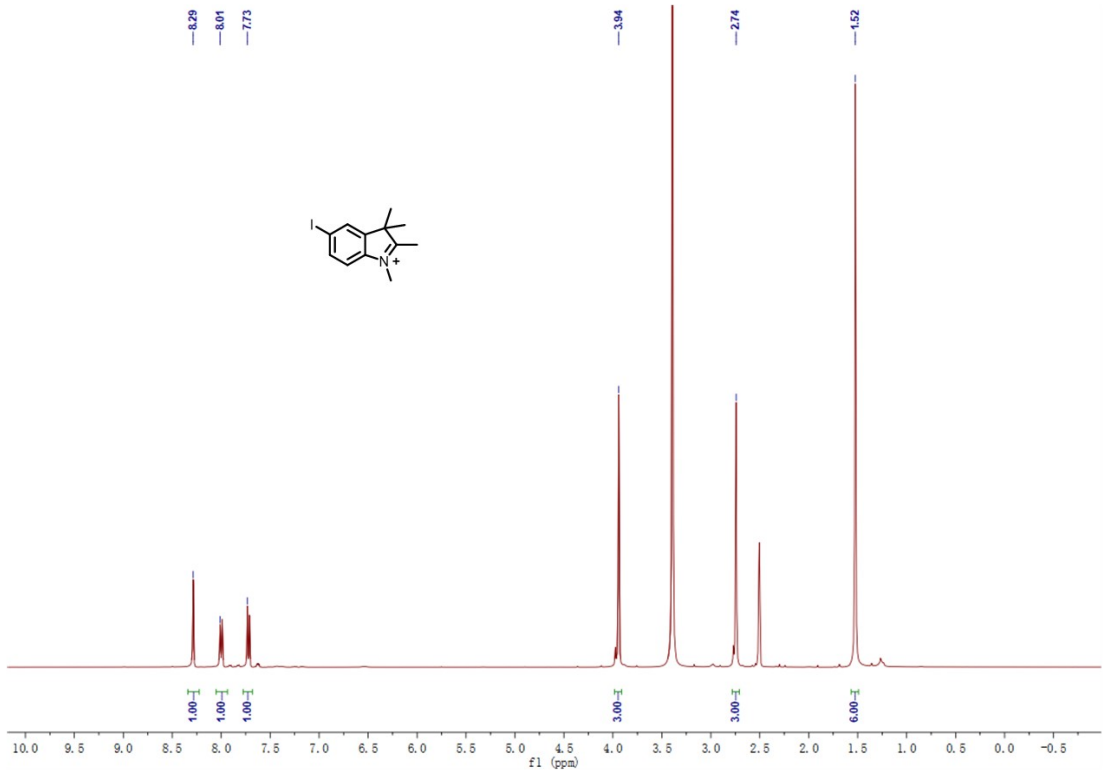

Fig. S44 ^{1}H NMR (400 MHz, 298 K, DMSO-d_6) spectrum for compound **7**.

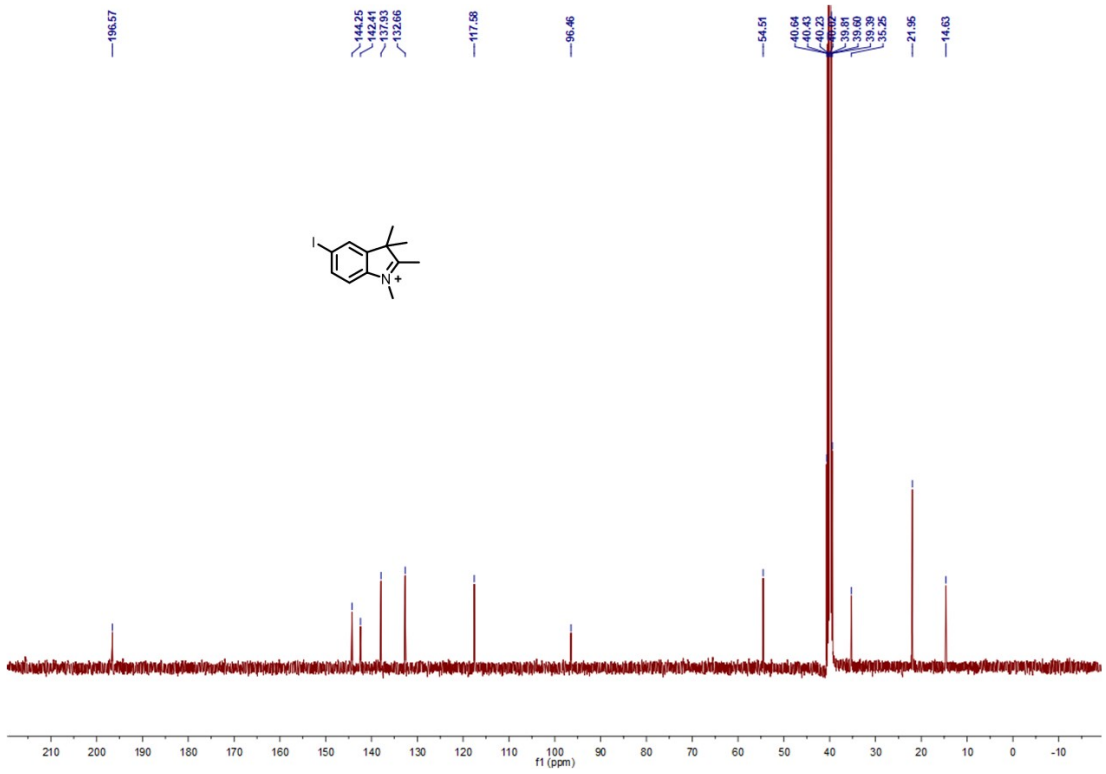

Fig. S45 ^{13}C NMR (100 MHz, 298 K, DMSO-d_6) spectrum for compound **7**.

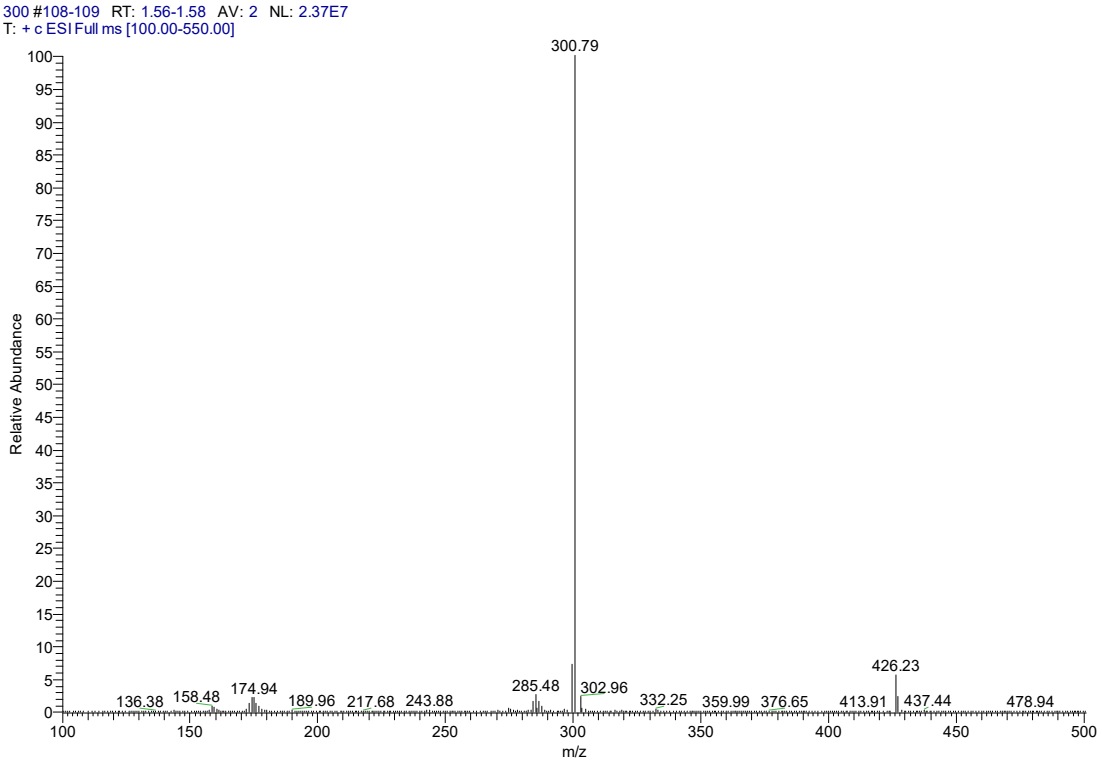

Fig. S46 HR-MS-ESI spectrum for compound **7**.

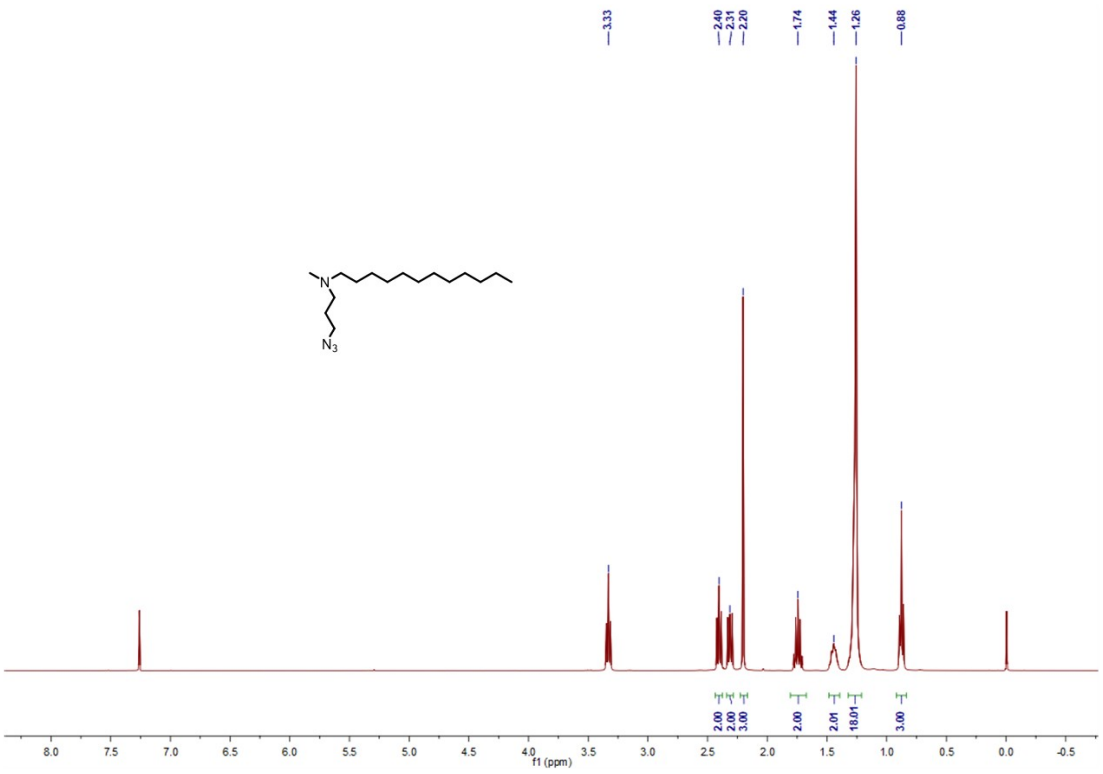

Fig. S47 ^{1}H NMR (400 MHz, 298 K, $CDCl_3$) spectrum for compound **9**.

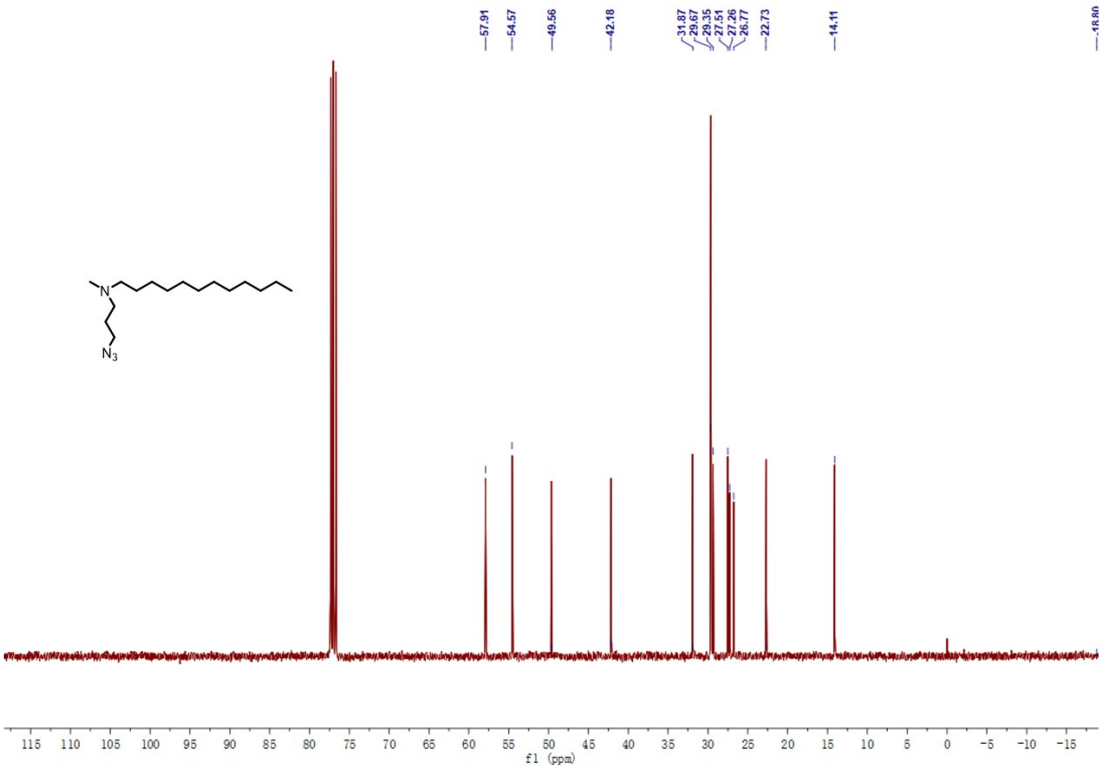

Fig. S48 ^{13}C NMR (100 MHz, 298 K, $CDCl_3$) spectrum for compound **9**.

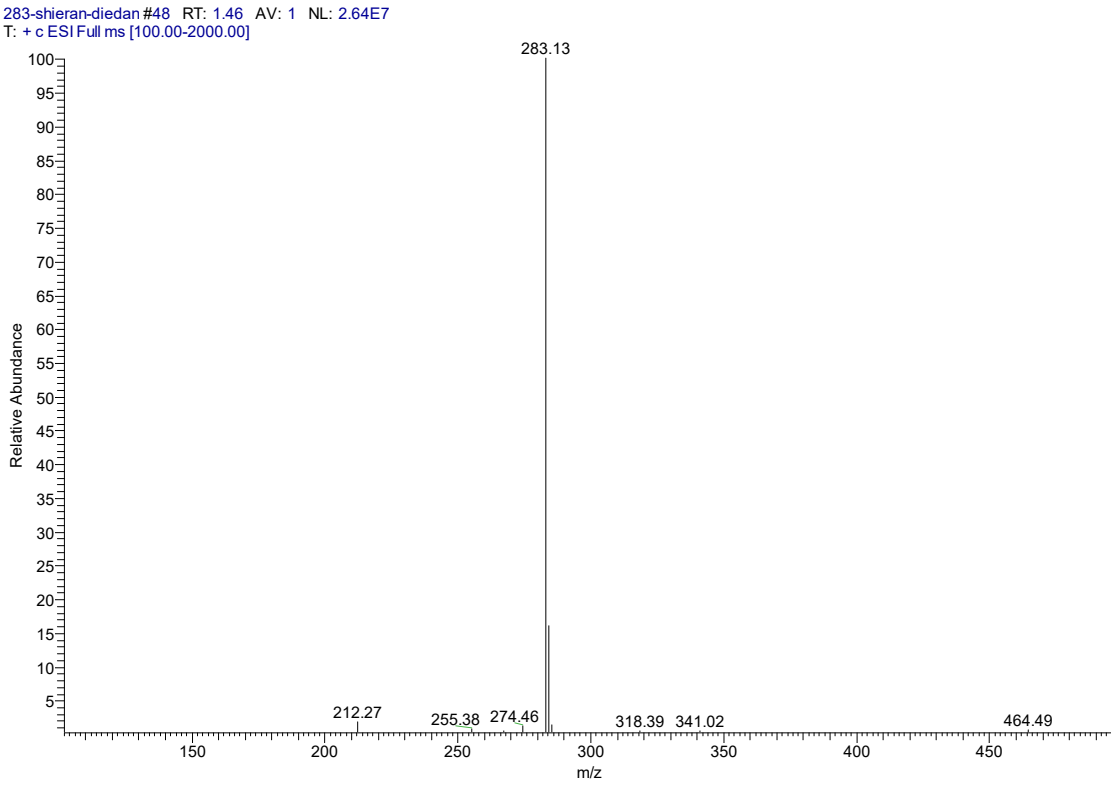

Fig. S49 HR-MS-ESI spectrum for compound **9**.

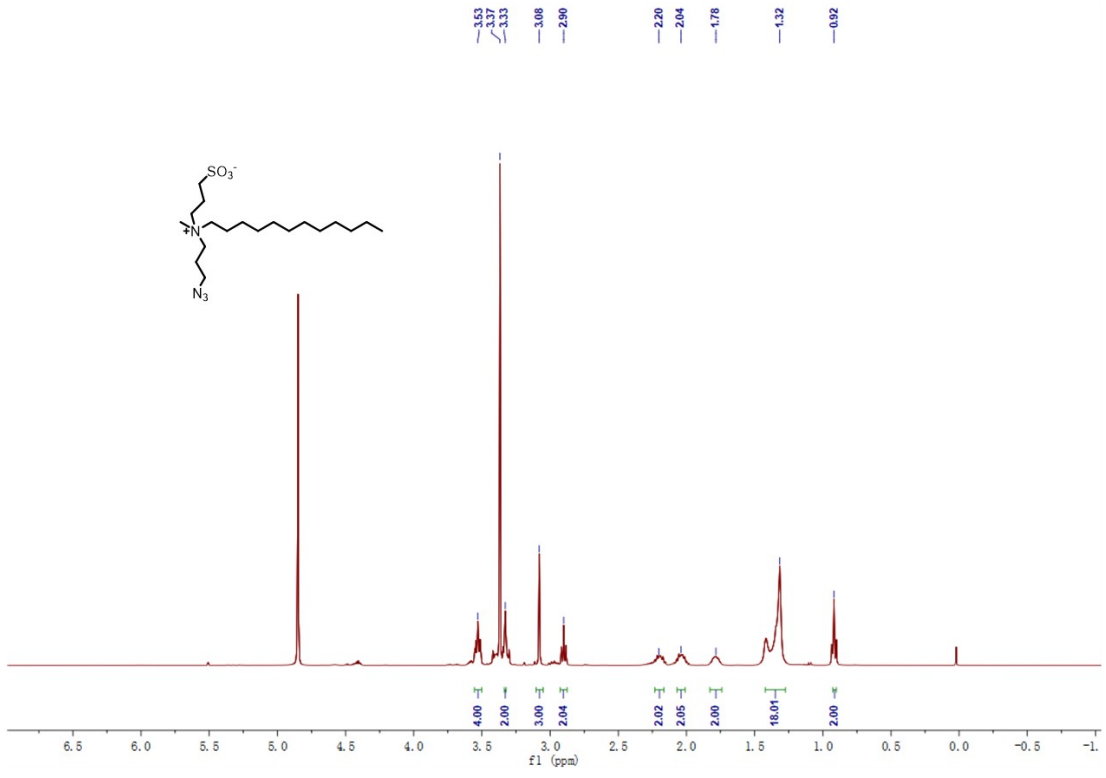

Fig. S50 ^{1}H NMR (400 MHz, 298 K, CD_3OD) spectrum for compound **Zwitterionic lipid**.

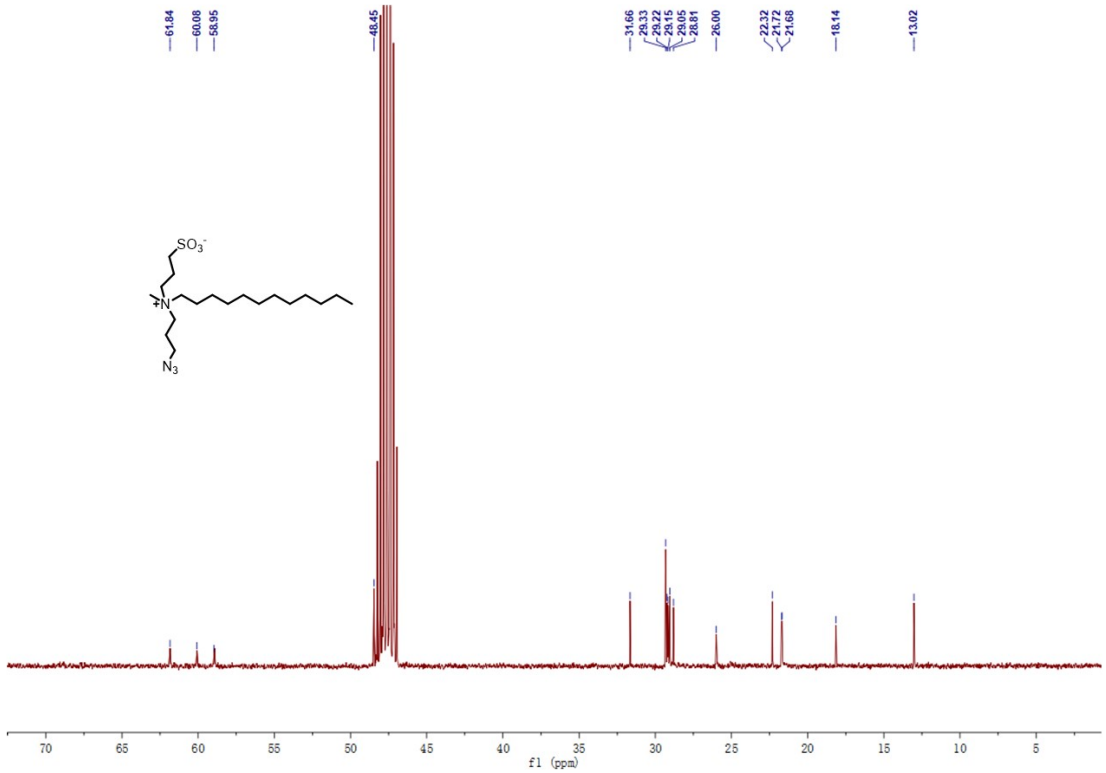

Fig. S51 ^{13}C NMR (100 MHz, 298 K, CD_3OD) spectrum for compound **Zwitterionic lipid**.

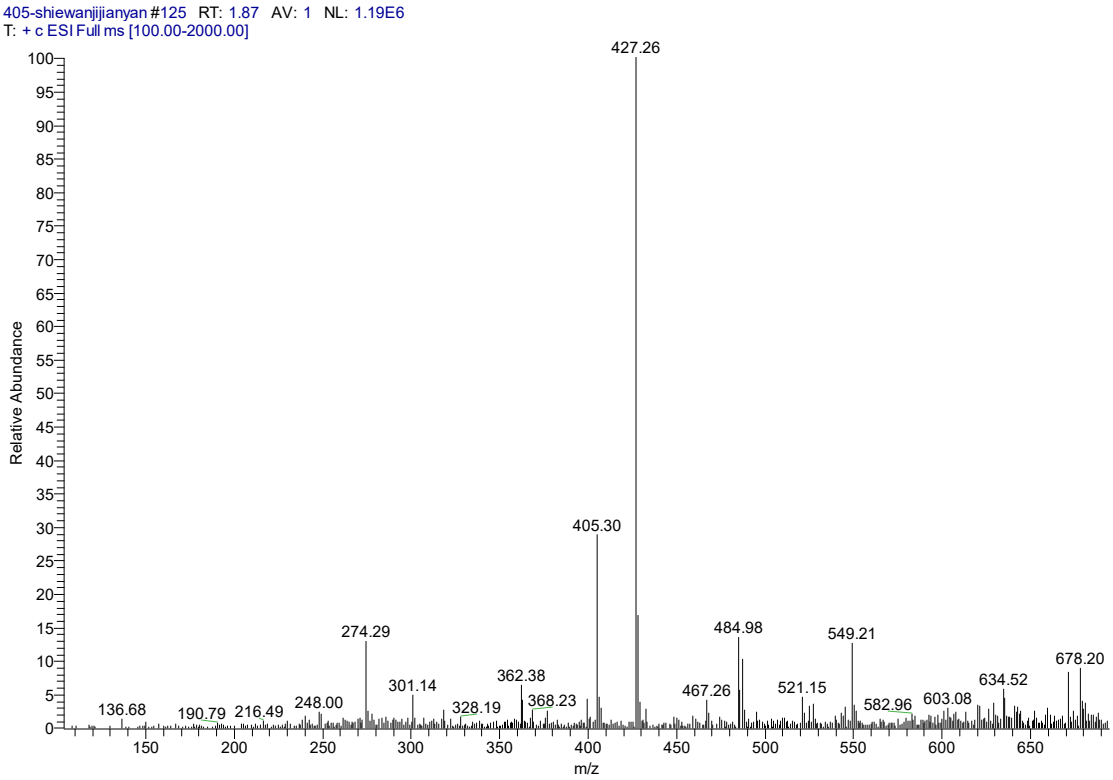

Fig. S52 HR-MS-ESI spectrum for compound **Zwitterionic lipid**.

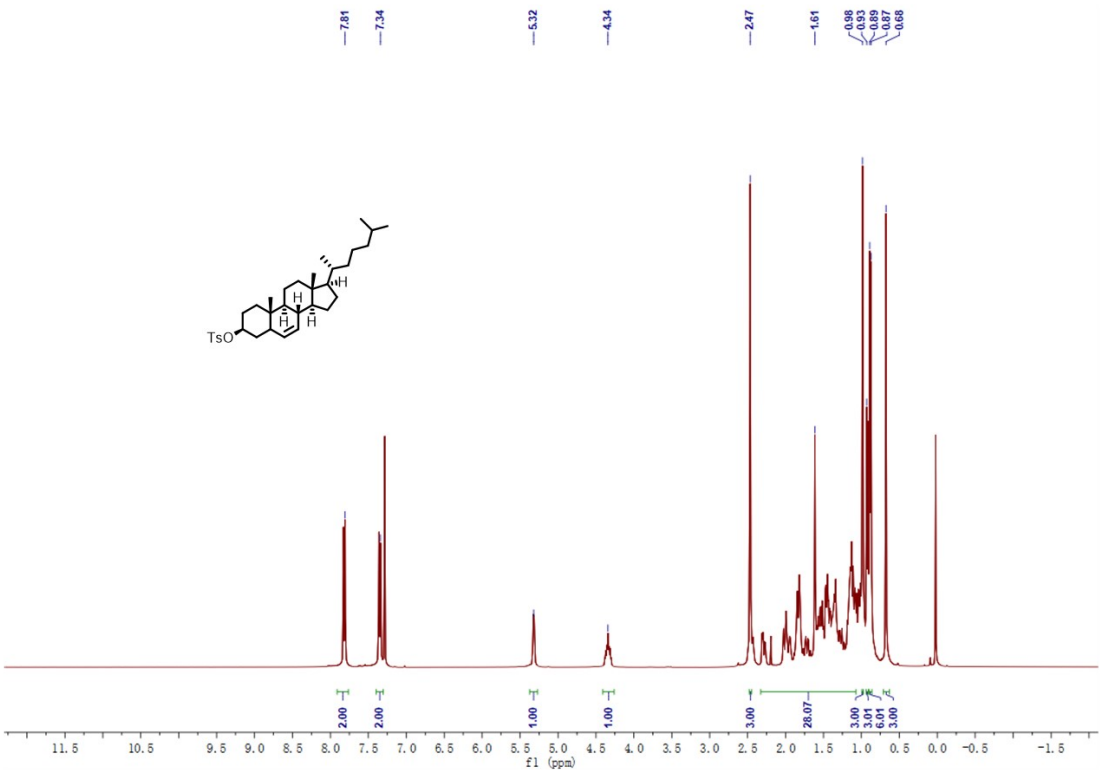

Fig. S53 ^{1}H NMR (400 MHz, 298 K, $CDCl_3$) spectrum for compound **10**.

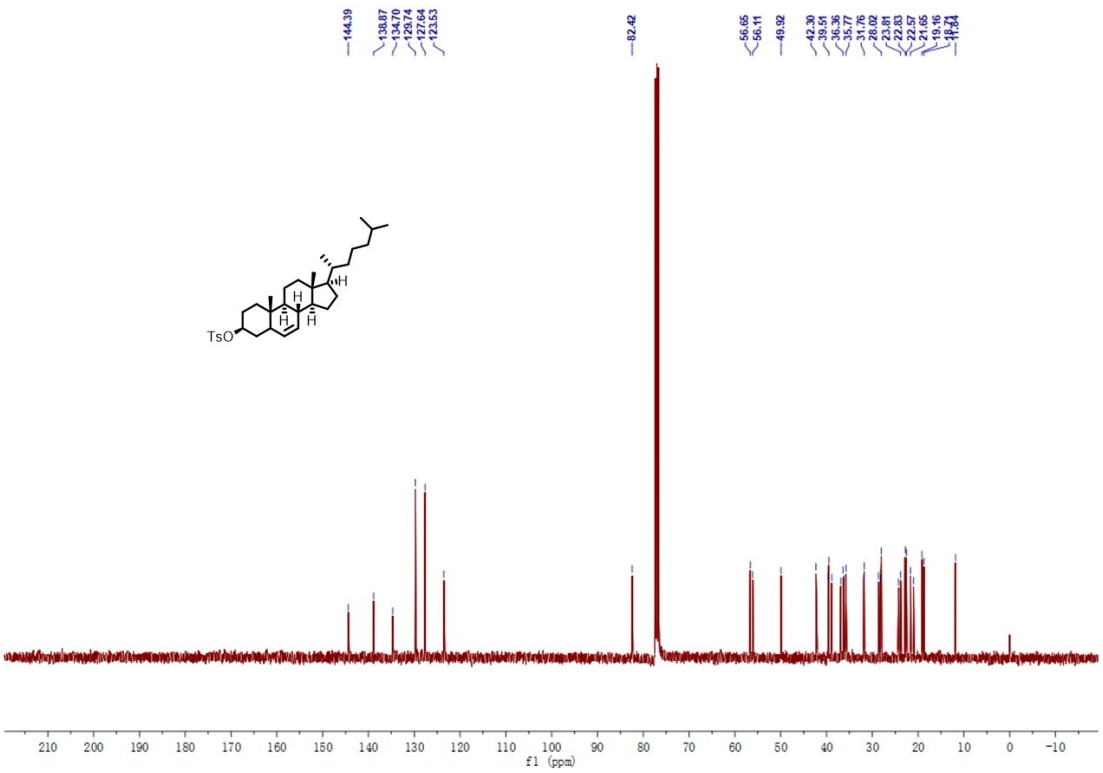

Fig. S54 ^{13}C NMR (100 MHz, 298 K, $CDCl_3$) spectrum for compound **10**.

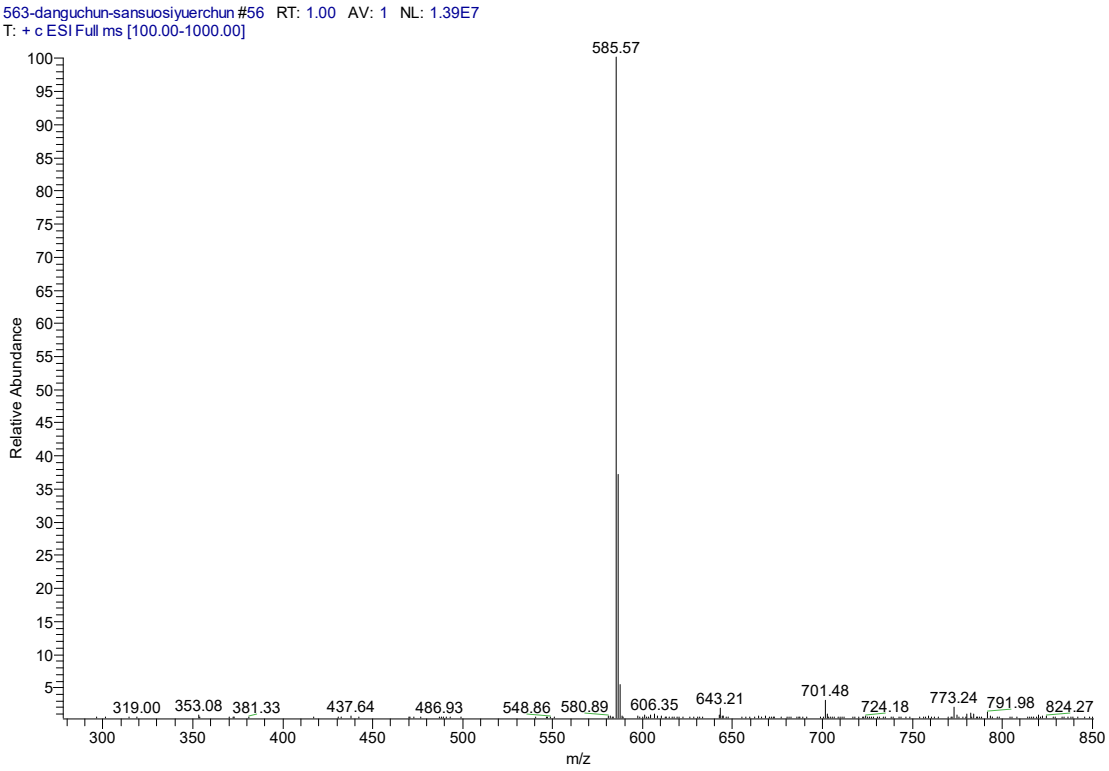

Fig. S55 HR-MS-ESI spectrum for compound **11**.

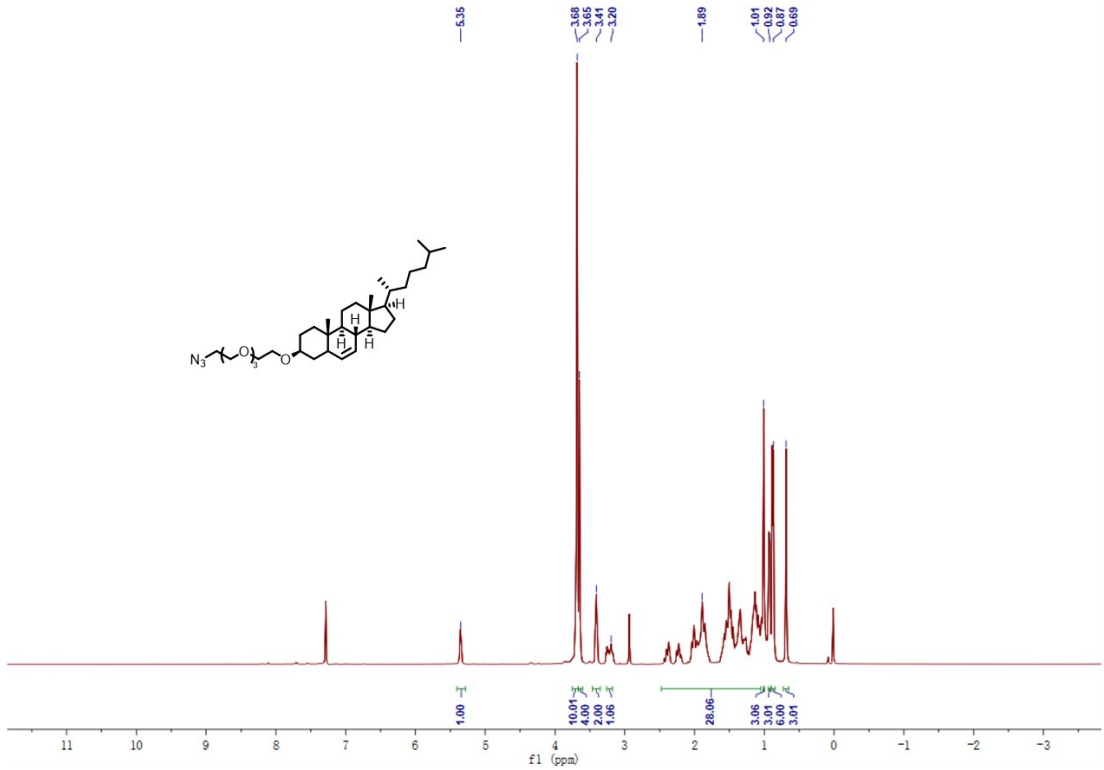

Fig. S56 ^{1}H NMR (400 MHz, 298 K, $CDCl_3$) spectrum for compound **Chol-PEG$_3$-N$_3$**.

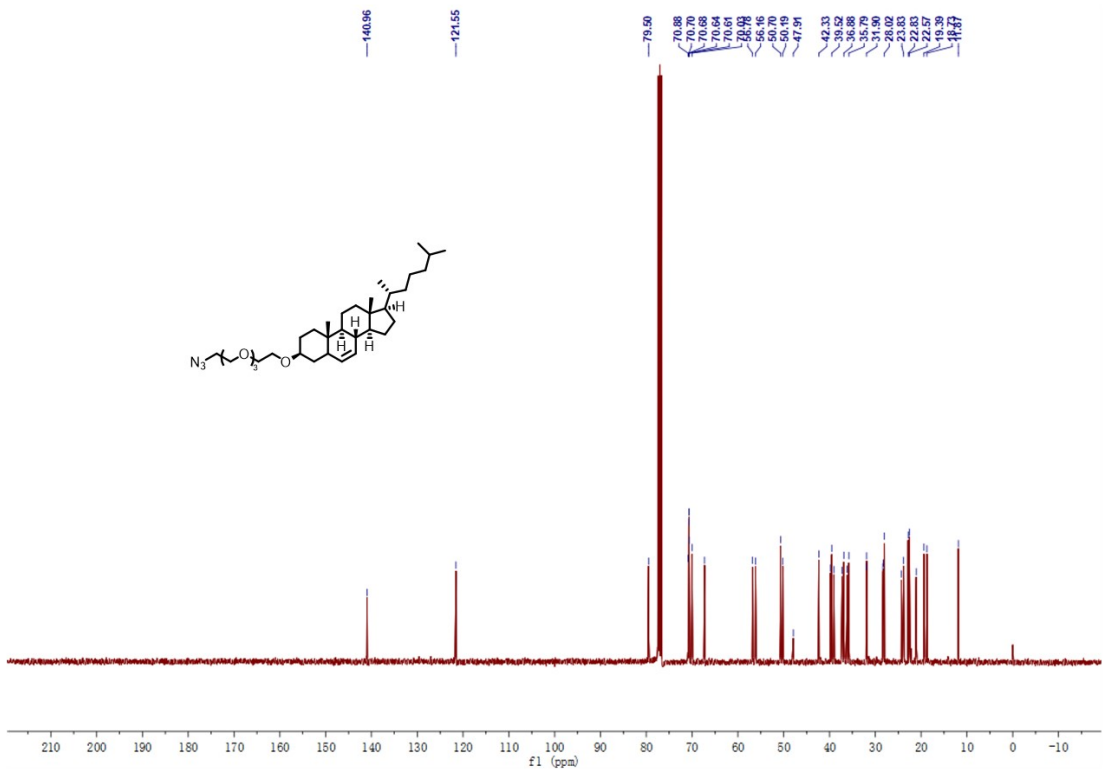

Fig. S57 ^{13}C NMR (100 MHz, 298 K, $CDCl_3$) spectrum for compound **Chol-PEG$_3$-N$_3$** .

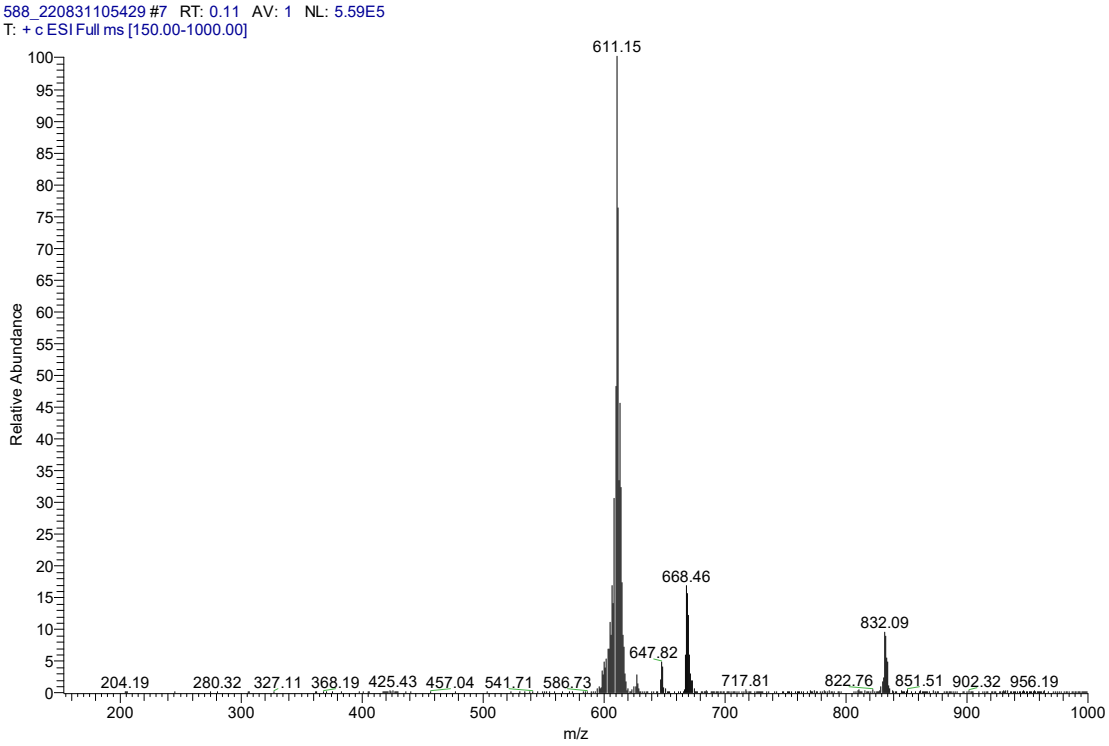

Fig. S58 HR-MS-ESI spectrum for compound **Chol-PEG$_3$-N$_3$**.

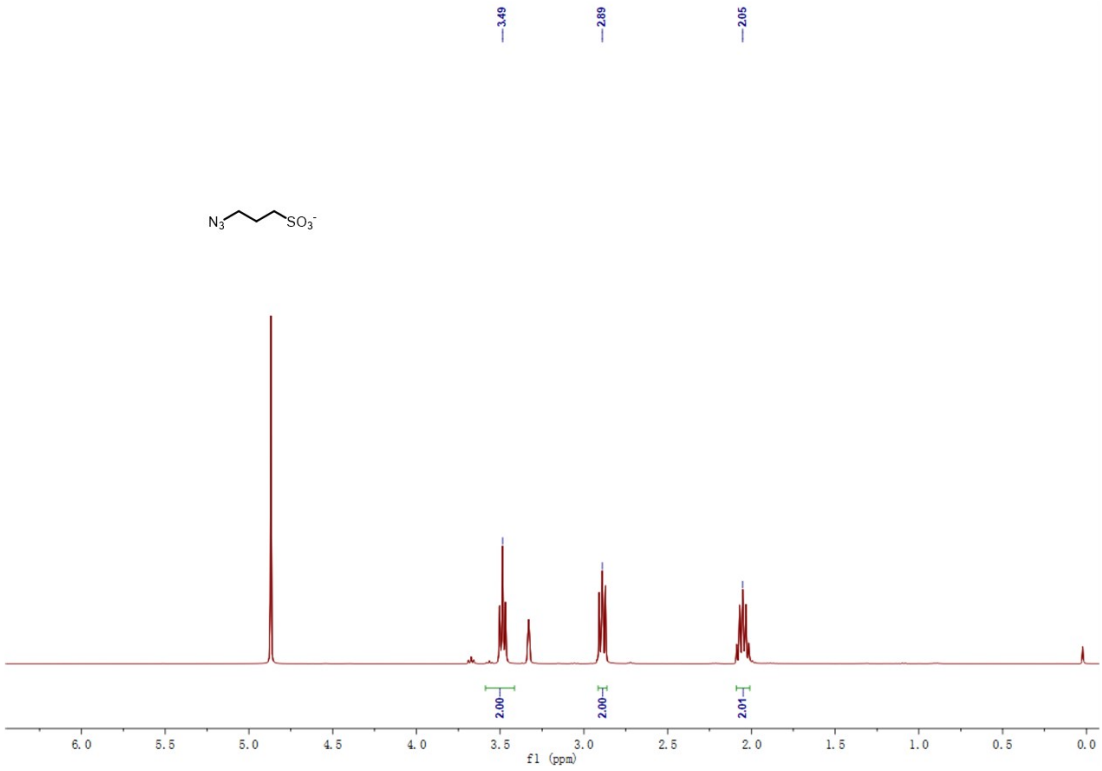

Fig. S50 ^{1}H NMR (400 MHz, 298 K, CD_3OD) spectrum for compound **13**.

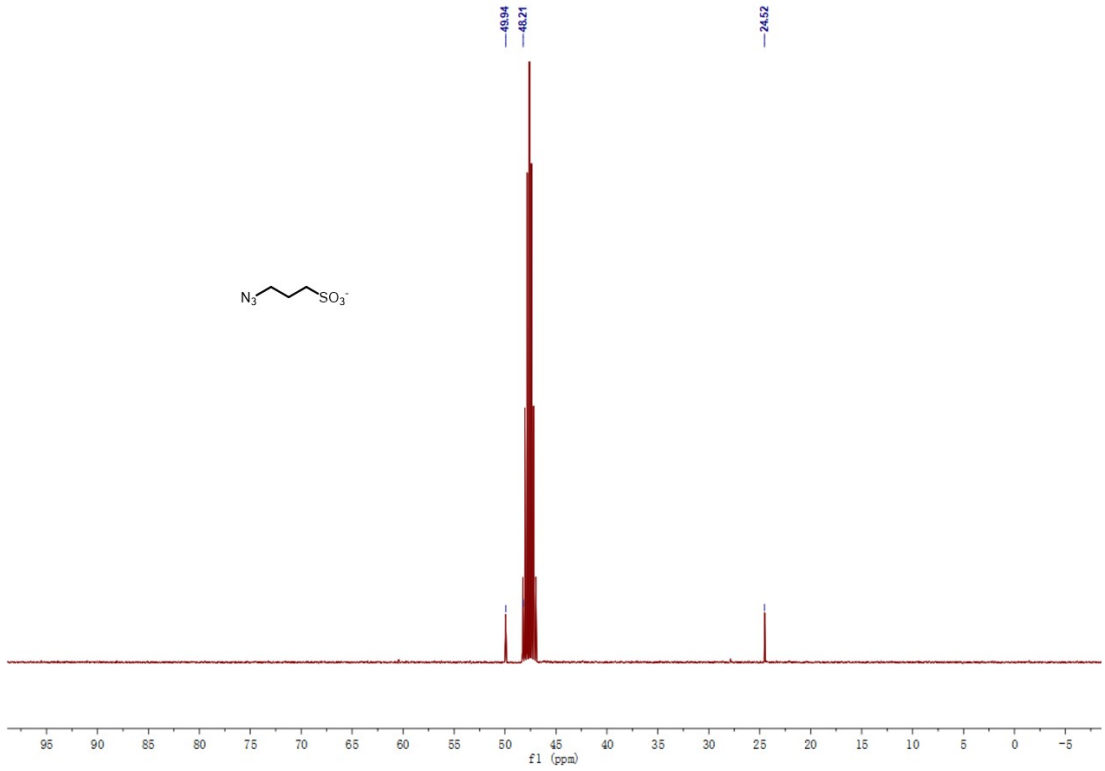

Fig. S60 ^{13}C NMR (100 MHz, 298 K, CD_3OD) spectrum for compound **13**.

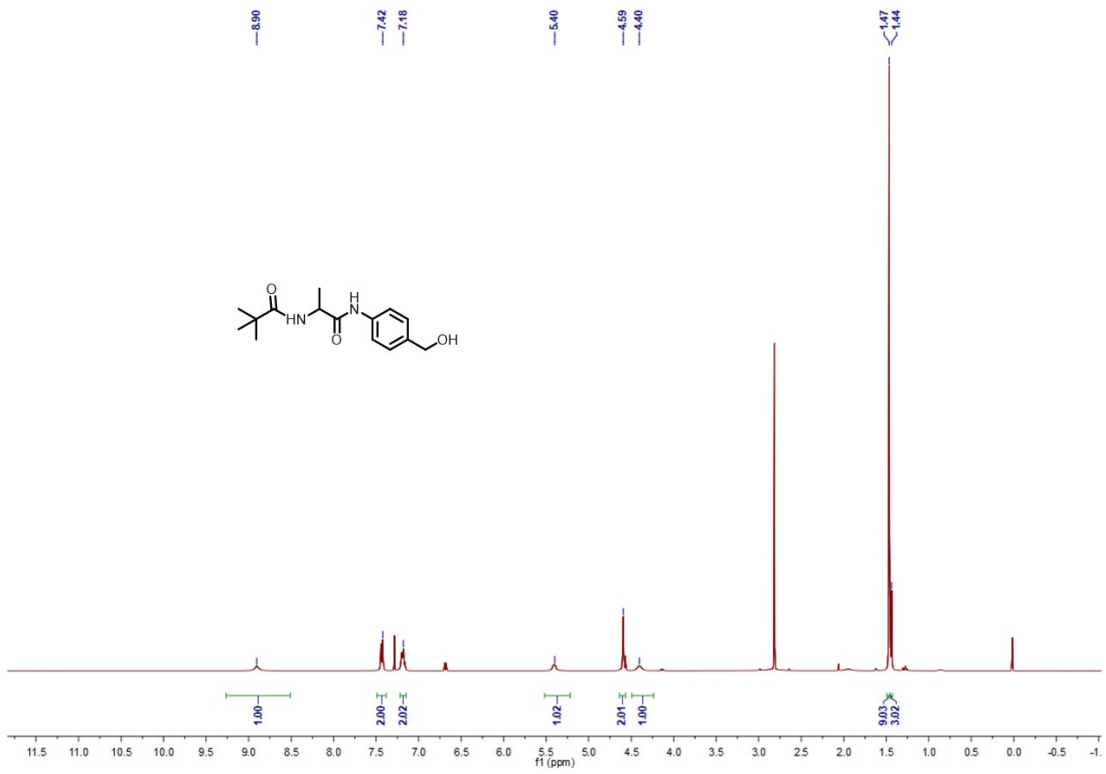

Fig. S61 ^{1}H NMR (400 MHz, 298 K, $CDCl_3$) spectrum for compound **14**.

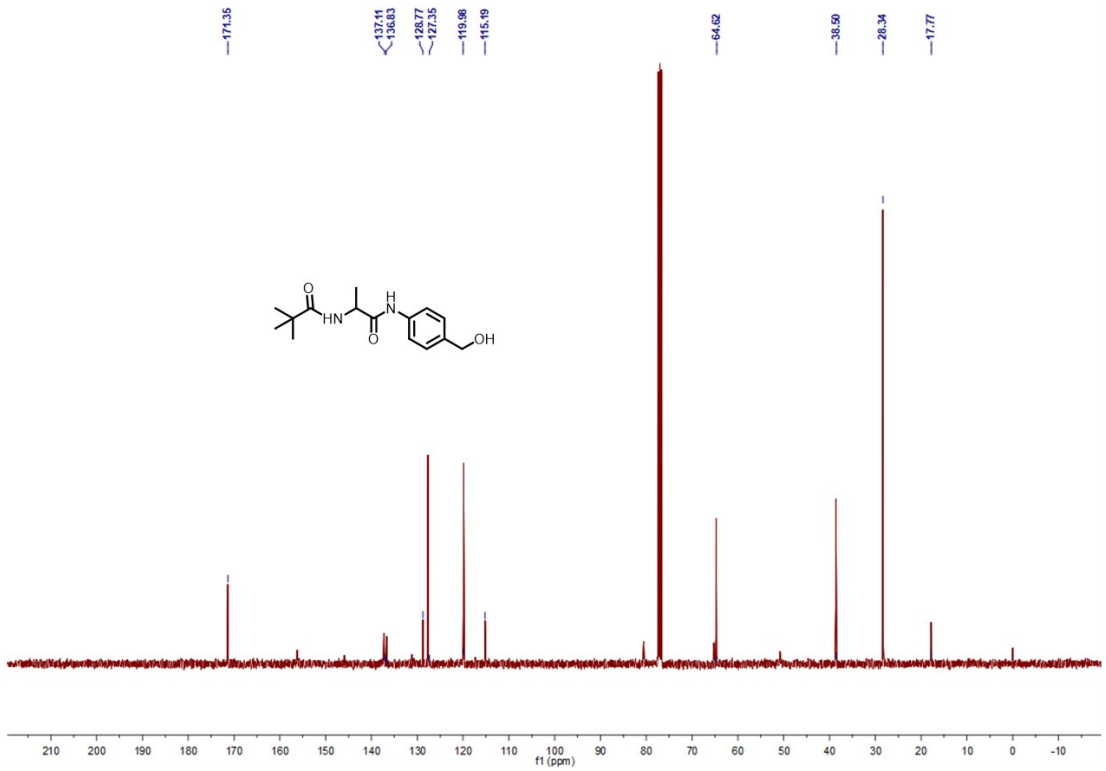

Fig. S62 ^{13}C NMR (100 MHz, 298 K, $CDCl_3$) spectrum for compound **14**.

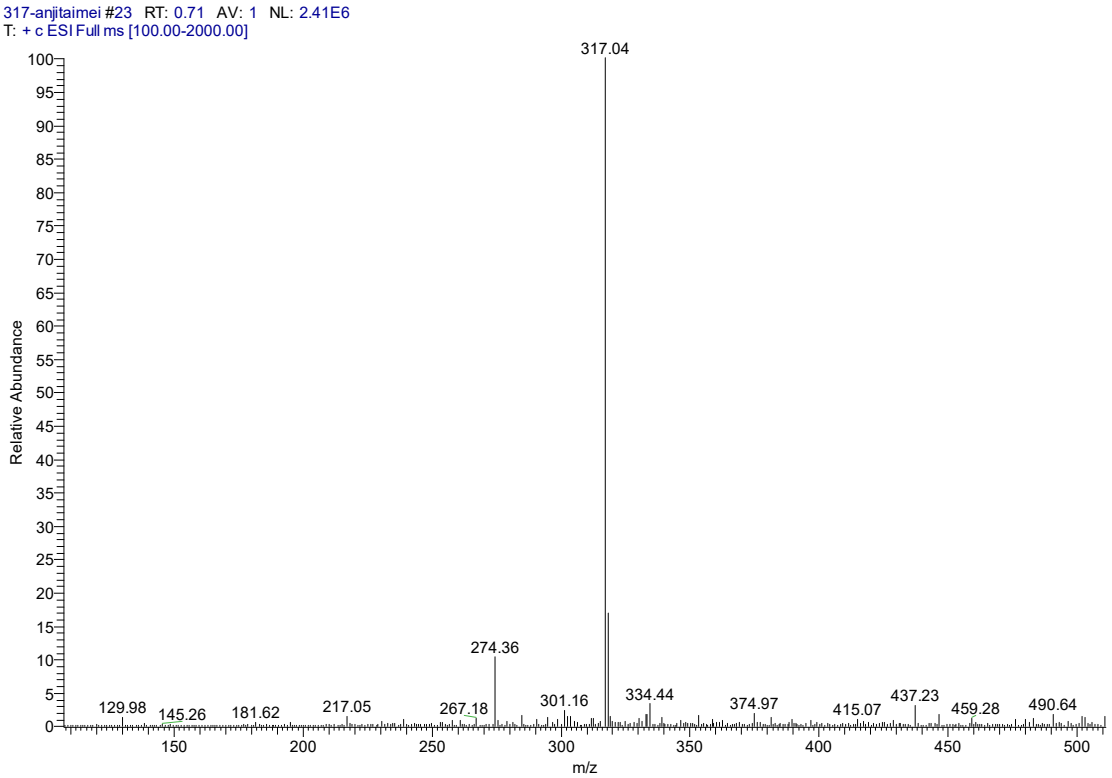

Fig. S63 HR-MS-ESI spectrum for compound **14**.

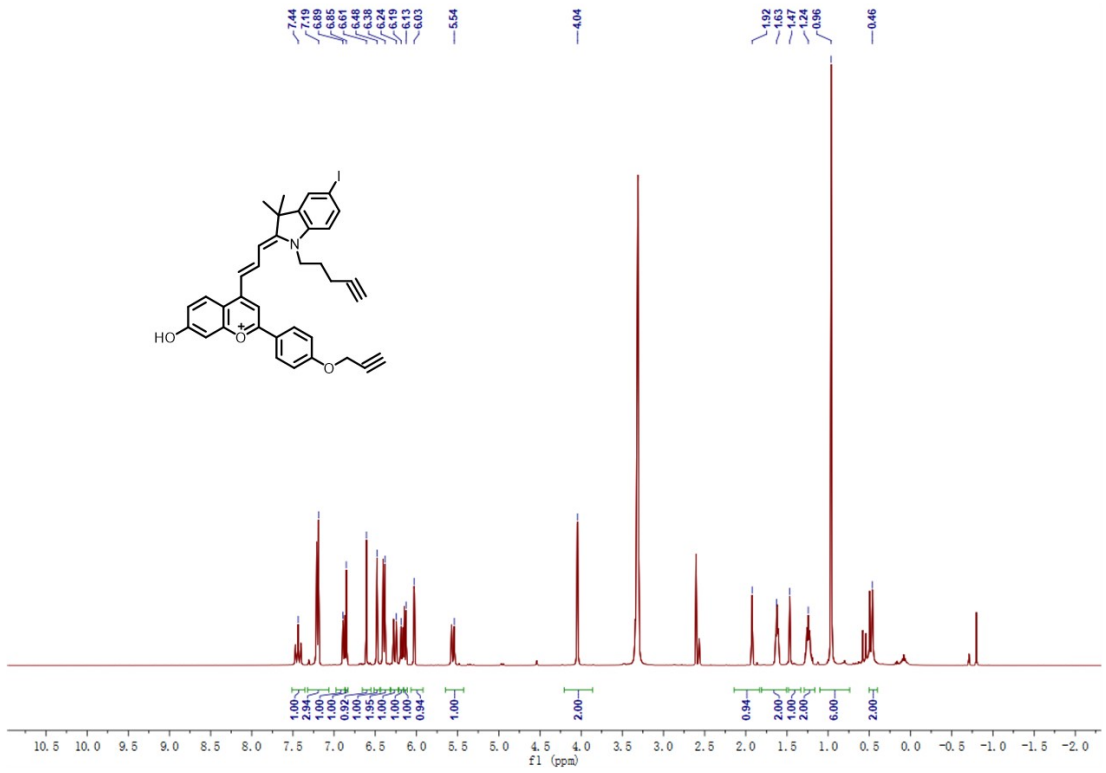

Fig. S64 ^{1}H NMR (400 MHz, 298 K, CD_3OD/ $CDCl_3$) spectrum for compound **PYCI-a**.

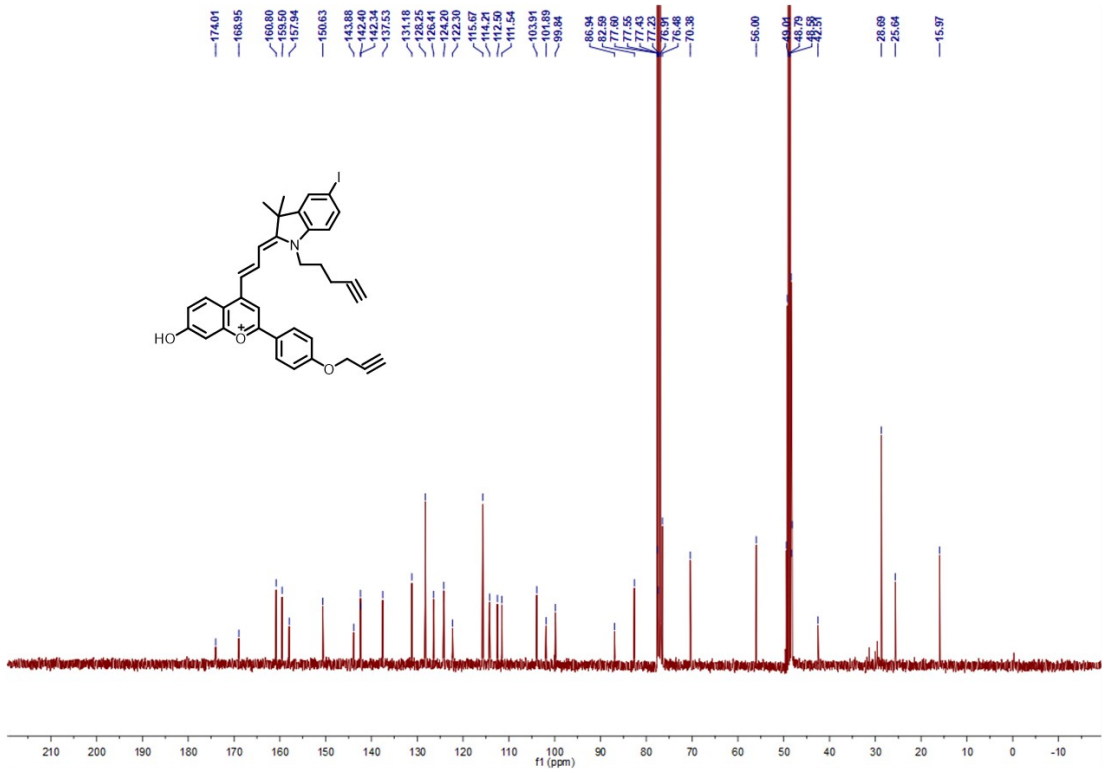

Fig. S65 ^{13}C NMR (100 MHz, 298 K, CD_3OD/ $CDCl_3$) spectrum for compound **PYCI-a**.

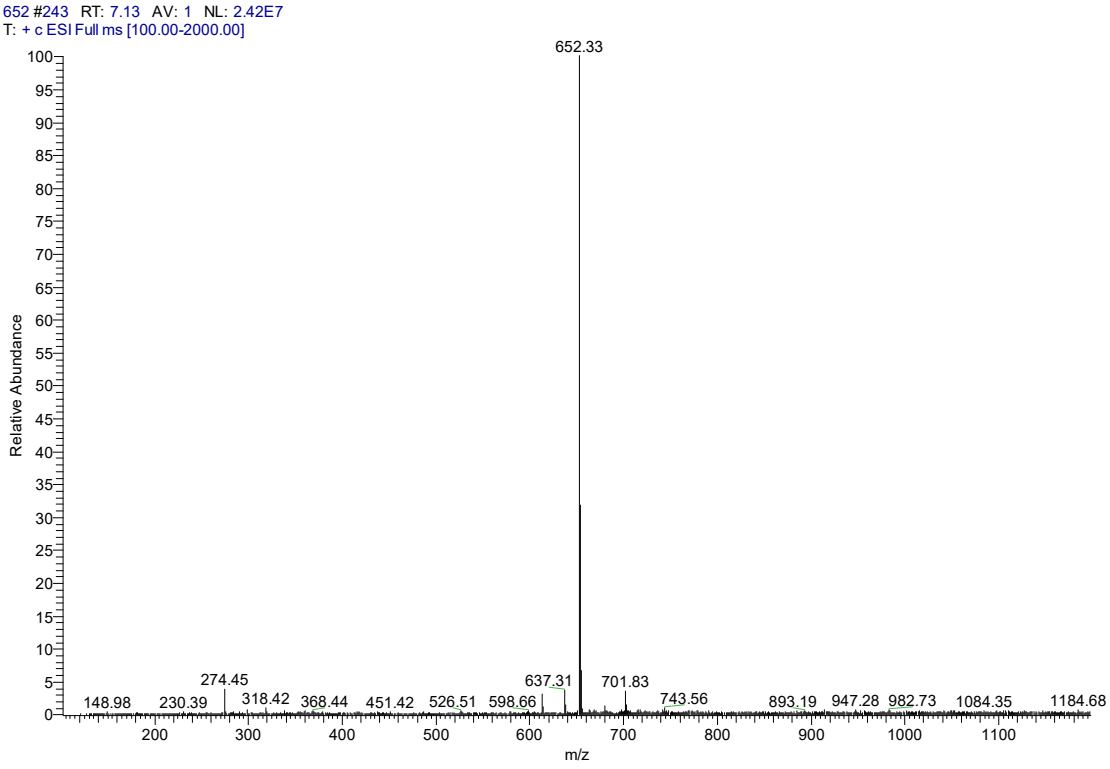

Fig. S66 HR-MS-ESI spectrum for compound **PYCI-a**.

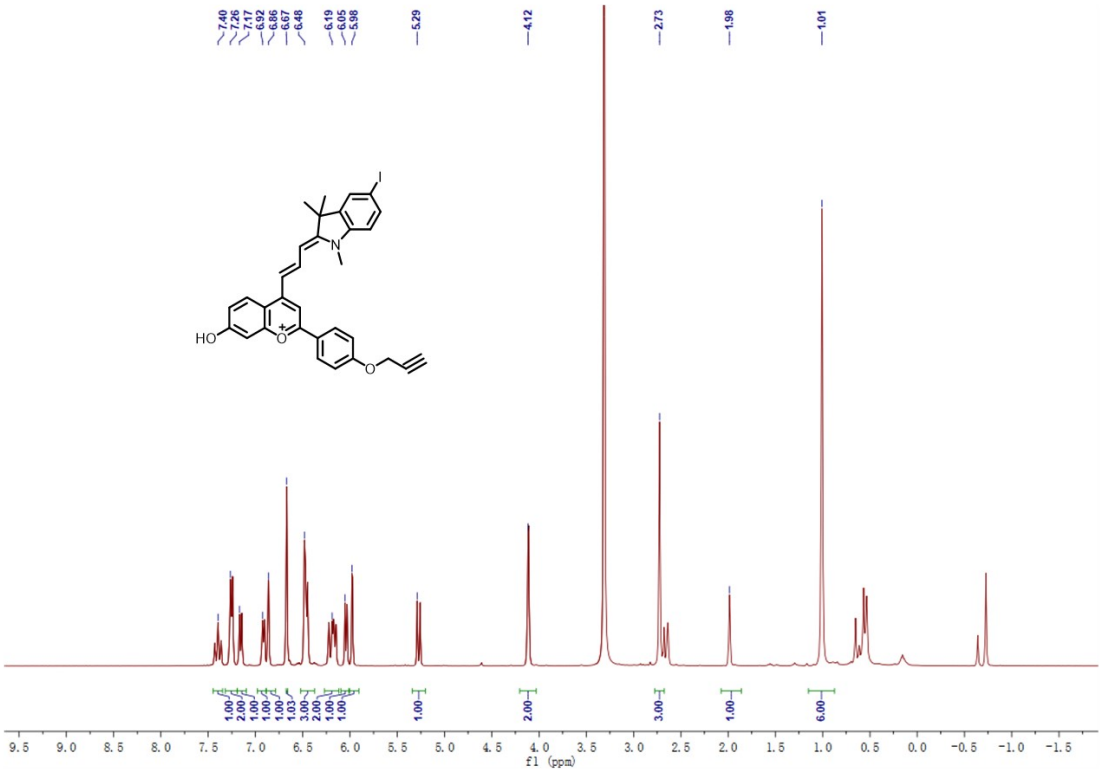

Fig. S67 ^{1}H NMR (400 MHz, 298 K, CD_3OD/ $CDCl_3$) spectrum for compound **PYCI-b**.

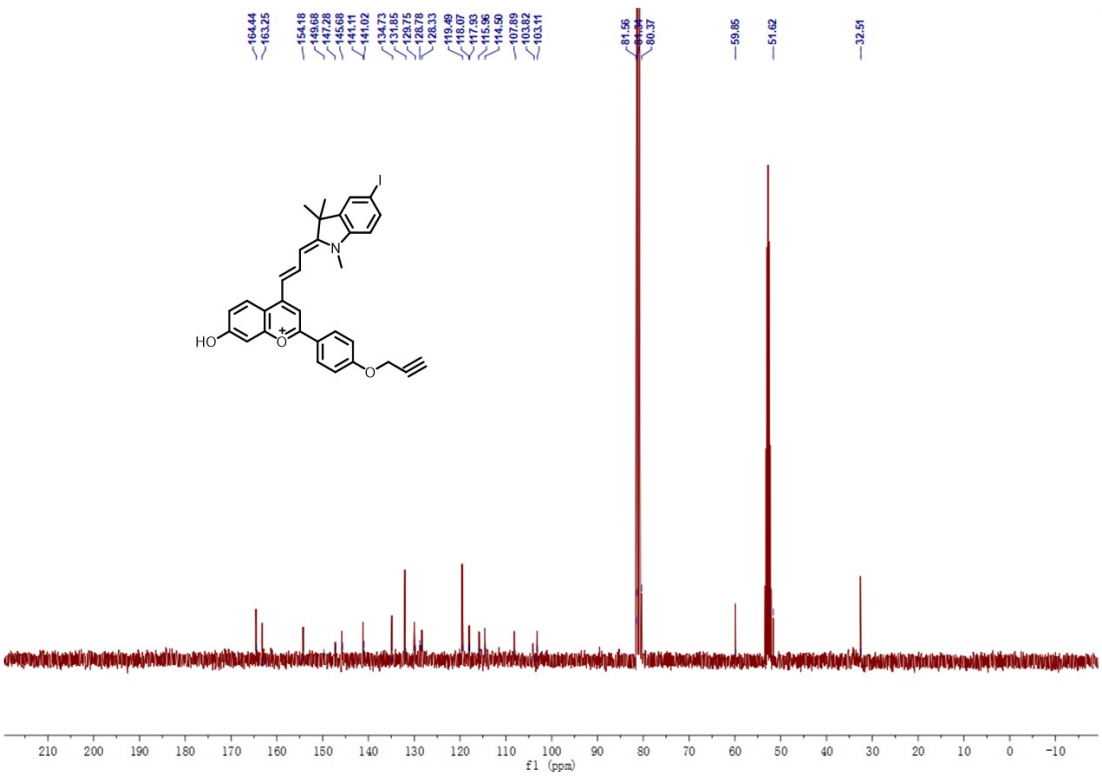

Fig. S68 ^{13}C NMR (100 MHz, 298 K, CD_3OD/ $CDCl_3$) spectrum for compound **PYCI-b**.

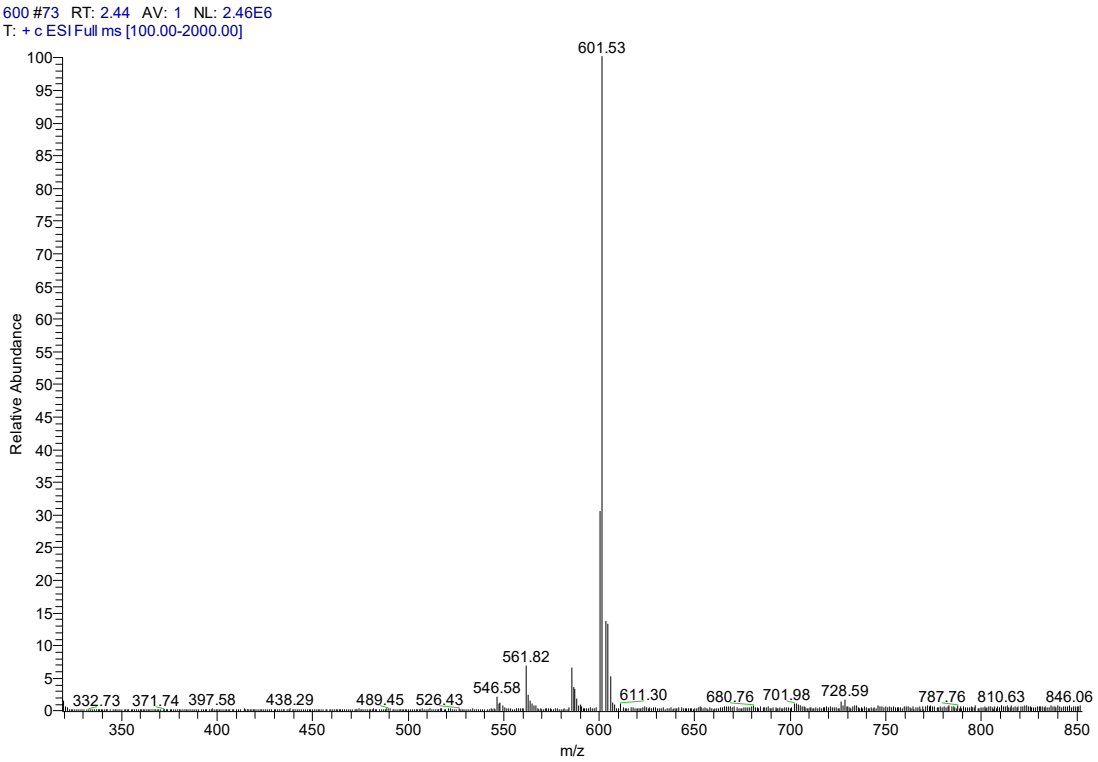

Fig. S69 HR-MS-ESI spectrum for compound **PYCI-b**.

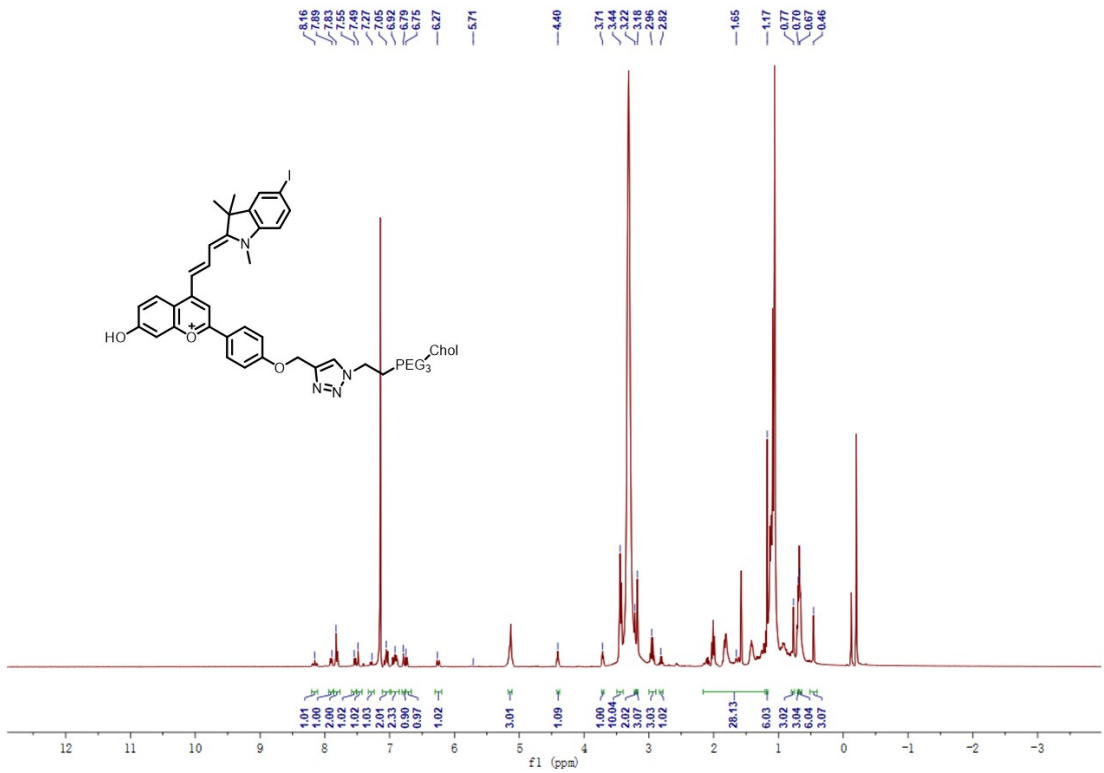

Fig. S70 ^{1}H NMR (400 MHz, 298 K, CD_3OD/ $CDCl_3$) spectrum for compound **PYCI1**.

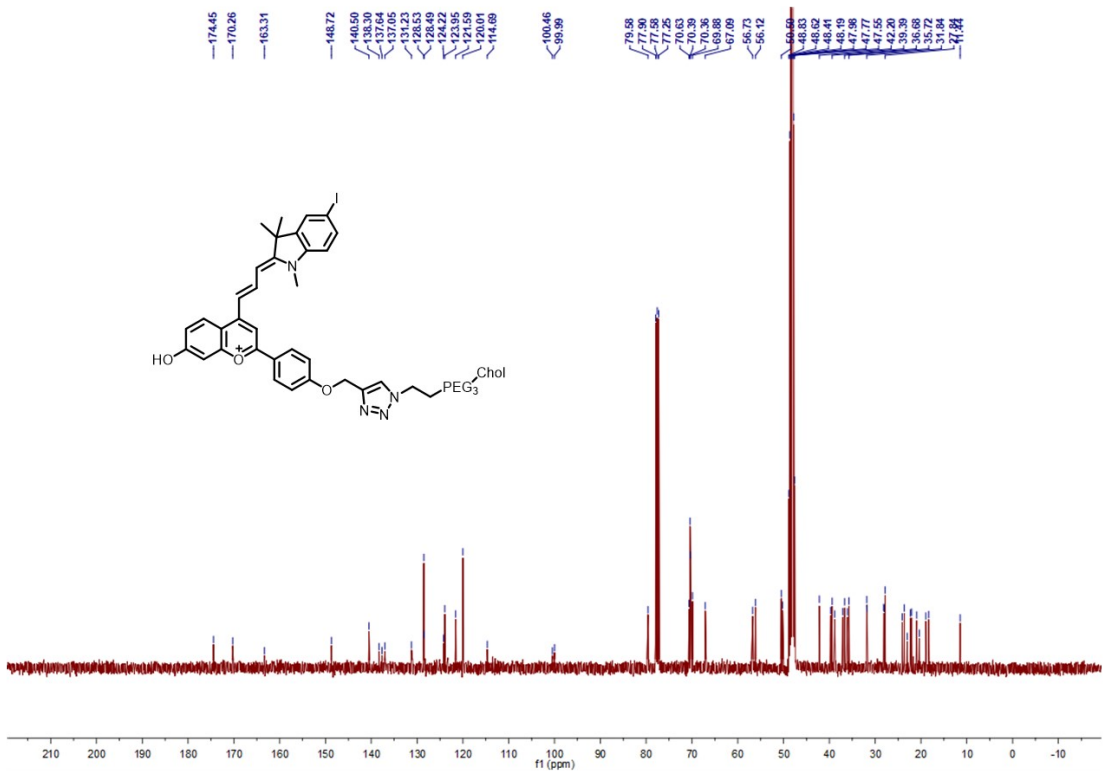

Fig. S71 ^{13}C NMR (100 MHz, 298 K, CD_3OD/ $CDCl_3$) spectrum for compound **PYCI1**.

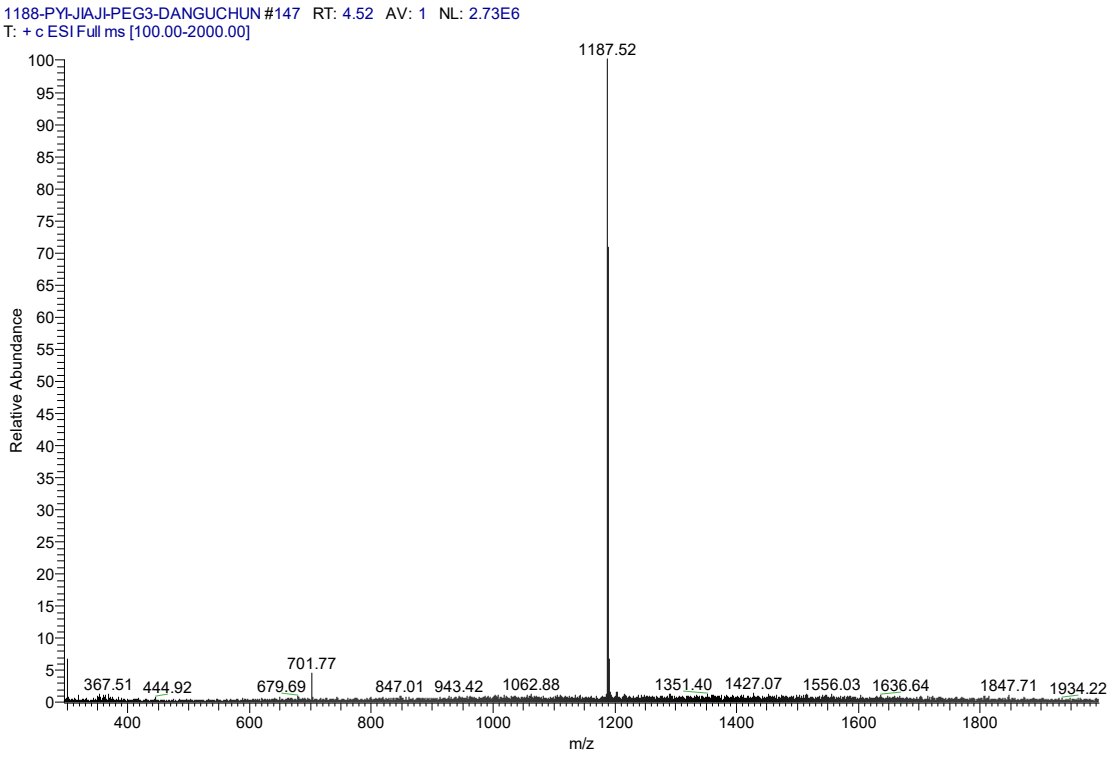

Fig. S72 HR-MS-ESI spectrum for compound **PYCI1**.

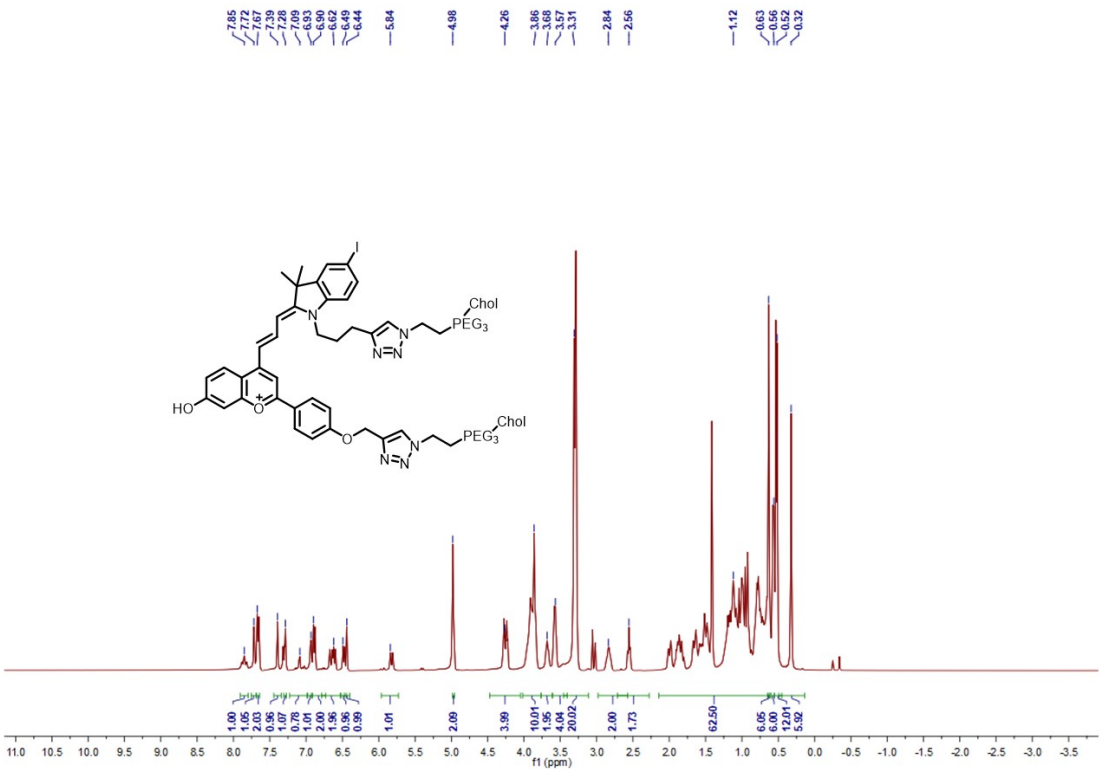

Fig. S73 ^{1}H NMR (400 MHz, 298 K, CD_3OD/ $CDCl_3$) spectrum for compound **PYCI2**.

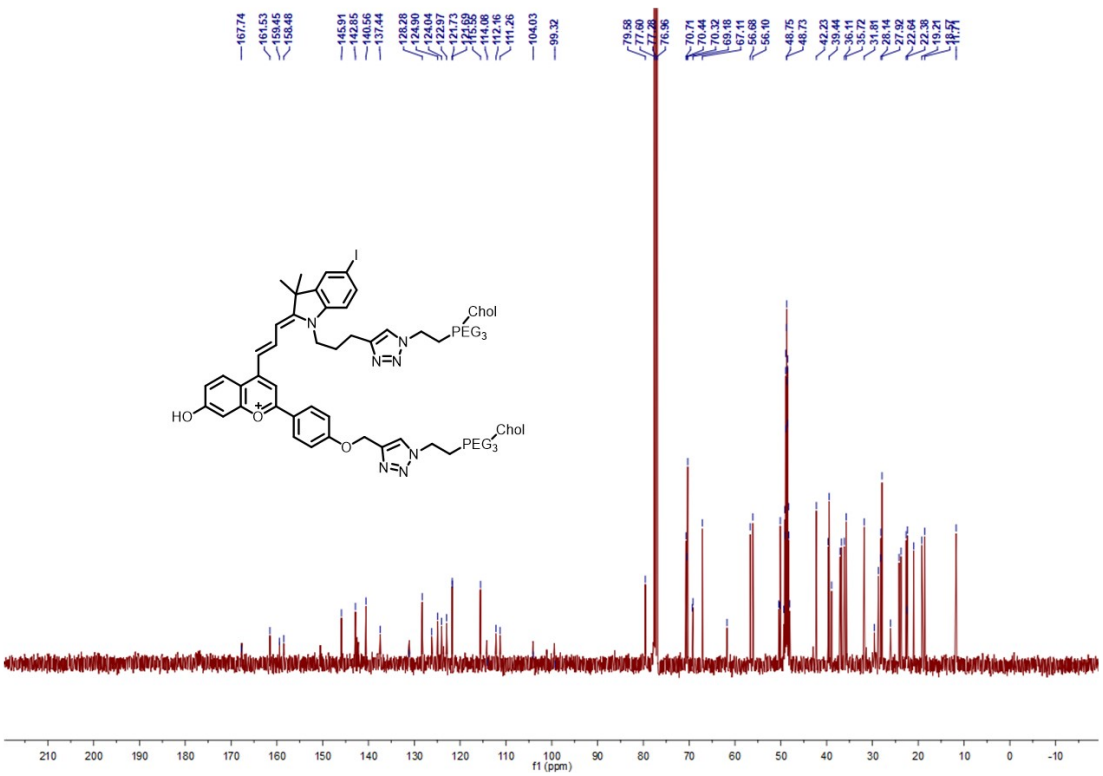

Fig. S74 ^{13}C NMR (100 MHz, 298 K, CD_3OD/ $CDCl_3$) spectrum for compound **PYCI2**.

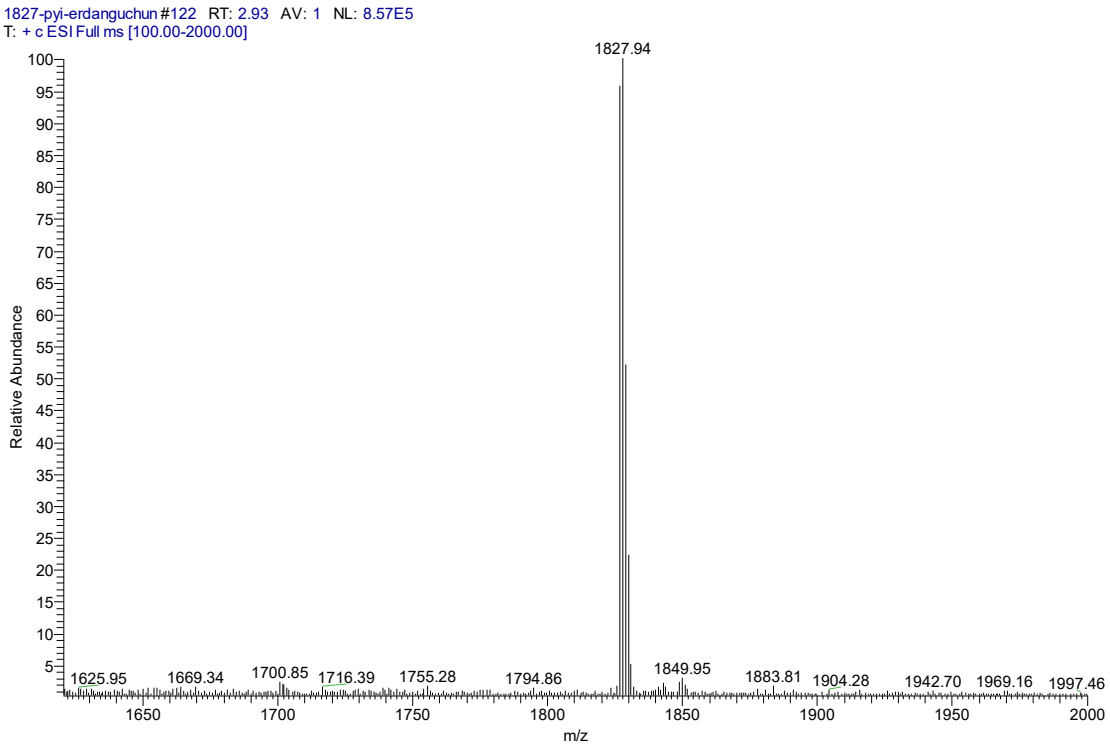

Fig. S75 HR-MS-ESI spectrum for compound **PYCI2**.

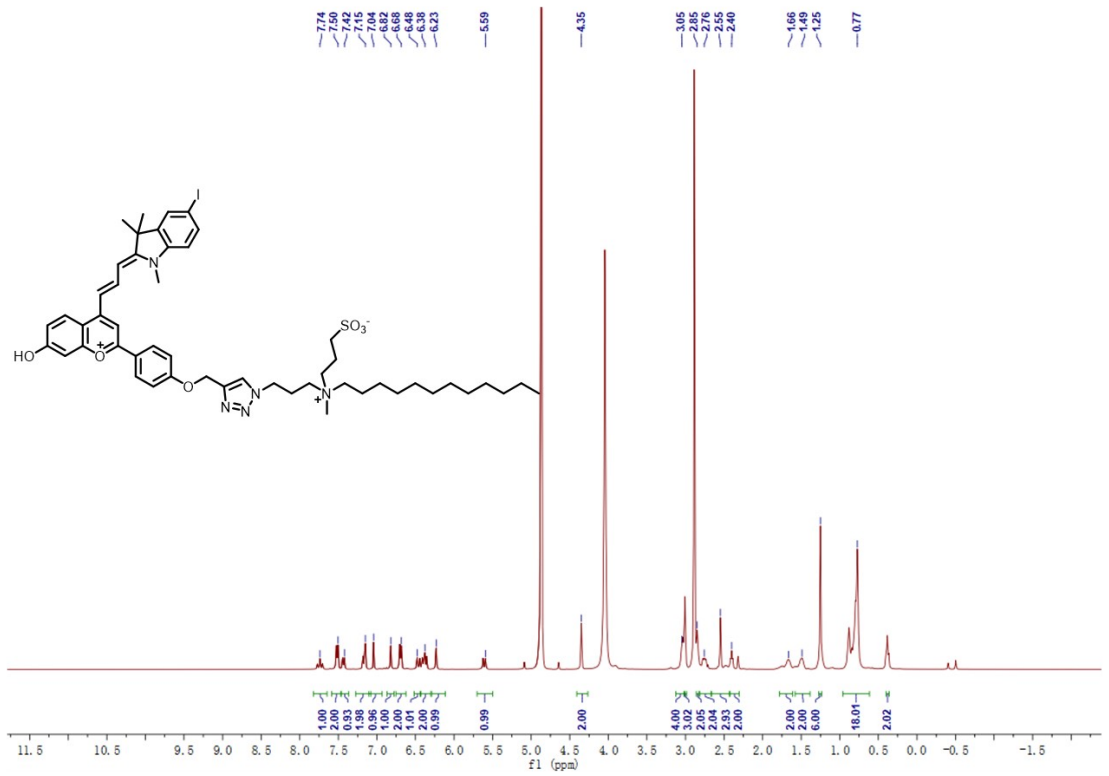

Fig. S76 ^{1}H NMR (400 MHz, 298 K, CD_3OD/ $CDCl_3$) spectrum for compound **PYCI3**.

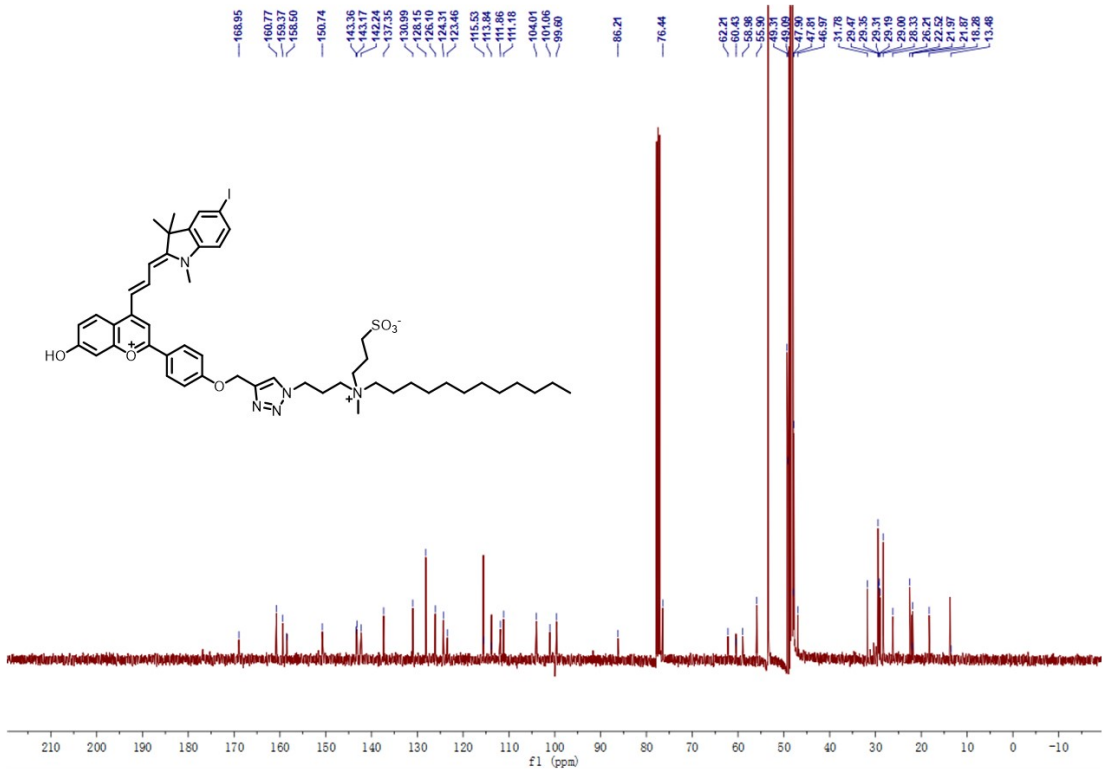

Fig. S77 ^{13}C NMR (100 MHz, 298 K, CD_3OD/ $CDCl_3$) spectrum for compound **PYCI3**.

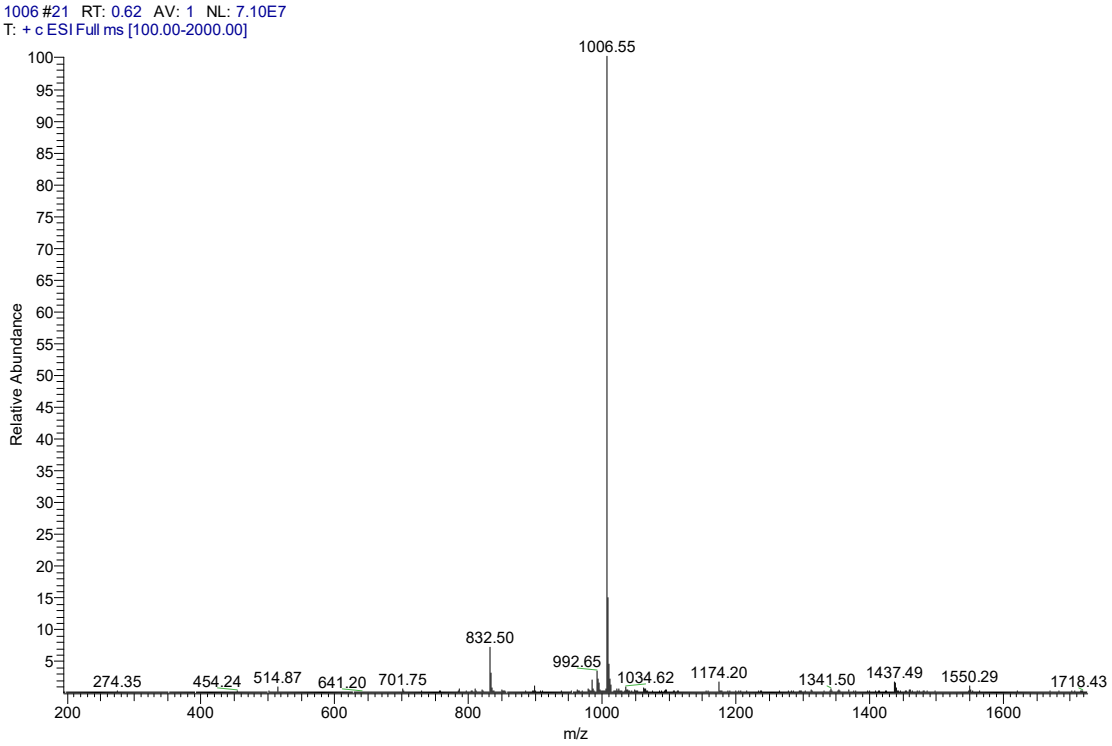

Fig. S78 HR-MS-ESI spectrum for compound **PYCI3**.

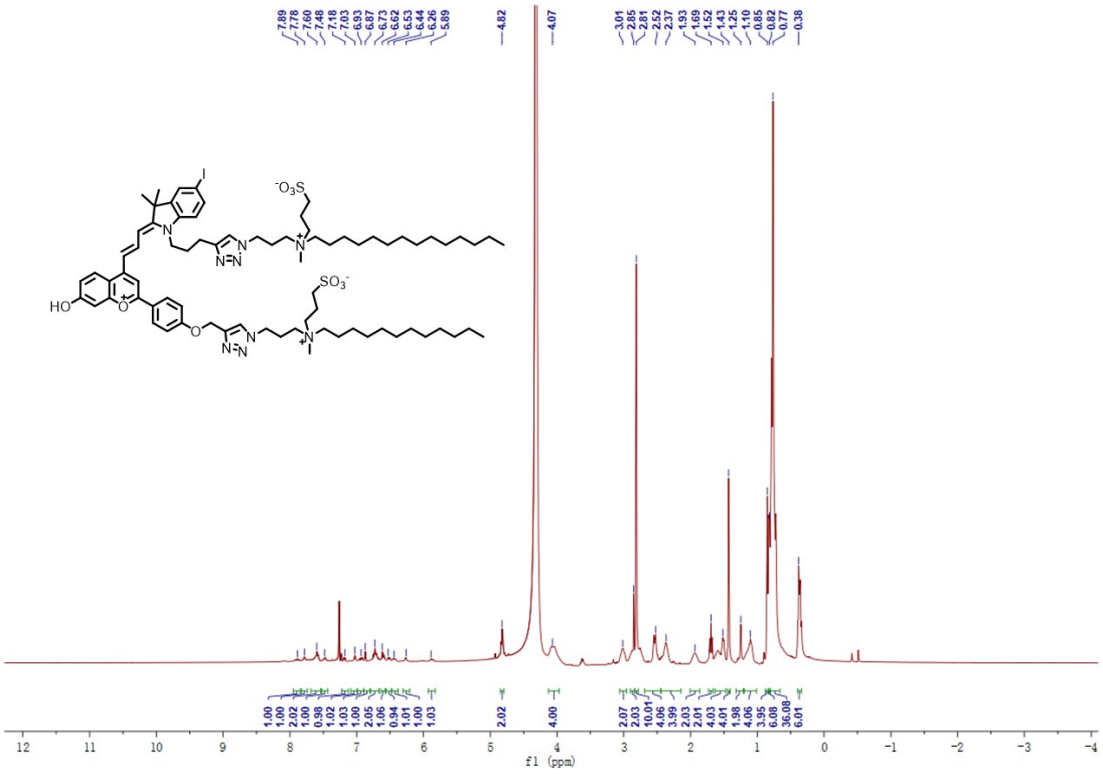

Fig. S79 ^{1}H NMR (400 MHz, 298 K, CD_3OD/ $CDCl_3$) spectrum for compound **PYCI4**.

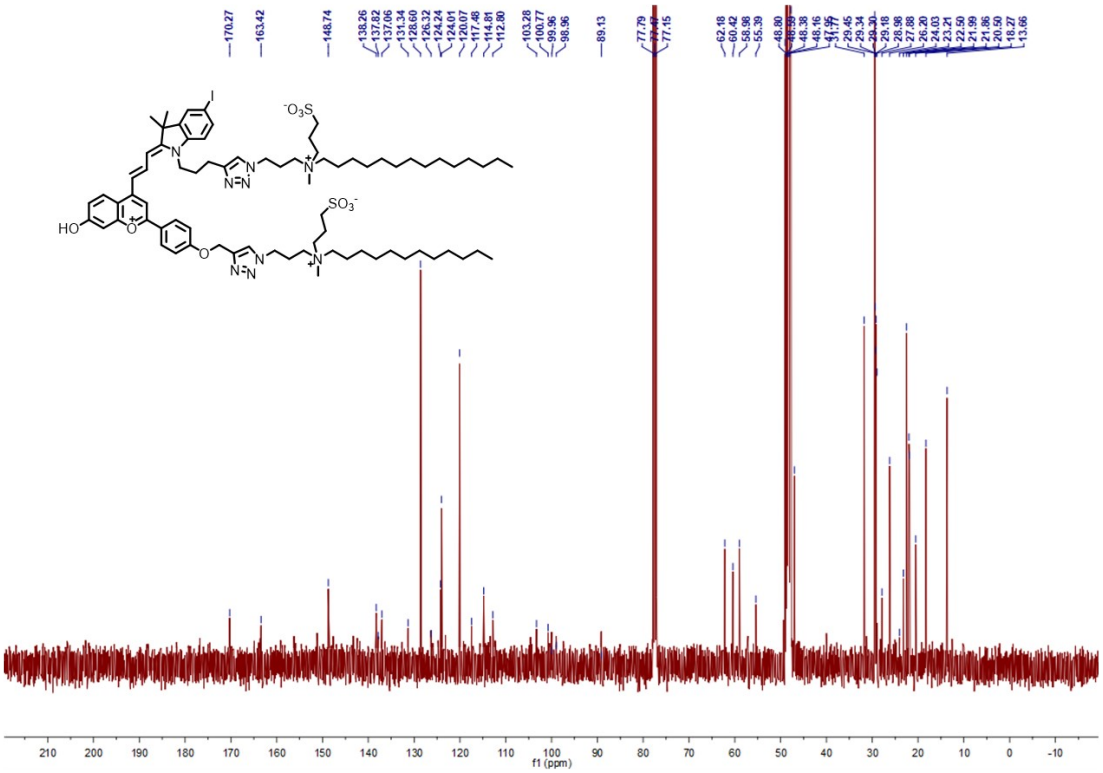

Fig. S80 ^{13}C NMR (100 MHz, 298 K, CD_3OD/ $CDCl_3$) spectrum for compound **PYCI4**.

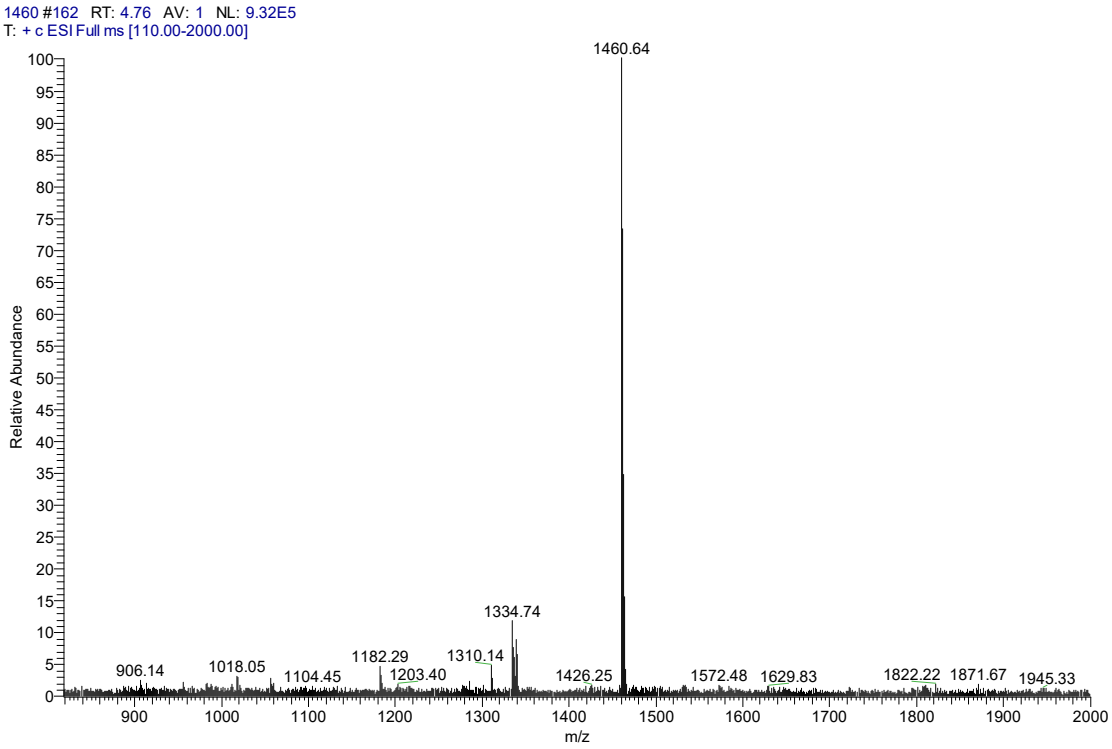

Fig. S81 HR-MS-ESI spectrum for compound **PYCI4**.

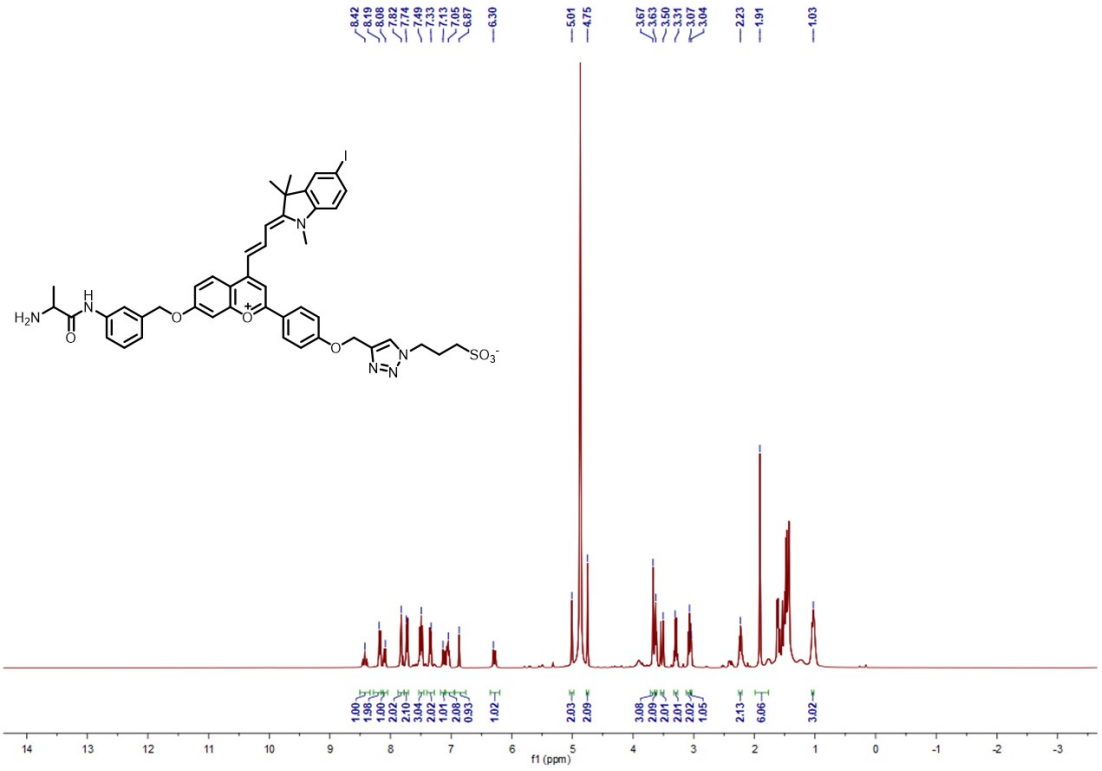

Fig. S82 ^{1}H NMR (400 MHz, 298 K, CD_3OD/ $CDCl_3$) spectrum for compound **aPYCI**.

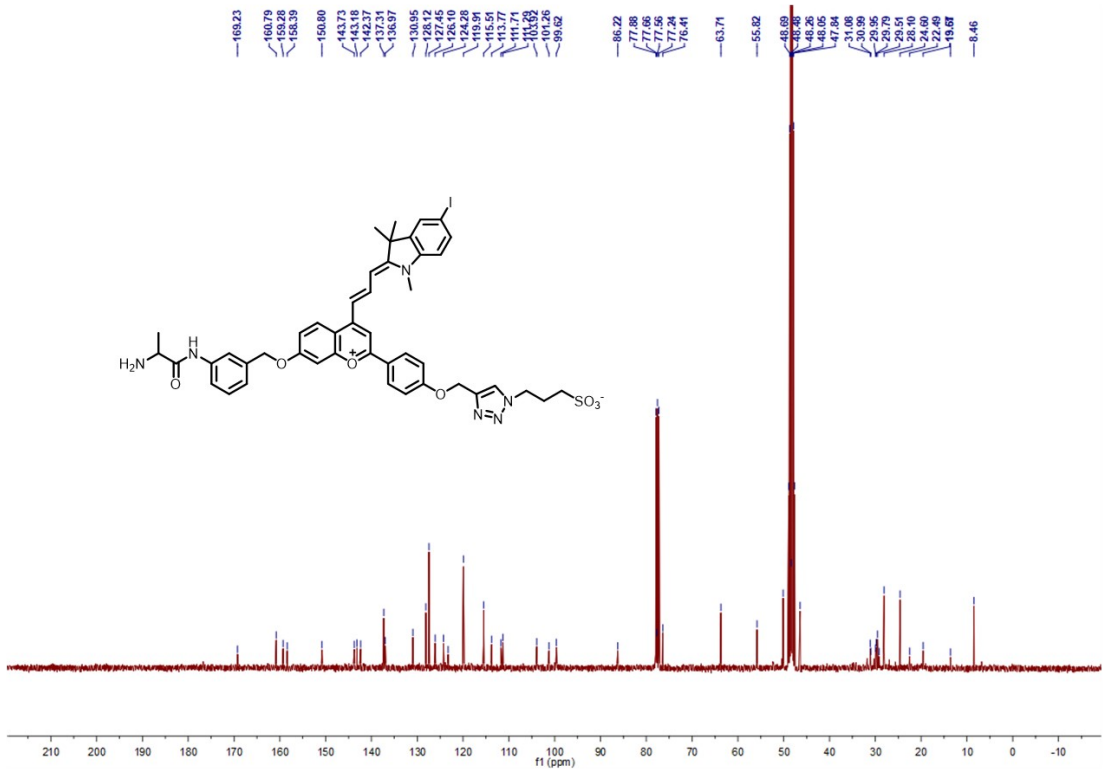

Fig. S83 ^{13}C NMR (100 MHz, 298 K, CD_3OD/ $CDCl_3$) spectrum for compound **aPYCI**.

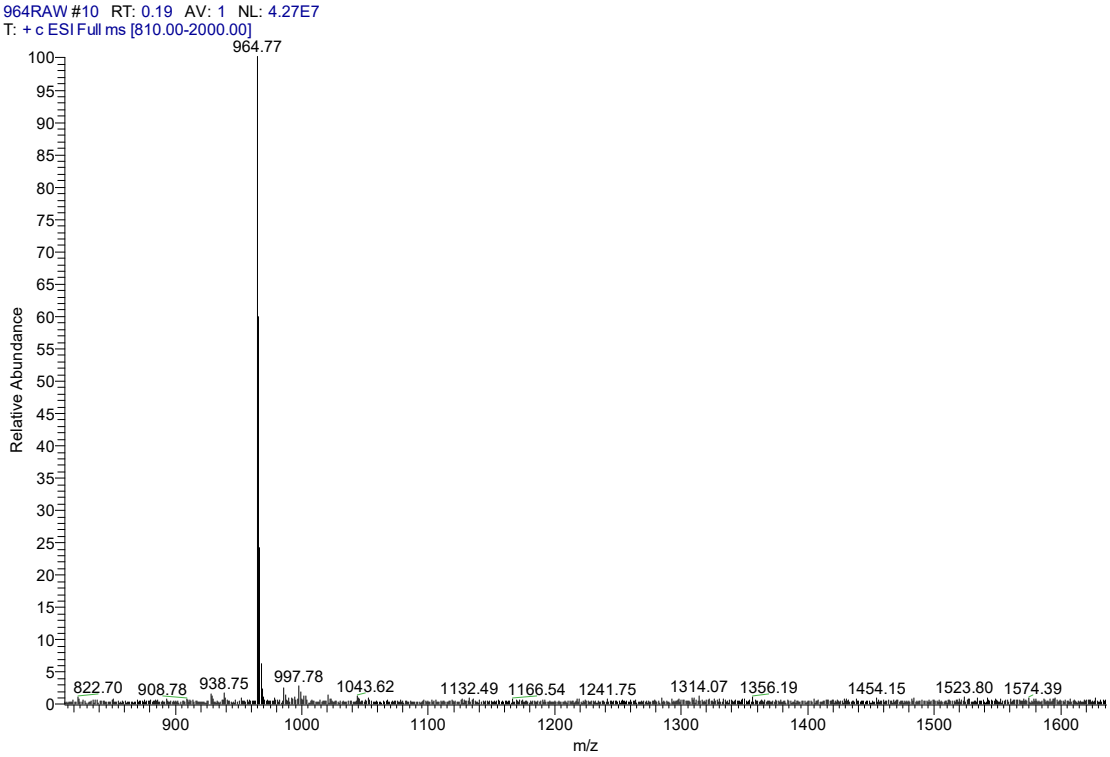

Fig. S84 HR-MS-ESI spectrum for compound **aPYCI**.

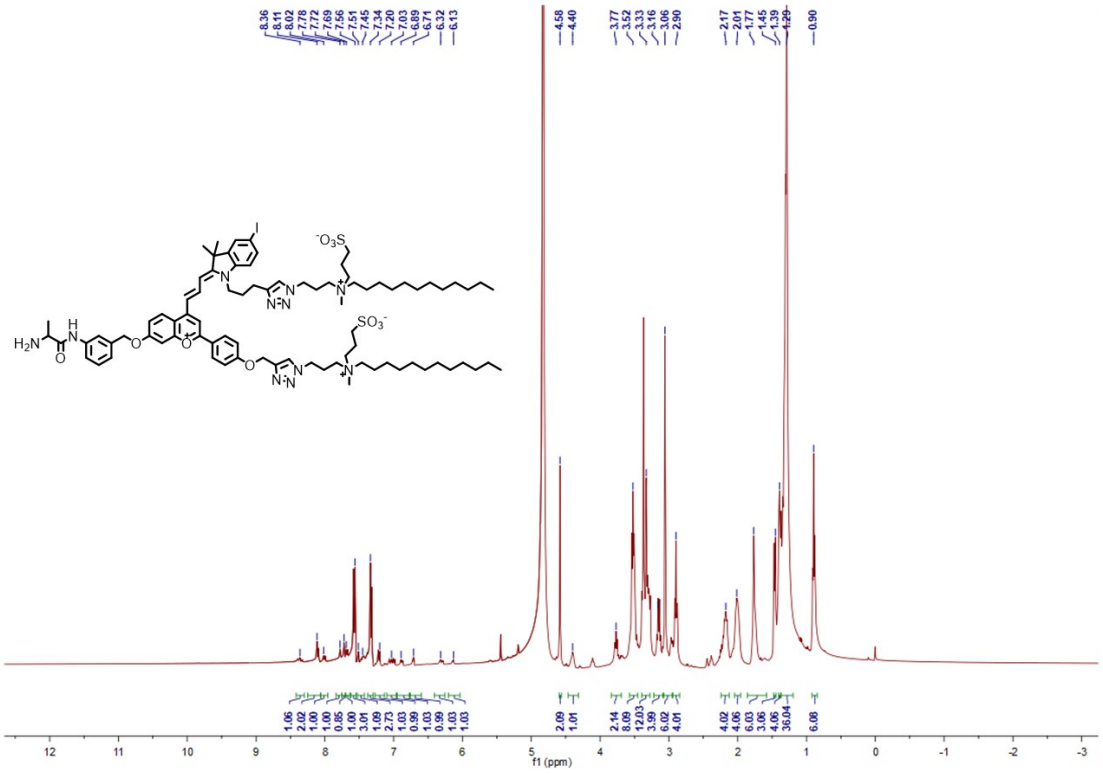

Fig. S85 ^{1}H NMR (400 MHz, 298 K, CD_3OD/ $CDCl_3$) spectrum for compound a**PYCI4**.

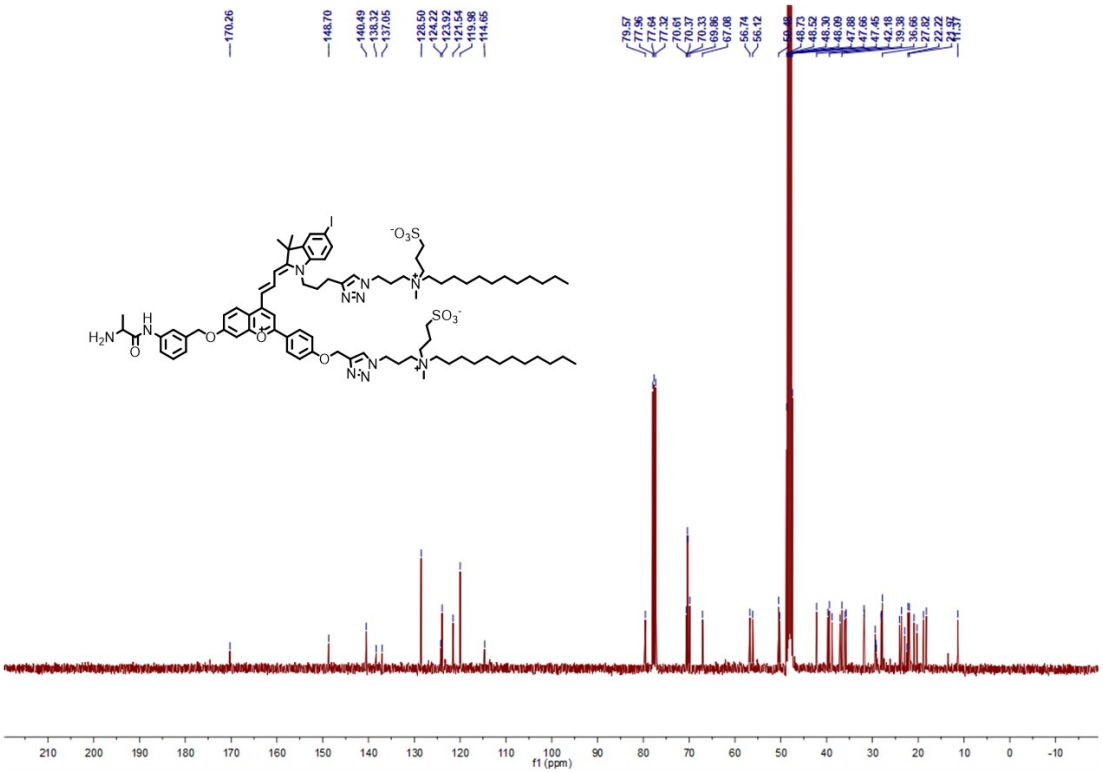

Fig. S86 ^{13}C NMR (100 MHz, 298 K, CD_3OD/ $CDCl_3$) spectrum for compound **aPYCI4**.

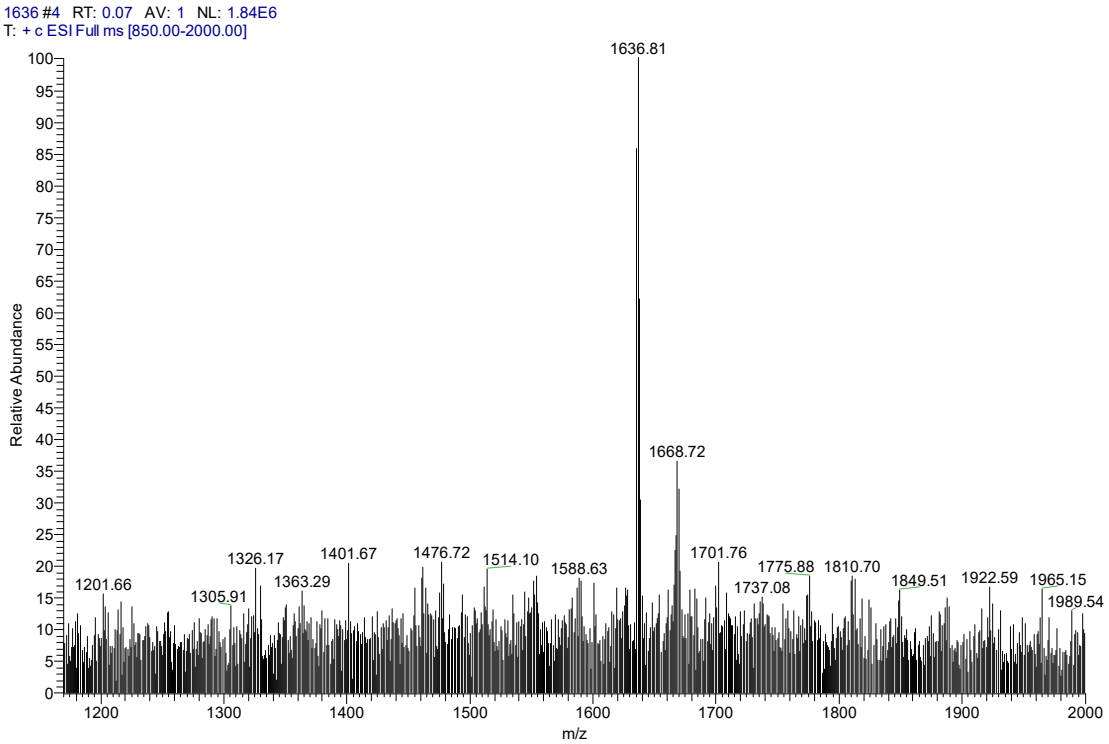

Fig. S87 HR-MS-ESI spectrum for compound **aPYCI4**.

4. References

1 X. M. Ding, Q. Z. Xu, F. G. Liu, P. K. Zhou, Y. Gu, J. Zeng, J. An, W. Dai and Z. S. Li, *Cancer Lett.*, 2004, **216**, 43-54.

2 X. Zhang, B. S. Rosenstein, Y. Wang, M. Lebwohl and H. Wei, *Free Radical Bio. Med.*, 1997, **23**, 980-985.

3 C. M. Krishna, J. E. Liebmann, D. Kaufman, W. DeGraff, S. M. Hahn, T. McMurry, J. B. Mitchell and A. Russo, *Arch. Biochem. Biophys.*, 1992, **294**, 98-106.

4 C. Yao, Y. Chen, M. Zhao, S. Wang, B. Wu, Y. Yang, D. Yin, P. Yu, H. Zhang and F. Zhang, *Angew. Chem. Int. Ed.*, 2022, **61**, e202114273.